

**STUDY OF MOLECULAR MECHANISMS OF SENSITIVITY AND
RESISTANCE TO EGFR-TARGETED THERAPY
IN LUNG CANCER**

by

ZHENFENG ZHANG

Submitted in partial fulfillment of the requirements
For the Degree of Doctor of Philosophy

Dissertation Adviser: Dr. Balazs Halmos

Department of Pathology, School of Medicine,
CASE WESTERN RESERVE UNIVERSITY

August, 2010

**CASE WESTERN RESERVE UNIVERSITY
SCHOOL OF GRADUATE STUDIES**

We hereby approve the thesis/dissertation of

ZHENFENG ZHANG

candidate for the Ph.D. degree *.

(signed) ALAN D LEVINE
(chair of the committee)

ZHENGHE WANG

PATRICK MA

WEI XIN

BALAZS HALMOS

CLIVE R HAMLIN

JOHN NEDRUD

(date) 04/28/2010

*We also certify that written approval has been obtained for any proprietary material contained therein.

TABLE OF CONTENTS

Table of Contents	iii
List of Tables	iv
List of Figures	v
Acknowledgements	vii
List of Abbreviations	ix
Abstract	xii
Chapter 1: Introduction.....	1
Chapter 2: DUSP6 is an ETS-regulated negative feedback mediator of	
oncogenic ERK signaling in lung cancer cells.....	38
Abstract.....	38
Introduction.....	40
Materials and Methods.....	44
Results.....	50
Discussion.....	70
Chapter 3: Overexpression of AXL as a novel acquired resistance	
mechanism to erlotinib in EGFR-mutated NSCLC cells.....	75
Abstract.....	75
Introduction.....	77
Materials and Methods.....	78
Results.....	82
Discussion.....	97
Chapter 4: Dissertation Discussion	100
Bibliography.....	122

LIST OF TABLES

Table		Page
Table 1-1	Classes and agents in development for treating NSCLC	7
Table 1-2	TAM Receptor Expression in Human Cancers	30
Table 1-3	Axl as a Therapeutic Target	37
Table 2-1	Effect of DUSP6 overexpression on H1975 cell cycle progression	67
Table 3-1	Genes upregulated in HCC827 cells upon erlotinib treatment	87
Table 3-2	Genes downregulated in HCC827 cells upon erlotinib treatment	87
Table 3-3	Genes upregulated in ER1 cells upon erlotinib treatment	88
Table 3-4	Genes downregulated in ER1 cells upon erlotinib treatment	88
Table 3-5	Genes upregulated in ER2 cells upon erlotinib treatment	88
Table 3-6	Genes downregulated in ER2 cells upon erlotinib treatment	88
Table 3-7	Genes upregulated in ER1 cells compared to HCC827 cells	89
Table 3-8	Genes downregulated in ER1 cells as compared to HCC827 cells	89
Table 3-9	Genes upregulated in ER2 cells as compared to HCC827 cells	90
Table 3-10	Genes downregulated in ER2 cells as compared to HCC827 cells	91
Table 4-1	Four-tier scoring system for IHC	104
Table 4-2	Correlation of AXL expression with clinicopathologic features of patients with NSCLC	115
Table 4-3	Study of correlaton of AXL expression with TKI resistance in NSCLC specimens	117

LIST OF FIGURES

Figure		Page
Figure 1-1	Cancer statistics: cancer incidence and mortality in 2009 and 5-year survival rates from 1975 to 2004	3
Figure 1-2	ALK fusion partners in lung cancer	10
Figure 1-3	Targeting the EGFR Signaling Pathway	13
Figure 1-4	Comparison of structures of gefitinib, erlotinib, and ATP	14
Figure 1-5	Gefitinib/erlotinib sensitizing or resistance mutations of EGFR in NSCLC	15
Figure 1-6	EGFR crystal structures illustrate atom-level of mechanisms of TKI sensitivity and resistance	28
Figure 1-7	Structural Features of DUSP6	24
Figure 1-8	Structure, binding, and activation of TAM receptors by their ligands	28
Figure 1-9	Axl signaling pathways lead to platelet aggregation, cell survival, proliferation, regulation of proinflammatory cytokine production, and regulation of the actin cytoskeleton.	33
Figure 2-1	DUSP6 expression in NSCLC cell lines and primary patient samples	52
Figure 2-2	DUSP6 is regulated by EGFR/ERK inhibition in NSCLC cell lines	54
Figure 2-3	Downregulation of DUSP6 by erlotinib is mediated by the ERK-responsive ETS family transcription factor ETS1 through direct binding to the DUSP6 gene promoter	59
Figure 2-4	DUSP6 protein localizes to the cytoplasm and functions as a negative regulator for ERK activity	63
Figure 2-5	DUSP6 overexpression inhibited H1975 cell growth through a combination of increased apoptosis and decreased cell proliferation	66
Figure 2-6	Introduction of DUSP6 siRNA reduced DUSP6 protein levels resulting in	69

increased ERK activity and cellular proliferation

Figure 2-7 Model of MAPK pathway signal transduction

71

Comparison of growth and signaling of parental HCC827 and erlotinib-resistant
Figure 3-1 HCC827 cells

84

Figure 3-2 AXL is overexpressed in resistant ER1 cells

86

SiRNA-mediated AXL knockdown restores erlotinib sensitivity in ER1 cells
Figure 3-3 leading to cell death and is accompanied by inhibition of AKT and ERK activity

95

Figure 3-4 Inhibition of AXL by XL880 restores erlotinib sensitivity in ER1 cells

96

Model of oncogenic RTK switch of EGFR-TKI resistance in lung cancer with
Figure 3-5 AXL overexpression

98

Figure 4-1 A cluster of CpG islands are found in the promoter region of DUSP6 gene

108

Figure 4-2 There is a CpG island within the promoter area of the AXL gene

113

Figure 4-3 AXL protein expression in 9 NSCLC cell lines.

119

ACKNOWLEDGEMENTS

I would like to thank all people who have helped and inspired me during my doctoral study.

I especially would like to thank my advisor, Dr. Balazs Halmos. His perpetual energy, intelligence and enthusiasm in research had motivated me to continue to do research. I am so grateful that he has given me so much freedom with my project and the confidence to keep at it when all seemed grim, and he was always accessible and gave me the guidance to recover when my steps faltered. No words of gratitude can possibly do any justice for the helps and supports Balazs gave me in the past three years.

I was lucky enough to have supports from my previous advisor Dr. Alan Levine who is also the chairman of my thesis committee. In the first three years of my graduate studies, Alan has led me hand by hand to the scientific research world. He has always kept an eye on my progress and growth and even my English as a scientist in the past six years. I would like to show my gratitude to his guidance, support and great patience.

It is my great pleasure to thank the following wonderful scientists during my graduate studies, especially the members of my thesis committee, Drs Wei Xin, John Nedrud, Zhenghe John Wang, Patrick Ma, and Clive Hamlin for their constructive scientific suggestions that have been proved extremely valuable for my project. I am also grateful to Drs. Zhiwei Yu and Rom Leidner for inspiring me with insightful ideas and their

valuable friendships when I was getting bored in my mind, and was during the work in the middle of night.

Lastly, I owe my deepest gratitude to my family who have always provided unconditional love and support: my parents, my wife, and my lovely daughter and son. This dissertation is impossible without them. I am most grateful to my wonderful wife for walking along with me on the long road of doctoral study. She always gave me confidence, encouragement and inspiration to deal with difficulties in my life. Finally for the two little ones whom I owe most – my daughter Cynthia and my son Ryan, I am so grateful for the sunshine you give me to my life. Only smiles left without any unhappiness and worries together with you.

LIST OF ABBREVIATIONS

Ab - antibody

ALK - anaplastic lymphoma kinase

BrdU - bromo-deoxyuridine

CML - chronic myelogenous leukemia

DAC - deoxyazacytidine

DNMT - DNA methyltransferase

DUSP - dual specificity phosphatase

EGFR - epidermal growth factor receptor tyrosine

EML4 - echinoderm microtubule-associated protein-like 4

Erk - extracellular signal regulated kinase

FBS - fetal bovine serum

FISH - fluorescence in-situ hybridization

FNIII - fibronectin type III

GAPDH - Glyceraldehyde-3-phosphate dehydrogenase

Gas - growth-arrest-specific gene

GFP - green fluorescent protein

GIST - gastrointestinal stromal tumor

HDAC - histone deacetylase

HGFR - hepatocyte growth factor receptor

HUVEC - human umbilical vein endothelial cells

Ig - immunoglobulin

IHC - Immunohistochemistry

KIM - kinase interaction motif

LCM - laser capture microdissection

LOH - loss of heterozygosity

MAPK - mitogen activated protein kinase

MKP - dual-specificity MAPK phosphatase

MET - mesenchymal-epithelial transition factor receptor

mTOR - mammalian target of rapamycin

MTS - tetrazolium compound [3-(4,5-dimethylthiazol-2-yl)-5-(3-carboxymethoxyphenyl)-2-(4-sulfophenyl)-2H-tetrazolium

NCAM - neural cell adhesion molecule

NES – nuclear export signal

NSCLC - non-small cell lung cancer

NuLi-1 - human airway epithelial cell line

PARP - poly ADP ribose polymerase

PI - propidium iodide

PI-3K - phosphatidylinositol-3 kinase

PLC - phospholipase C

PTEN - phosphatase and tensin homologue

PTK - protein tyrosine kinase

RTK - receptor tyrosine kinase

RT-PCR - reverse transcription-polymerase chain reaction

SCLC - small cell lung cancer

SDS-PAGE - sodium dodecyl sulfate polyacrylamide gel electrophoresis

siRNA - small interfering RNA

Src - homology-2 (SH-2)

STAT - signal transducer and activator of transcription

TCA - trichloroacetic acid

TGF - transforming growth factor

TKI - tyrosine kinase inhibitor

TSA - trichostatin A

TSG - tumor-suppressor gene

VEGFR - vascular epithelial growth factor receptor

Study of Molecular Mechanisms of Sensitivity and Resistance to EGFR-Targeted Therapy in Lung Cancer

ABSTRACT

By

ZHENFENG ZHANG

Lung cancer is still the leading cause of cancer-related death worldwide. EGFR-targeted tyrosine kinase inhibitors (TKI), such as erlotinib and gefitinib, have dramatic clinical effects on EGFR-dependent lung cancers and are used as first-line therapy for patients with EGFR-mutant lung tumors. However, eventually all tumors acquire secondary resistance to the drugs and progress. Sensitivity to such EGFR-TKI is determined by activating mutations in EGFR tyrosine kinase domain whereas resistance to the TKI can be conferred by EGFR secondary mutations such as EGFR T790M and MET activation. Using a T790M-mutant H1975 NSCLC cell line which is gefitinib-resistant but sensitive to an irreversible EGFR inhibitor CL-387,785 allowed us to compare the target gene changes by treatment with gefitinib or CL387,785 in a transcriptional profiling study. We identified several dual specificity phosphatases (DUSPs) among the most highly and immediately regulated genes upon EGFR inhibition. DUSPs act as natural terminators of MAPK signal transduction and we demonstrate a tumor suppressive role of DUSP6 via

targeting ERK activity. We also show that the regulation of DUSP6 is mediated at the promoter level by ETS1, a well-known nuclear target of activated ERK, indicating an important negative feedback loop in NSCLC. Furthermore, we developed an erlotinib-resistant NSCLC cell model and explored mechanisms of such resistance. We discover a novel mechanism of erlotinib resistance involving overexpression of AXL. Further studies confirm that co-treatment using erlotinib along with AXL knockdown or pharmacological inhibition resensitizes these resistant cells leading to cell death. These results suggest that an oncogenic switch from EGFR-dependent to EGFR/AXL-codependent signaling can lead to secondary EGFR-TKI resistance in NSCLC. In summary, our findings provide novel options for the improved targeting of EGFR-dependent tumors by the identification of DUSP6 and AXL as important modulators of EGFR sensitivity/resistance.

CHAPTER 1

INTRODUCTION

1.1. Lung cancer as a public health issue

Lung cancer is a major global health problem, and still remains the second most common cancer among both men and women, accounting for the most cancer-related deaths in America, and late diagnosis is a fundamental obstacle to improving lung cancer outcomes (1).

Only 15% of all lung cancer patients are alive 5 years or more after diagnosis (Fig. 1-1).

Lung cancer is a unique disease in that the etiologic agent is an industry. About 90% of cases are caused by voluntary or involuntary (second hand) cigarette smoking. Reduction of lung cancer mortality will require effective public health policies to prevent initiation of smoking, Federal Drug Administration (FDA) oversight of tobacco products and other tobacco control measures (National Comprehensive Cancer Network, Clinical Practice Guidelines in Oncology: Non-Small Cell Lung Cancer, volume 2, 2008).

Symptoms: People with early stages of lung cancer rarely have symptoms and common symptoms of this disease include persistent cough, sputum streaked with blood, dyspnea, weight loss, chest pain, recurrent pneumonia or bronchitis. Symptomatic patients are more likely to have chronic obstructive pulmonary disease.

Classification: The World Health Organization divides lung cancer into 2 major classes based on its biology, therapy, and prognosis: non-small cell lung cancer (NSCLC) and small cell lung cancer (SCLC). This histological distinction is important since these two groups differ in terms of their likelihood to metastases and response to available therapies for

common clinical management. Histopathological diagnosis is to separate out SCLC because SCLC is treated as a systemic disease, significantly different from that for NSCLC. SCLCs represent approximately 15%–20% of lung cancer cases, and are the most aggressive of lung tumors, metastasizing early and widely. They have high initial response to chemotherapy and radiotherapy, but are virtually incurable by all available therapeutic means. Most patients have distant metastasis on diagnosis, thus, even with active treatment, the mean survival after diagnosis is about 1 year.

NSCLCs include adenocarcinoma, squamous cell (epidermoid) carcinoma, and large-cell carcinoma and are grouped together because their prognosis and management are similar. NSCLCs represent approximately 80%–85% of all lung cancers and are less often metastatic and less responsive to chemotherapy by comparison to SCLC. Approximately 10% of all lung carcinomas have a combined histology, including two or more of the above types. Adenocarcinoma is the most common type of NSCLC in the United States and is also the most frequently occurring cell type in nonsmokers. Recently, gene expression profiling (using RNA microarrays) has identified subtypes of lung adenocarcinomas (ie, bronchioid, squamoid, magnoid), which correlate with stage-specific survival and metastatic pattern. Bronchioid tumors were associated with increased survival in early-stage disease, whereas, squamoid tumors were associated with increased survival in advanced disease (2).

Pathologic Evaluation: The purpose of pathologic evaluation is to classify the lung cancer, determine the extent of invasion, and establish the cancer involvement status of the surgical margins, and determine the molecular abnormalities of lung cancer that may be able to predict for sensitivity and resistance to epidermal growth factor receptor tyrosine-kinase inhibitors (EGFR-TKI), such as erlotinib and gefitinib (3, 4).

Treatment: Current treatments for lung cancer include surgical resection, platinum-based chemotherapy, radiation therapy, adjuvant therapy, and recently developed biological targeting therapy (targeting EGFR or VEGF, for example) alone or in combination dependent on the histological type (SCLC or NSCLC) and stage of the cancers at diagnosis. Despite an overall poor outlook with all available treatment, some patients with earlier stage of lung cancers have been cured by lobectomy or pneumonectomy or radiation-based therapies, emphasizing the continued need for early diagnosis and adequate prompt therapy.

Cancer Incidence and Mortality: 2009			Five-Year Survival Rates: 1975-2004 (select cancers)		
Cancer Type	Estimated Deaths	Estimated New Cases	Cancer Type	1975-1977 (%)	1984-1986 (%)
All sites*	562,340	1,479,350	All cancers	50	54
Lung and bronchus	159,390	219,440	Prostate	69	76
Colon	49,920	106,100	Thyroid	93	94
Breast	40,610	194,440	Testis	83	93
Pancreas	35,240	42,470	Melanoma‡	82	87
Prostate	27,360	192,280	Breast	75	79
Non-Hodgkin's lymphoma	19,500	65,980	Hodgkin's lymphoma	74	79
Liver and intrahepatic bile duct	18,160	22,650	Endometrial	88	84
Ovary	14,600	21,550	Bladder	74	78
Esophagus	14,530	16,470	Cervical	70	68
Bladder	14,330	70,980	Kidney	51	56
Kidney and renal pelvis	12,980	57,760	Rectum	49	57
Brain	12,920	22,070	Colon	52	59
Stomach	10,620	21,130	Non-Hodgkin's lymphoma	48	53
Multiple myeloma	10,580	20,580	Larynx	67	66
Acute myeloid leukemia	9,000	12,810	Oral§	53	55
Melanoma	8,650	68,720	Leukemia	35	42
Chronic lymphocytic leukemia	4,490	15,490	Ovary	37	40
Cervical	4,070	11,270	Brain	24	29
Soft tissue	3,820	10,660	Multiple myeloma	26	29
Larynx	3,660	12,290	Stomach	16	18
Gallbladder	3,370	9,760	Esophagus	5	10
Endocrine system	2,470	39,330	Lung	13	13
Pharynx	2,230	12,610	Liver	4	6
Tongue	1,910	10,530	Pancreas	2	3
Mouth	1,810	10,750			5
Other oral cavity	1,650	1,830			
Thyroid	1,630	37,200			
Bones and joints	1,470	2,570			
Acute lymphocytic leukemia	1,400	5,760			
Childhood cancer†	1,380	10,730			
Hodgkin's lymphoma	1,290	8,510			
Small intestine	1,110	6,230			
Vulva	900	3,580			
Ureter	790	2,270			
Vagina/other genital (female)	770	2,160			
Anus/anal canal	710	5,290			
Chronic myeloid leukemia	470	5,050			
Testis	380	8,400			
Penis	300	1,290			
Eye	230	2,350			

* Incidence and mortality figures for all sites include cancers not listed in table, including nonepithelial skin cancers; other digestive, respiratory, oral, and endocrine cancers; other types of leukemia; and unspecified primary sites.

† Oral cancers include those of the nose, mouth, tongue, throat, and pharynx. Childhood cancers include leukemia, brain and nervous system, neuroblastoma, Wilms tumor, Hodgkin's lymphoma, rhabdomyosarcoma, retinoblastoma, osteosarcoma, and Ewing sarcoma in children ages 0-14.

‡ Other skin cancers—including squamous cell and basal cell skin cancers—occur in more than 1 million people in the United States each year, and are not included in this table.

§ Oral cancers include those of the nose, mouth, tongue, throat, and pharynx.

Figure 1-1. Cancer statistics: cancer incidence and mortality in 2009 and 5-year survival rates from 1975 to 2004 (5).

1.2. Tumorigenesis of Lung cancer

Cancers develop as a result of an accumulation of inherited and somatic mutations in oncogenes and tumor-suppressor genes (TSGs). For lung cancer, better understanding of oncogenes and tumor suppressor genes involved in the pathogenesis of lung cancer holds the promise of improving early diagnosis, increasing the number of available prognostic markers, and possibly leading to new effective therapies. However, our understanding of the genetic abnormalities underlying the development of lung cancer remains quite limited (6). Besides classical tumor suppressors, such as p53, p16, and retinoblastoma and the k-ras oncogene, recently a few lung-specific oncogenes have been identified. Specifically, molecular abnormalities have been found in EGFR, ERBB2, kRas, bRaf, MET, and ALK oncogenes that occur in mutually exclusionary fashion with each other (7-10), indicating the complementary roles of these oncogenes in lung carcinogenesis.

K-RAS: K-RAS belongs to the RAS family of oncogene and accounts for more than 90% of RAS mutations in NSCLC. K-RAS mutations have been detected in 15-30% of NSCLC, with the majority occurring in codons 12 and 13, in particular codons 12 (>90%). The mutations lead to impaired GTPase activity and subsequent constitutive activation of RAS signaling, which is downstream of EGFR leading to activation of proliferative and anti-apoptotic pathways such as the ERK signaling pathway. The prognostic significance of K-RAS mutations in NSCLC remains unclear. A 2005 meta-analysis involving 28 studies showed a worse survival for NSCLC with K-RAS mutations (11). However, in other studies including the multivariate analysis of BR. 21, K-RAS mutation was not prognostic for poorer survival (12).

Several lines of evidence suggest that K-RAS mutation is a predictor of resistance to EGFR-TKIs in NSCLC and indeed biological rationale would suggest the same. It was first reported in 2005 in a retrospective review of NSCLC patients treated with EGFR TKIs that patients with k-Ras mutant tumors were refractory to either erlotinib or gefitinib (7, 10). In the TRIBUTE study, patients with k-Ras mutations had shorter time to progression and overall survival when treated with chemotherapy plus erlotinib than those treated with chemotherapy alone or those with wild type k-Ras regardless of treatment type (3). The BR.21 study showed that a survival benefit from erlotinib was seen in patients with wild type k-Ras (Hazard Ratio(HR)=0.69, p=0.03) but not in patients with k-Ras mutations (HR=1.67, p=0.31), although the interaction *P* value was 0.09 (12). A recent systematic review and meta-analysis of 17 studies in advanced NSCLC (165 of 1008 patients with k-Ras mutations) showed that k-Ras mutations were significantly associated with resistance to EGFR TKIs with a specificity of 0.94 (13). Taken together, patients with k-Ras mutant tumors are very unlikely to respond to EGFR TKIs and accordingly k-Ras mutations can potentially serve as a negative biomarker to identify patients who are unlikely to derive major benefit from EGFR TKI therapy. On the other hand, despite strong evidence for k-Ras mutations to be a good predictor of the lack of benefit of EGFR-targeting monoclonal antibodies such as cetuximab and panitumumab in advanced colorectal cancer, the presence of k-Ras mutations was not found to predict lesser benefit from cetuximab in NSCLC patients in the previously listed FLEX and BMS099 trials (14).

The mutational status of k-Ras is usually investigated by direct sequencing (DS). This method depends on the tumor cellularity to be more than 20% to be reliable and can be challenging for small samples. To overcome these problems, more sensitive techniques have

been developed, including mutant-enriched sequencing (ME-sequencing). In one study involving 83 patients with lung adenocarcinoma, DS detected k-Ras mutations in 19% of tumors, whereas ME-sequencing identified mutations in 36% of samples (7, 15).

MET: Mesenchymal-epithelial transition factor receptor (MET), also known as hepatocyte growth factor receptor (HGFR) and located in chromosome 7, is a novel target in NSCLC (16). Deregulation of the HGF/MET signaling pathway can occur through HGF or MET overexpression (leading to paracrine and/or autocrine mechanisms for receptor activation), MET gene amplification, and mutations (17, 18). MET amplification in NSCLC, which has been associated with poor prognosis in early stage disease, is a relatively uncommon event occurring in 1-5% of unselected cases (19, 20). However, it has been recently shown that EGFR mutant NSCLCs with acquired resistance to erlotinib or gefitinib can display MET amplification or HGF overexpression (21-23). These events are seen in over 20% of TKI-resistant tumors and MET amplification is a pre-existing genetic abnormality that is selected after exposure to EGFR TKIs (24). Although MET copy number has been evaluated using quantitative genomic PCR methods in cell line models (21), it seems FISH is a more robust method to detect amplification of this gene in clinical samples (20).

The interplay between the EGFR and MET pathways is extensive with cross-signaling occurring at multiple levels of downstream targets such as the PIK3/AKT and MAP kinase pathways (24, 25). Preclinical data suggests that combination of EGFR and MET TKIs can be a treatment strategy for EGFR mutated NSCLC either to delay acquired resistance or to treat tumors with co-existing EGFR activating mutations and MET amplification (16, 24). Multiple clinical trials of MET TKIs (including XL-184, ARQ-197, PF-02341066, SGX-523)

(Table 1-1) in combination with EGFR TKIs are underway, and will likely determine if inhibition of MET signaling will play a role in future therapies for NSCLC (26).

Table 1-1. Classes and agents in development for treating NSCLC

<i>Class</i>	<i>Agents</i>
Irreversible, dual EGFR/HER2 TKs	BIBW 2992, neratinib (HKI-272), MP-412 (AV-412), PF-299804, AEE78, XL647
ALK TKI	PF02341066
Antiangiogenesis agents	Aflibercept (VEGF Trap), sorafenib, cediranib, Neovastat (Ae-941), motesanib (AMG 706), thalidomide, vatalanib (PTK787/ZK 222584), sunitinib, axitinib (AG-013736), enzastaurin, pazopanib (GW786034B), brivanib (BMS-582664), telatinib (BAY 57-9352), CP-547,632, XL184, CEP-7055, BIBF 1120
Dual EGF/VEGF receptor inhibitors	Vandetanib (ZD6474), AEE788, XL647
IGF1R antibody	CP751, 871
MET TKI	ARQ197, XL184
Mtor	CCI-779, RAD009
HSP90	17-AAG, 17-DMAG, CNF1010
Immunotherapies/vaccines	PF-3512676, talactoferrin, belagenpumatucel-L, MAGE-A3/QS-21, BLB25
Apoptosis-inducing agents	Oblimersen
Vascular-disrupting agents	AS1404 (DMXAA)
HDAC inhibitors	Vorinostat, LBH-589, PDX-101, MS-275
Cell cycle inhibitors	E7070
Radiation sensitizers	Efaproxiral (RSR13)
Retinoid X receptor agonists	Bexarotene
Microtubule stabilizers/inhibitors	Paclitaxel poliglumex, BMS-275183, ABT-751

ALK: The fusion of the anaplastic lymphoma kinase (ALK) gene with echinoderm microtubule-associated protein-like 4 (EML4), both in chromosome 2, is the most recent oncogene found in NSCLC (27, 28). In 2007, EML4-ALK fusion genes was first identified as a transforming oncogene in mouse 3T3 fibroblasts from DNA of lung cancer in a Japanese man with a smoking history (27, 28). Rarer ALK fusion partners (TFG-ALK and KIF5B-ALK) have also been identified in NSCLC (29, 30) (Fig. 1-2). ALK translocations or mutations have also been described in other tumor types including anaplastic large cell lymphoma, inflammatory myofibroblastic tumors and neuroblastoma (31). ALK is a transmembrane protein, which has a kinase domain with 3 tyrosine-containing motifs (tyrosines 1278, 1282, and 1283 within the activation loop) and a C-terminus with binding sites for Src homology-2 (SH-2) and phospholipase C- γ (PLC γ) (31). ALK is not usually expressed in the lung (27). In cell line and mouse models, EML4-ALK is highly oncogenic, activates the PIK3-AKT-mTOR, MAPK-MEK-ERK and STAT pathways and induces lung tumors (27, 32). Since many EML4-ALK variants have been described, a common nomenclature using the position of the breakpoints in the EML4 (E) and ALK (A) genes has been devised (33). The most common variant is E13A20 followed by E20A20 (Fig 1-2). ALK translocations are found in 3-6% of all NSCLCs, and are more frequent in adenocarcinomas (specifically those with signet ring), younger patients and never smokers with NSCLC (34-38). ALK translocations are usually mutually exclusive with EGFR or k-Ras mutations and predict for a poor response to EGFR TKIs in patients with advanced NSCLC (37).

In pre-clinical models, cells with EML4-ALK are sensitive to ALK inhibitors (36, 39, 40). Initial results of an expanded cohort of ALK translocated NSCLC patients treated with PF-

02341066, a dual MET/ALK tyrosine kinase inhibitor (TKI) developed by Pfizer (Table 1-1), at a dose of 250 mg twice a day as part of a phase I trial (NCT00585195) have been recently presented. The response rate exceeds 65% and despite short follow-up most patients have been treated for more than 8-10 months prior to progression (37). PF-02341066 has already entered phase II (single agent use, NCT00932451) and III (randomized trial of PF-02341066 versus pemetrexed or docetaxel for second line therapy, NCT00932893) registration human studies for NSCLCs with ALK translocations.

The methods of detection of ALK translocations in NSCLC are rapidly evolving. In the original reports, archival clinical specimens were tested using isolated RNA and reverse transcription-polymerase chain reaction (RT-PCR) amplifications specific to ALK and its gene fusion partner (27, 29, 41). Immunohistochemical (IHC) detection of ALK epitopes with commercially-available antibodies has been extremely difficult in lung cancers and has failed to confirm most cases positive by RT-PCR (29, 35). Strategies to improve the accuracy of the available ALK IHC assays, including amplification of the signal with a tyramide cascade (35) or the intercalation of an antibody-enhanced polymer (29), can enhance the sensitivity of IHC. Another detection method for ALK translocations is fluorescence in-situ hybridization (FISH). Multiple reports have demonstrated that break-apart probes can identify ALK translocations in NSCLC (29, 35, 37, 41). Specifically, a commercially available break apart probe (Vysis LSI ALK Dual Color, Break Apart Rearrangement Probe, Abbott Molecular, Des Plaines, IL) has been used as the screening test to detect ALK translocated patients in the setting of clinical trials (37) and this test was chosen by Pfizer and the Food and Drug Administration as the method of choice for screening tumors of NSCLC

patients for the registration phase III trial of PF-02341066. Therefore, it seems ALK FISH will enter the clinic as a standard test prior to IHC or RT-PCR.

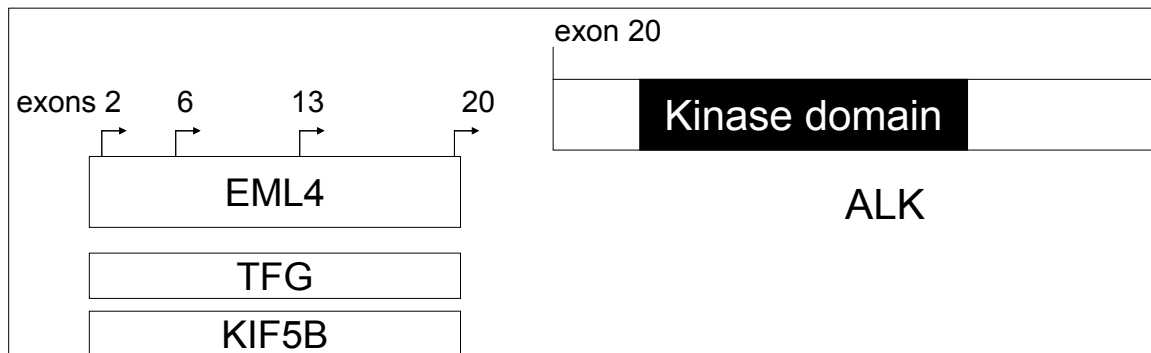


Figure 1-2. ALK fusion partners in lung cancer. Indicated by arrows are some of the common EML4 breakpoint fusion areas. In all cases described to date, the ALK gene is fused either at or around exon 20 and always prior to the kinase domain of ALK.

1.3. Targeted therapy for lung cancer

Current nonspecific, nonselective treatment of patients with NSCLC with chemotoxic chemotherapy results in only a modest increase in survival at the cost of significant toxicity to the patient; therefore, more effective, less toxic agents are needed (42). Recently various molecular targeted therapies have been developed for the treatment of lung cancers. EGFR-targeted and anti-angiogenesis (Bevacizumab (43)) drugs were developed and commonly used in current treatment of lung cancers. Bevacizumab is a recombinant humanized monoclonal antibody that binds and sequesters VEGF which is a pivotal mediator of angiogenesis.

A number of other targeted agents are at various stages of clinical research, such as irreversible EGFR TKI, dual TK inhibitors (Table 1-2), cyclo-oxygenase-2 inhibitors (44), the apoptosis promoter exisulind (45), proteasome inhibitors (46), bexarotene (47) and

vaccines (48). Future areas of research include Ras proto-oncogene inhibition, phosphoinositide 3-kinase inhibition (PI3K), histone deacetylase inhibition, and tumor suppressor gene replacement (49).

1.4. EGFR-targeted therapy in NSCLC

The EGFR is a well studied oncogene and belongs to a family of closely related growth factor receptor tyrosine kinases that includes EGFR (ErbB1), HER2/neu (ErbB2), HER3 (ErbB3), and HER4 (ErbB4) (50). Upon ligand binding, these receptors homodimerize or heterodimerize resulting in autophosphorylation, activation, and subsequent activation of intracellular signaling cascades such as the RAS/RAF/MEK/ERK, PI3K/Akt, and Jak/Stat signaling pathways (Fig. 1-3). This family has been shown to be important for proper regulation of many developmental, metabolic, and physiologic processes mediated by EGF, transforming growth factor- α , and multiple other ligands. In numerous cancers, including glioblastomas, breast cancer, and non-small-cell lung cancer, there is often a transforming deregulation of EGFR family kinase activity (51). EGFR can contribute to oncogenesis via at least three major mechanisms: overexpression of EGFR ligands, amplification of EGFR, and mutational activation of EGFR (52). EGFR is normally found on the surface of epithelial cells and is often overexpressed in a variety of human malignancies. Recent analyses have reported EGFR overexpression in 62% of NSCLC cases, and its expression is correlated with a poor prognosis (53), making EGFR and its family members prime candidates for the development of targeted therapeutics. Presence of EGFR-activating mutations represents critical biological factors for proper patient selection. There is a significant association between EGFR mutations, especially exon 19 deletion, and response to TKIs (54, 55).

Lung cancer cells with the EGFR activating mutations are dependent on survival signals transduced by the mutated EGFR receptors (so called oncogene addiction) and will die if this addictive function is removed or inhibited by a targeted drug, whereas the bystander normal cells with no addiction to the mutant EGFR are much less sensitive to the drug. EGFR-targeted drugs include tyrosine kinase inhibitor (TKI) (Table 1-1), such as erlotinib and gefitinib (Fig. 1-4), primarily used in lung cancer treatment and produced significant clinical responses in 10% to 30% of all NSCLC patients (56-58), and humanized monoclonal antibody against extracellular structure of EGFR such as cetuximab and panitumumab, primarily used in colorectal cancer and head/neck cancer (59).

A number of clinical studies have demonstrated an approximately 75% response rate to erlotinib or gefitinib in patients presenting with EGFR-mutant tumors (60, 61). The recent IPASS Phase III clinical trial that compared gefitinib with standard chemotherapy as a first-line treatment for Asian patients with lung adenocarcinomas, with no smoking history or only a light usage revealed that the determinant of clinical efficacy is the presence of an EGFR mutation and not the clinical background of the patient (62). Progression-free survival (PFS) of patients with EGFR mutation treated with gefitinib was around 10 months, whereas the PFS for those treated with platinum doublet chemotherapy was around 6 months. Overall, the frequency of these mutations is approximately 5% to 20% depending on the population studied and is significantly more common in East Asians, women, nonsmokers, and patients with adenocarcinoma histology (63). Recent and ongoing clinical studies demonstrate the feasibility of EGFR-driven patient selection. EGFR mutation testing is commercially available, and current research efforts will define how best to incorporate EGFR mutational status into treatment paradigms. EGFR amplification as determined by EGFR-fluorescent in

situ hybridization and overexpression are other predictive and prognostic factors undergoing intense investigation (64, 65).

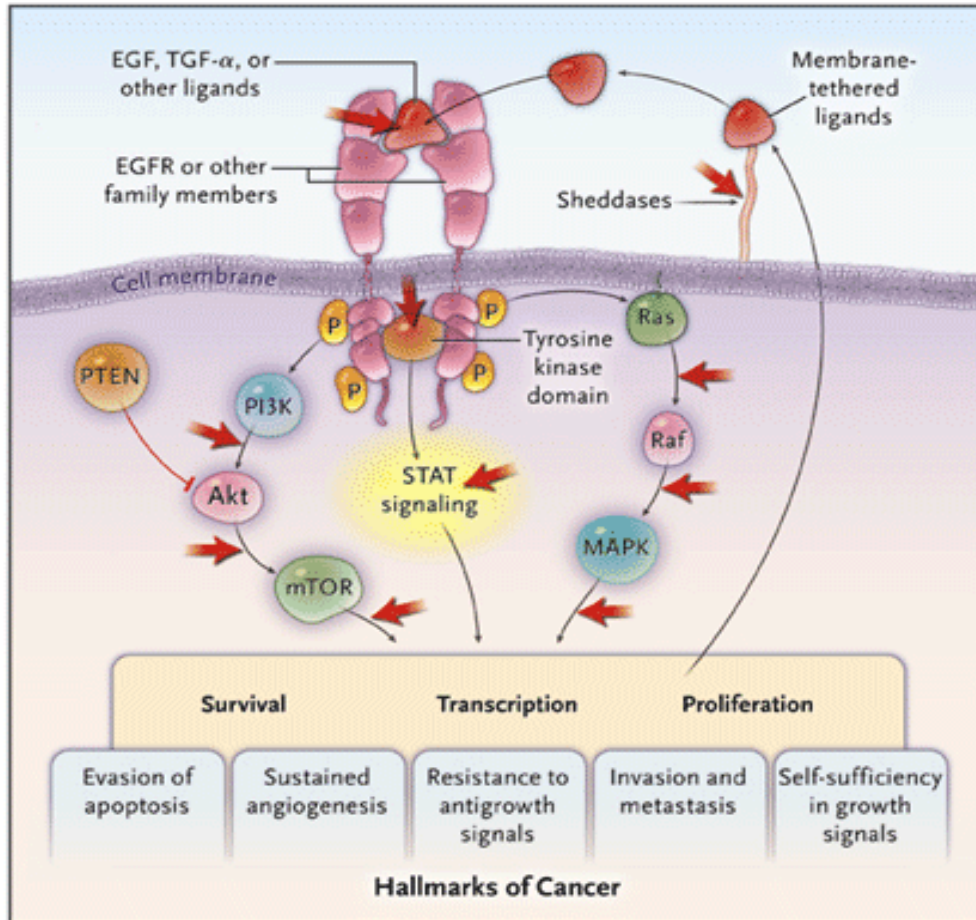


Figure 1-3. Targeting the EGFR Signaling Pathway. EGFR dimerization results in the activation of tyrosine kinases, which is followed by stimulation of three major signaling pathways, eventually leading to the activation of five of the six hallmarks of cancer (with the exception of limitless replication) (66). The classic mutations of the EGFR kinase domain result in ligand-independent activation of the pathway. EGFR TKIs interfere with the kinase activity of the gene and prevent downstream signaling. Activation of EGFR signaling also leads to an autocrine loop resulting from the formation and release of ligands. The ligands require release from their membrane-bound precursor forms by the activity of sheddase proteins. Red arrows indicate targets of therapies in current clinical use or in trials (67).

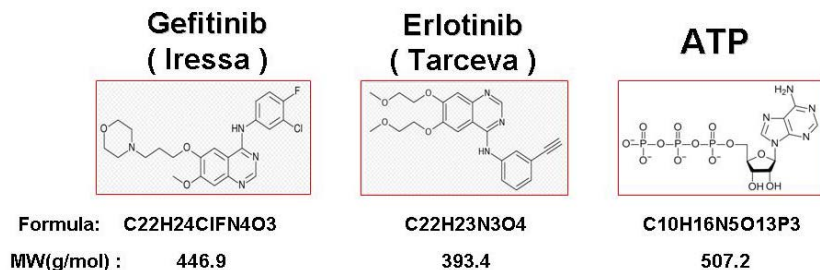


Figure 1-4. Comparison of structures of gefitinib, erlotinib, and ATP. Gefitinib and erlotinib have similar chemical structures as that of ATP, and smaller molecular weights (MW) than ATP. Gefitinib and erlotinib are therefore also called small molecule inhibitors.

1.5. EGFR activating mutations

The most prevalent and well studied EGFR somatic activating mutations occur in NSCLC. Recent clinical trials demonstrated EGFR mutations as a predictive factor of the efficacy of gefitinib compared with chemotherapy in the first-line setting (62). There are three broad classes of activating somatic mutations in EGFR-TK. These are categorized as class (i) in-frame deletions in exon 19, (ii) single-nucleotide substitutions that cause an amino acid alteration, and (iii) in-frame duplications and/or insertions in exon 20 (68). The majority of the documented activating kinase domain mutations can be classified as either class (i) or class (ii). Class (i) mutations are in-frame deletions that almost always include amino acid residues leucine-747 to glutamic acid-749 (LRE) and are located at the N-terminus of the kinase domain C-helix (Fig. 1-4). These deletions account for approximately 45% of the activating EGFR-TK domain mutations. Class (ii) mutations are dominated by a single point mutation in exon 21 that substitutes an arginine for a leucine at codon 858 (L858R). This point mutation has the highest prevalence of any single activating EGFR kinase domain point mutation and accounts for approximately 40-45% of EGFR-TK activating mutations (Fig. 1-4). An additional 4% of EGFR-TK activating mutations result in glycine-719 (G719) mutation to serine, alanine, or cysteine, and a further 6% have been found to be other

missense mutations. Class (iii) mutations account for the remaining 5% of EGFR-TK activating mutations. Although patients who present with “classical” activating EGFR-TK domain mutations, often respond to anilinoquinazoline-based small-molecule inhibitors, gefitinib, and erlotinib (69), evidence is accumulating that some of these activating mutations are more susceptible to treatment with certain kinase inhibitors than others (60, 70-72). The molecular-level reasons for these differences in response are not clear.

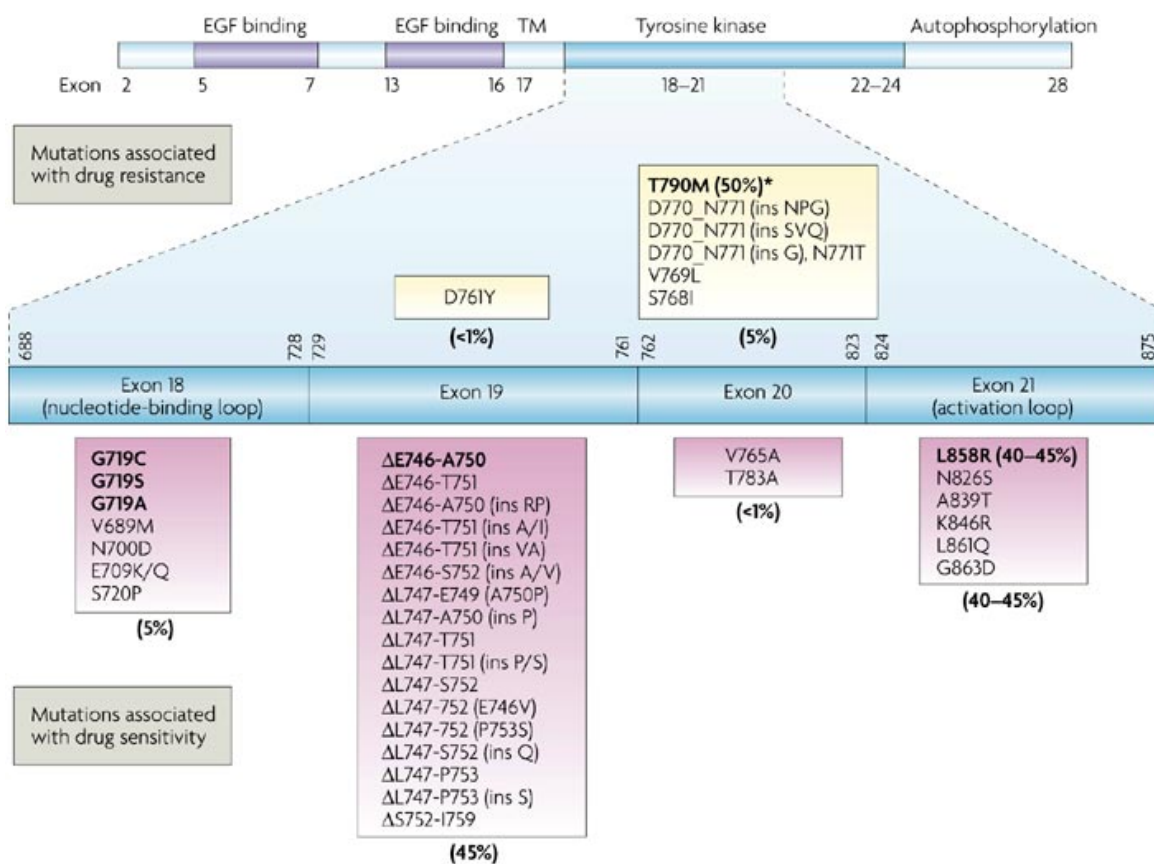


Figure 1-5. Gefitinib/erlotinib sensitizing or resistance mutations of EGFR in NSCLC.
All the EGFR mutations reported to date are on exon 18 through 21, affecting the tyrosine kinase domain of EGFR (9).

1.6. Molecular mechanisms of EGFR activation

The molecular mechanisms for improper activation of EGFR-TK and its targeted inhibition are being made increasingly clear by emerging insights of crystallographic structures of the EGFR TK domain.

Wild type EGFR activation: Protein kinase activity is generally regulated by the conformational state of the catalytic domain. The catalytic domain conformation, either active or inactive, governs the ability of the kinase to transfer a phosphate from bound ATP to peptide substrate, and thus controls downstream signaling. Regulation of protein kinases often includes two components: Firstly, the correct amino acid residues must be oriented to facilitate phosphate transfer; secondly, the peptide substrate binding site must not be occluded. Creation or removal of these conditions is often a critical step in the regulation of protein kinase activity. Two regions of kinase domains that are frequently reoriented to meet, or break, these conditions are the activation loop and the C-helix. The activation loop in an active kinase is extended away from the cleft to allow peptide substrate binding while a catalytic glutamate residue (part of the C-helix) forms an ionic interaction with a lysine residue that coordinates the α and β phosphates of ATP (73) (Fig. 1-5A). In the inactive conformation, the activation loop often changes conformation dramatically to preclude the binding of peptide substrate, while the C-helix rotates away, pulling with it the critical catalytic glutamate residue. A conformational equilibrium between the active and inactive kinase states is often modified by phosphorylation and dephosphorylation events, most frequently occurring on the activation loop of protein kinases. Usually receptor TK ligand (eg, cytokine, growth factor) binding to the extracellular portion of the receptor is followed by dimerization of the receptor. This allows transphosphorylation of the cytoplasmic kinase domains, on their activation loops and elsewhere, and results in consequent kinase activation and downstream signaling. In the EGFR family, however, ligand binding to the receptor does not result in immediate activation loop phosphorylation and activation loop phosphorylation is not required for kinase activity (74), thus, the mechanism of activation for EGFR has remained elusive. Recent studies propose a major EGFR activating mechanism to be driven by protein-protein interactions (75). In the inactive state of EGFR, ordered parts of the activation loop fold into a helix. In this conformation, the activation loop prevents C-helix

rotation toward the catalytic cleft, thereby keeping the catalytically important lysine and glutamate residues distant from one another. On ligand-induced dimerization of the EGFR, the intracellular kinase domains are brought into close proximity, allowing an asymmetric kinase domain dimer to occur. This tail-to-head interaction mediates an equilibrium shift to favor the active state. This knowledge may allow development of drugs to interrupt the asymmetric dimer formation and consequent activation, a potentially interesting avenue to explore as a therapeutic entry point for tumors overexpressing EGFR.

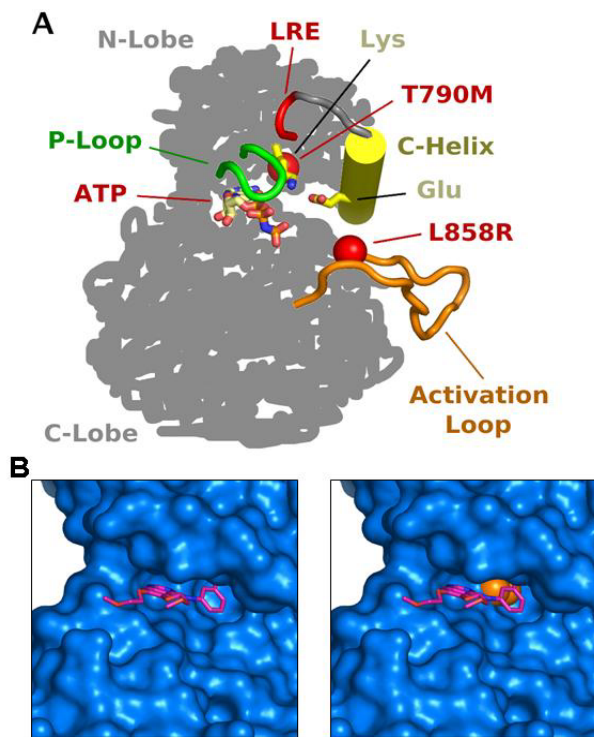


Figure 1-6. EGFR crystal structures illustrate atomic-level mechanisms of TKI sensitivity and resistance. A. Illustration of the active-state locations of the major structural regions of EGFR-TK. The position of ATP analog AMP-PNP in the catalytic cleft and the locations of the catalytic glutamic acid (Glu) and lysine (Lys) residues are shown. B. Left, Erlotinib snugly fits into the ATP-binding pocket of EGFR blocking its function; Right, T790M mutant EGFR has a bulkier 790 methionine (M, orange) protruding into the ATP-binding pocket, leads to steric hindrance disallowing erlotinib to bind and also leads to higher ATP affinity and thereby oncogenicity.

Activation of mutant EGFR: Improper EGFR activation for many of the somatic EGFR mutants frequently seen in NSCLC is likely mediated by a conformational shift between active and inactive states of EGFR-TK that favors the activated state, thereby leading to increased activation and consequent oncogenicity (76). EGFR L858R mutation accounts for approximately 40-45% of all EGFR-TK activating mutations in NSCLC. Examination of the active and inactive conformation EGFR-TK crystal structures reveals the side chain of leucine-858 (L858) to be in two dramatically different local environments (Fig. 1-5A). In the active state, L858 is exposed on the protein's surface; however, in the inactive state, L858 is found in a closely packed hydrophobic pocket. It is expected from the active and inactive EGFR-TK crystal structures that replacement of small hydrophobic leucine with a large polar arginine will destabilize the inactive EGFR-TK conformation and stabilize the active conformation. Because the L858R mutation favors a solvent-exposed surface environment for residue 858, this mutation will push the conformational equilibrium that exists between the active and inactive states toward the active, catalytically competent conformation. The atomic-level driving mechanisms for improper EGFR activation by somatic mutations will not be identical. This may result in differential responses to allosteric or ATP-competitive small-molecule kinase inhibitors and may have significant implications for drug design and therapeutic use. One potential clinical implication of the development of mutant-specific inhibitors could improve the therapeutic window. These drugs could potentially lead to reduced off-target adverse effects because they would have less specificity for the wild-type EGF receptor. This might lead to both better tolerance of these drugs and improved efficacy because stronger target inhibition could be accomplished. The development of such drugs could also assist in the selection of rational combination regimens that might limit the development of resistance further extending the clinical benefit of these compounds.

1.7. Mechanisms of TKI inhibition

EGFR activation by dimerization or other structural mechanisms generally results in intermolecular autophosphorylation of key tyrosine residues in the activation loop of catalytic TK domains via the transfer of gamma-phosphates from bound ATP. Small molecule TKIs, like gefitinib and erlotinib competitively interfere with the ATP-binding site on the active loop of the EGFR, therefore block EGFR activity. Importantly, the presence of

mutations in the TK domain correlates with tumor drug sensitivity to TKIs. Those activating mutations may result in conformational changes that lead to increased activity as well as TKI sensitivity based on the fact that both gefitinib and erlotinib preferentially bind to the active conformation of the receptor, the favored state in mutant molecules. For example, the binding affinity of gefitinib to the L858R mutant of EGFR is 20-fold tighter than that of wt-EGFR (77). This might explain in part why gefitinib or erlotinib leads to such a high likelihood of response in EGFR-mutant tumors, whereas their activity against tumors with EGFR overexpression is more modest.

Irreversible inhibitors, such as CL-387,785 and HKI-272 besides functioning as ATP-mimetic inhibitors similar to erlotinib and gefitinib also form a covalent bond with the crucial cysteine residues, Cysteine797 within EGFR or Cysteine805 within ERBB2, in the active site of the respective enzymes. Because only EGFR and ERBB2 rather than ERBB4 have cysteines at these corresponding positions, irreversible ERBB inhibitors show very high specificity for both wt and mutated forms of EGFR and ERBB2 (78).

1.8. Primary and Acquired resistance to EGFR-TKI in NSCLC

Although activating mutations of EGFR correlate with sensitivity to growth inhibition by first-generation reversible TKIs, such as erlotinib or gefitinib, resistance to them develops eventually in almost all of the patients (79). Resistance to EGFR inhibitors can be categorized as primary or acquired resistance. Primary resistance affects patients who are initially refractory to treatment; whereas acquired resistance affects patients who initially respond to treatment but subsequently experience a loss of response (80).

Certain molecular factors have been identified predictive of response, such as increased EGFR gene copy number and activating mutations within the EGFR TK domain (9, 63, 81). Thus, patients without these characteristics are more likely to present with primary resistance to EGFR TKIs. Multiple other mechanisms have been implicated in the primary resistance to EGFR TKIs, such as the presence of insertion mutations in exon 20 of EGFR that precludes

the binding of gefitinib and erlotinib to the EGFR TK domain conferring resistance. Although these mutations typically develop during treatment with EGFR inhibitors, they have been detected before drug exposure and are believed to have a role in primary resistance (69, 82, 83). In addition, mutations in the K-RAS oncoprotein, a downstream mediator of EGFR signaling, are significantly associated with primary resistance (3, 10, 84, 85)

The acquisition of resistance to the targeted inhibition of kinases in cancer is by now a well-documented phenomenon in several of cancer types. Although the importance of the cancer stem cell is firmly established for drug resistance, the etiology of acquired resistance is still the subject of some debate. In the case of EGFR-TK, there are currently only two documented resistance point mutations to the gefitinib and erlotinib, T790M (56, 86) and aspartic acid-761 to tyrosine (D761Y) (Fig. 1-4) (87). The T790M point mutation in EGFR kinase domain has been reported to be the most common secondary resistance mutation, accounting for about 50% of tumors relapsed from prior TKI therapy (86). The T790M mutation is located at the gatekeeper position in the kinase ATP-binding cleft, a structural location often documented to interfere with inhibitor binding; imatinib resistance mutations threonine-315 to isoleucine (T315I) in BCR-Abl (88) and threonine-670 to isoleucine (T670I) in Kit (89) are both at the same structural location. Substitution of the threonine at codon 790 with methionine results in an alteration of the topology of the ATP-binding pocket (Fig. 1-5B,C) and restores the affinity of the EGFR protein to ATP to be higher than the affinity of EGFR to EGFR-TKI, resulting in resistance to EGFR-TKI (90). The irreversible inhibitors of EGFR-TK, Cl-387,785 (Wyeth; Madison, NJ), HKI-272 (Wyeth), EKB-569 (Wyeth) and Cl-1033 (Pfizer) seem to effectively inhibit T790M (9) and are under clinical development for this indication (Table 1-1). These drugs covalently bind to cysteine-797 of EGFR, however,

atomic-level details of how they overcome the T790M mutation has not yet been described, we therefore eagerly await crystallographic descriptions of their modes of inhibition.

The second major mechanism of acquired resistance is the amplification of the MET oncogene that activates ERBB3/PI3k/AKT signaling in lung cancer (21). MET amplification was found in 4 (22%) of 18 lung cancer biopsy samples obtained from patients with acquired resistance to gefitinib or erlotinib (21).

Given that T790M and MET amplification collectively account for approximately 60% of the acquired resistance cases, there are clearly additional mechanisms that underlie resistance to EGFR TKIs. Other mechanisms that have been implicated in acquired resistance include altered EGFR trafficking (91), expression of insulin-like growth factor-1 (92), amplification of mutant EGFR or hyperactivation of components of downstream signaling pathways (93), and expression of the ABCG2 drug-efflux transporter (94).

Currently no adequate treatment option is available for patients who experienced erlotinib or gefitinib failure. A more clinically advanced dual EGFR/HER2 irreversible inhibitor Neratinib (HKI-272) has showed some promise for NSCLC patients who had progressed on erlotinib or gefitinib in a phase I preliminary study (95) and another multi-target TKI, XL647 with activity against EGFR, HER2, and VEGFR2 also has been reported disease control in patients who relapsed after earlier benefit from erlotinib or gefitinib, or who had a documented T790M mutation in a ongoing phase II trial (96) (Table 1-1).

1.9. Mutant EGFR signaling targets

Although somatic EGFR mutations have been reported to mediate oncogenic effects by altering downstream signaling and antiapoptotic mechanisms (97), the exact signaling events that result from these somatic mutations are not completely understood.

Our previous transcriptional profiling study of mutant EGFR target genes compared differentially expressed genes in the "resistant" gefitinib-treated and the "sensitive" CL-387,785-treated H1975 cells and identified cyclin D1 as one of the pivotal downstream target genes in EGFR-driven NSCLC cancers (98). Interestingly we also noted that several dual specificity phosphatases (DUSPs) were among the most highly and immediately regulated genes. Therefore we initiated a study focusing on the role of DUSP6 on NSCLC.

1.10. Oncogenic MAP kinase signaling and its terminators

Mitogen-activated protein kinases (MAPK) constitute a highly conserved family of kinases that relay information from extracellular signals to downstream effectors that control diverse cellular processes such as proliferation, differentiation, migration , survival and apoptosis (99). Three major groups of MAPK have been characterized in mammalian cells based on sequence similarity, differential regulation by agonists and substrate specificity. These are the classical p42 and p44 MAPKs (also known as extracellular signal-regulated kinases ERK2 and ERK1 respectively,) the c-Jun amino-terminal kinases JNK1, 2 and 3 and the four p38 MAPKs (α , β , δ and γ) (100). It is well known that abnormalities in MAPK signalling pathways have been implicated in a wide range of human cancers. The classical ERK pathway has long been associated with the ability of cancer cells to grow independently of

normal proliferation signals and is deregulated in approximately 30% of human tumors. Oncogenic abnormalities are also found in upstream components of the ERK MAPK signalling pathways, including overexpression or activating mutations of receptor tyrosine kinases (EGFR, Eph, etc), activating mutations of the Ras GTPase and mutations in the serine/threonine MAPK kinase kinase, B-Raf (101).

A balance between the activities of upstream activators and various negative regulatory mechanisms of MAPK signaling, which terminate its activation, determines its biological outcomes. It is now clear that a major point of control of MAPK signaling is through the activities of a family of MAPK phosphatases. The requirement for phosphorylation on both threonine and tyrosine residues for activating the MAPK mean that dephosphorylation of either residue is sufficient for kinase inactivation. This can be achieved by serine/threonine phosphatases, tyrosine specific phosphatases or by dual-specificity phosphatases and studies in a wide variety of model organisms from yeast to man have demonstrated that all three major classes of protein phosphatase can perform this task *in vivo*. However, by far the largest group of protein phosphatases that serve to specifically regulate the phosphorylation and activity of mammalian MAPKs are the dual-specificity MAPK phosphatases (MKPs) (102). The MKPs constitute a distinct subgroup of ten catalytically active enzymes so far within the larger cysteine-dependent dual specificity phosphatases (DUSP) family (103). While DUSP1 (MKP-1), DUSP4 (MKP-2), and DUSP9(MKP4), dephosphorylate both ERKs and p38 and JNK, the phosphatases DUSP5 (Hvh-3), DUSP6 (MKP-3), and DUSP7(MKP-X) specifically target ERK1/2 MAPKs (102).

1.11. DUSP6 structure and functions involved in tumorigenesis

DUSP6 is a cytoplasmic dual specificity protein phosphatase that specifically binds to and inactivates the ERK1/2 MAP kinases in mammalian cells. The highly conserved C-terminal domain of MKPs contains a tyrosine-specific phosphatase signature sequence HCXXXXXR at the active site, where cysteine acts as the enzymatic nucleophile and arginine interacts directly with the phosphate group on phosphotyrosine or phosphothreonine (58) (Fig. 1-6). The amino-terminal noncatalytic domain of DUSP6 contains a leucine-rich nuclear export signal (NES) necessary and sufficient for nuclear export of the phosphatase (104).

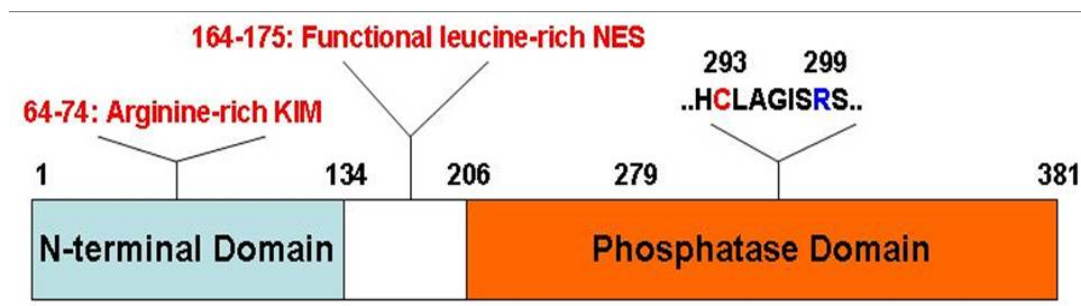


Figure 1-7. Structural Features of DUSP6. The highly conserved C-terminal domain of DUSP6 contains a tyrosine-specific phosphatase signature sequence HCXXXXXR at the active site. N-terminal region of DUSP6 has a specific arginine-rich kinase interaction motif (KIM) (105) and a functional leucine-rich nuclear export signal (NES).

DUSP6 has been identified as a potential novel tumor suppressor gene in pancreatic cancer since loss of DUSP6 expression might synergize with activating-mutated k-Ras resulting in increased activation of ERK1/2 MAP kinase and thus contribute to the development of the

malignant and invasive phenotype in pancreatic cancer. Furthermore, the reintroduction of active DUSP6 into cultured pancreatic cancer cells resulted in suppression of cell growth and increased levels of apoptosis (106). DUSP6 was identified as one of only three genes which are uniquely expressed in myeloma cells harboring a constitutively active mutant N-ras gene and is also overexpressed in human melanoma cell lines with potent activating mutations in B-raf and in breast epithelial cells stably expressing H-Ras (107-109), suggesting that the over-expression of DUSP6 seen in response to activating-mutated Ras or Raf might represent a compensatory increase in the negative feedback control of the ERK1/2 MAPK pathway, which lies downstream of these activated oncogenes. In support of this, the tetracycline-induced expression of a functional fusion protein between DUSP6 and green fluorescent protein (GFP) in H-ras transformed fibroblasts following injection into nude mice resulted in a large delay in tumor emergence and growth as compared to the untreated control group (110).

1.12. DUSP6 and NSCLC

Overall, the fact that DUSP6 functions as a natural negative regulator of oncogenic ERK MAPK signaling strongly suggest that it plays an important tumor suppressor role in a variety of cancer types. However, the function of DUSP6 is unknown in lung cancer, even though upregulated DUSP6 gene expression combined with other 4 genes was recently demonstrated to be associated with an increased risk of recurrence and decreased overall survival in the NSCLC tumors using risk scores based on microarray and decision-tree analyses of 125 frozen tumor specimens from patients with NSCLC (111). We believe that DUSP6 overexpression represents hyperactivation of the ERK pathway in this subset of

cancers and also hypothesize that progressive loss of DUSP6 expression can contribute to tumor progression and metastasis. Our previous work screened downstream mediators of oncogenic EGFR signaling in lung cancer by gene chip studies of 22,000 genes in tyrosine kinase inhibitor (TKI)-resistant lung cancer cell line H1975 and identified CyclinD1 and DUSP6 as one of the most highly and early downregulated genes upon TKI inhibition (98). Similarly, in microarray studies of downstream effectors of ErbB2 signaling, we found DUSP6 as one of the earliest and most highly downregulated genes in ErbB2-positive lung and breast cancer cells treated with EGFR and ErbB2 inhibitors. We plan to focus on the analysis of the functional role of DUSP6 on EGFR signaling in lung cancer. Better understanding of such MAPK phosphatases might identify novel critical effectors of EGFR activation/blockade and provide new targets for therapeutic interventions of lung cancer.

1.13. TAM family of RTK

Receptor tyrosin kinases (RTKs) are well known involved in tumorigenesis of NSCLC and served as targets for therapy. In NSCLC, only a few RTKs (e.g., EGFR and MET) have been thoroughly investigated (112).

Structure and function: TAM is a new class of the RTK subfamily that transduces crucial extracellular signals inside cells (113). TAM family of RTK includes Tyro3, AXL, and Mer, and is characterized by a conserved sequence within the kinase domain and adhesion molecule-like extracellular domains (Fig. 1-7). This small family of RTKs regulates an intriguing mix of processes, including cell proliferation, survival, cell adhesion and migration, blood clot stabilization, and regulation of inflammatory cytokine release. Genetic or

experimental alteration of TAM receptor function can contribute to a number of disease states, including coagulopathy, autoimmune disease, retinitis pigmentosa, and cancer (114).

The TAM family is distinguished from other RTKs by a conserved sequence, KW (I/L)A(I/L)ES, within the kinase domain and adhesion molecule-like domains in the extracellular region (Fig. 1-7A). More specifically, two immunoglobulin-like (Ig) domains and two fibronectin type III (FNIII) domains comprise nearly the entire ectodomain of each family member. These motifs are thought to be important in cell-cell contacts and mimic the structure of neural cell adhesion molecule (NCAM), which contains five Ig domains and two FNIII domains (115). Although the TAM receptors share extracellular motifs with some RTKs, the MET RTK family (composed of Met and Ron) is most closely related to the TAM family on the basis of amino acid sequence of the kinase domain (116). The MET and TAM receptors activate common signaling molecules resulting in similar functions (117).

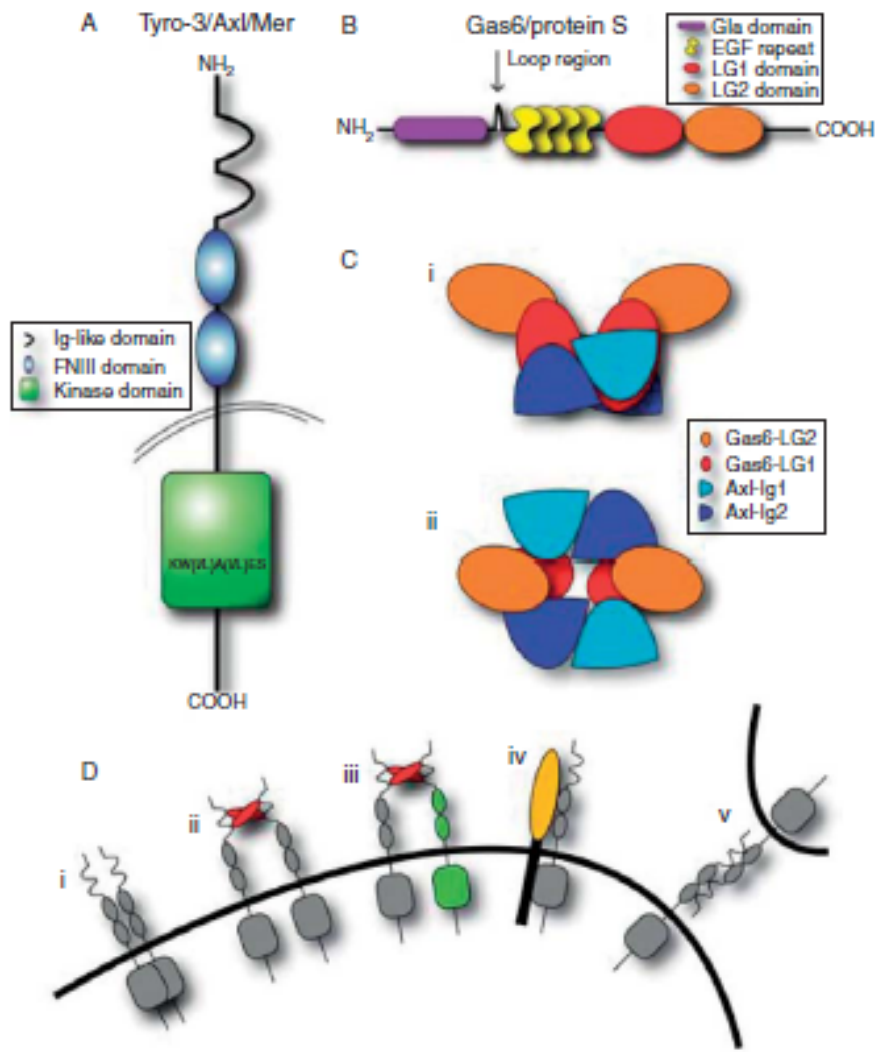


Figure 1-8. Structure, binding, and activation of TAM receptors by their ligands. (A) Domain organization of Tyro-3, Axl, and Mer. The conserved sequence within the kinase domain is indicated. (B) Domain structure of the TAM receptor ligands, Gas6 and Protein S. Protein S contains thrombin cleavage sites in the loop region and has not been shown to activate Axl. (C) Axl binds to Gas6 with 2:2 stoichiometries as shown from the side (i) and from the top (ii). No ligand/ligand or receptor/receptor contacts were observed in crystals of the minimal complex containing the two LG domains of Gas6 and the two Ig domains of Axl. (D) Possible means of TAM receptor activation include: (i) ligand-independent dimerization, (ii) ligand-dependent dimerization, (iii) heteromeric dimerization of two different TAM receptors, (iv) Heterotypic dimerization with a non-TAM receptor, and (v) trans-cellular binding of extracellular domains (114).

Although expression of TAM receptor mRNA has been observed in embryonic tissues (118-120), single, double, and even triple knockouts are viable without obvious signs of developmental defects at birth (121-123). These data suggest that the TAM RTKs are largely nonessential for embryogenesis. Conversely, TAM adult knockout mice develop diverse phenotypes in a wide range of tissues revealing some of the most prominent cellular functions of TAM receptors. In adult tissues, Tyro-3, Axl, and Mer exhibit widespread distribution with overlapping but unique expression profiles. Tyro-3 is most abundantly expressed in the nervous system, and is also found in ovary, testis, breast, lung, kidney, osteoclasts, and retina as well as a number of hematopoietic cell lines including monocytes/macrophages and platelets (124, 125). Axl is expressed ubiquitously (126), with notable levels found in the hippocampus and cerebellum as well as monocytes/macrophages, platelets, endothelial cells, heart, skeletal muscle, liver, kidney, and testis (124, 127). Within the hematopoietic lineages, Mer is expressed in monocytes/macrophages, dendritic cells, NK cells, NKT cells, megakaryocytes, and platelets. High levels of Mer expression are also detected in ovary, prostate, testis, lung, retina, and kidney. Lower levels of Mer are found in heart, brain, and skeletal muscle (124, 125, 127). Tyro-3, Axl, and Mer also display ectopic or overexpression in numerous cancers, including myeloid and lymphoblastic leukemias, melanoma, breast, lung, colon, liver, gastric, kidney, ovarian, uterine, and brain cancers (Table 1-2), and overexpression of TAM receptors is sufficient to transform cells. However, the pattern differs for each family member, e.g. Mer is found in lymphoid leukemia while Axl is not (125).

Table 1-2. TAM Receptor Expression in Human Cancers (114).

Cancer	Axl	Mer	Tyro-3
Myeloid leukemias (AML, CML)	+		+
Lymphoid leukemias (ALL)		Ect	
Erythroid leukemia	+		
Megakaryocytic leukemia	+		
Mantle cell lymphoma		+	
Multiple Myeloma			+
Uterine endometrial cancer	+		
Gastric cancer	+	+	
Colon cancer	+		
Prostate cancer	+	+	
Thyroid cancer	+		
Lung cancer	+		
Breast cancer	+	+	
Ovarian cancer	+		
Liver cancer	+		
Renal cell carcinoma	+		
Astrocytoma/Glioblastoma	+		
Pituitary adenoma		+	
Melanoma	+	+	
Osteosarcoma	+		
Rhabdomyosarcoma		+	

1.14. AXL signaling

AXL (Greek word anexelekto or uncontrolled), a transforming gene, was isolated from patients with chronic myelogenous leukemia (CML) (126). Ligand binding induces receptor dimerization and subsequent trans-autophosphorylation of tyrosine residues within the cytoplasmic domain of TAM (Fig. 1-7D). The autophosphorylation either leads to phosphorylation of other substrates or constitutes docking sites that recruit signaling molecules containing SH2, PTB, or other phosphotyrosine-binding domains allowing RTKs and other proteins to form macromolecular signaling complexes. Three tyrosine residues (Y-779, Y-821, and Y-866) within the C-terminal domain of Axl have been proposed as

potential autophosphorylation sites (128). These three sites, and in particular Y-821, mediate interaction of Axl with a number of signaling molecules including phospholipase C (PLC), PI3K, and Grb2. All of the interactions identified were dependent on Axl tyrosine kinase activity; however, the studies do not provide clear evidence that tyrosine residues 779, 821, and 866 are indeed sites of autophosphorylation. Future generation of phospho-site-specific antibodies will greatly aid our ability to address these types of questions.

An increasingly common theme in cell signaling literature is cross-talk between receptor systems. Ligand-independent heterotypic receptor dimerization of Axl with interleukin-15 receptor alpha (IL-15R α) has been reported in immortalized and primary fibroblasts (129) (Fig. 1-8D). Binding of IL-15 to IL-15R α , not Axl, leads to Axl-mediated phosphorylation of IL-15R α as well as Axl phosphorylation, although it is not known whether this is a direct action of the Axl kinase domain. Thus, IL-15 transactivates the Axl receptor and downstream signaling molecules, including PI3K, Akt, and ERK.

Gas6/Axl signaling promotes the growth and survival of numerous cell types. These effects are likely mediated by Gas6/Axl-induced activation of the MAPK/ERK and PI3K signaling pathways (Fig. 1-8). Gas6 also stimulates phosphorylation of Bad, a target of Akt commonly associated with prosurvival signaling (130, 131). Other survival pathways downstream of Gas6–Axl signaling via PI3K/Akt include phosphorylation of NF κ B, increased expression of antiapoptotic proteins such as Bcl-2 and Bcl-x L , and inhibition of proapoptotic proteins such as caspase 3 (132, 133). Another Gas6/Axl-induced survival pathway may involve PI3K activation of the small GTPases Rac and Rho as well as the downstream kinases Pak and JNK (130). A number of studies have suggested a physical association between Axl and

various signaling molecules. For example, coimmunoprecipitation experiments demonstrated association of EGFR/Axl chimera and several coexpressed GST fusion proteins in 293 cells. The same study also revealed that tyrosine 821 of Axl mediates binding to PLC γ , p85 α and p85 β subunits of PI3K, Grb2, Src, and Lck (128). Axl tyrosine 866 also contributes to PLC γ binding while tyrosine 779 may constitute a nonessential, low affinity site of interaction with p85 α and p85 β . The interaction of Src and Lck likely involves additional contacts *in vivo* as the Axl mutant receptor Y821F effectively coimmunoprecipitated both SFKs from 293 cells. Yeast two-hybrid experiments confirmed the interaction of Axl with PI3K and Grb2 while identifying four novel proteins which potentially interact with Axl: suppressor of cytokine signaling (SOCS)-1, Nck2, Ran-binding protein in microtubule organizing center (RanBPM), and C1-TEN (134).

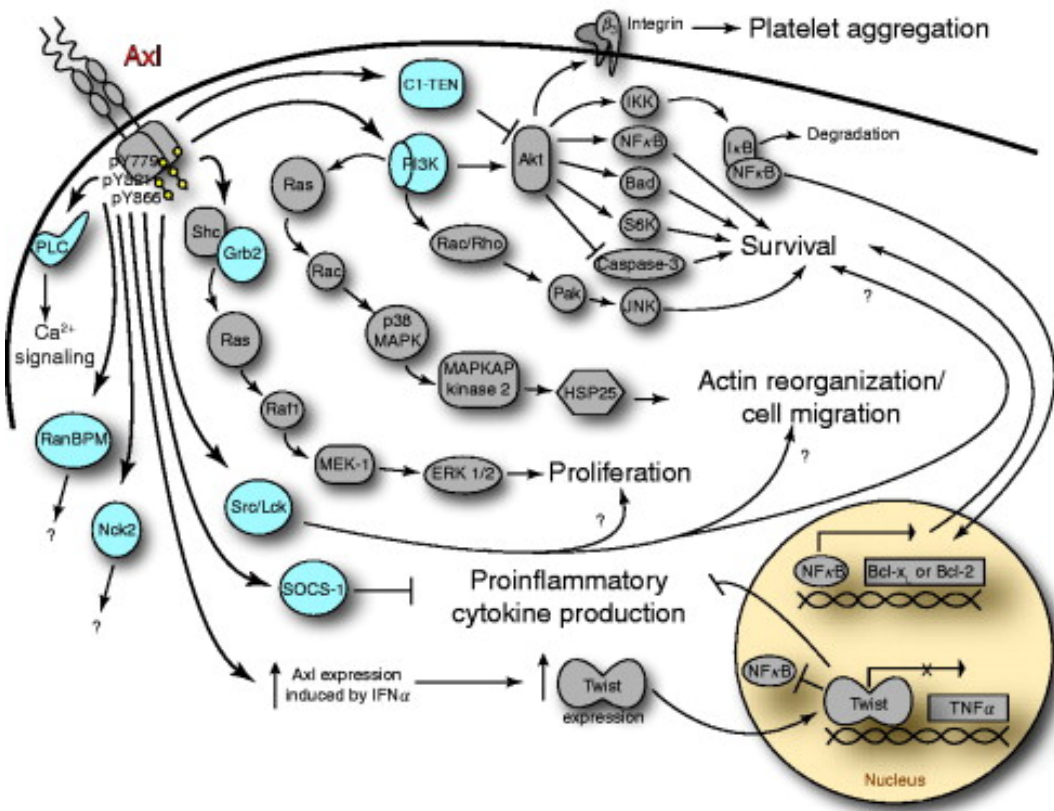


Figure 1-9. Axl signaling pathways lead to platelet aggregation, cell survival, proliferation, regulation of proinflammatory cytokine production, and regulation of the actin cytoskeleton. Molecules in blue have been shown to associate with Axl through either a direct or indirect interaction. Tyrosines 779, 821, and 866 of Axl are phosphorylated (yellow circles) and mediate interactions with a number of signaling molecules. It remains unknown whether these residues are sites of autophosphorylation or whether they are substrates for another protein tyrosine kinase (114).

1.15. Deactivation of AXL

Cellular control of RTK signal attenuation is important as aberrant or continued receptor signaling can lead to pathological states, including cancer. Cells have developed numerous methods for inactivation of RTKs, including antagonistic ligands, hetero-oligomerization with kinase inactive mutants, phosphorylation of inhibitory residues by other kinases, dephosphorylation of activating residues by phosphatases, and receptor endocytosis accompanied by ligand dissociation, receptor degradation, or both (135). Only a few of these pathways have been explored as possible mechanisms for TAM receptor regulation.

A putative tyrosine phosphatase C1-TEN has been shown to bind Axl and overexpression of C1-TEN correlates with reduced cell survival, proliferation, and migration of 293 cells (136), consistent with C1-TEN-mediated Axl inactivation. Soluble forms of Axl, produced by proteolytic cleavage and release of the ectodomain, can be detected in murine and human plasma, which binds to Gas6 and can act as a ligand sink and inhibit normal cellular functions of the full-length RTK (137). In the same regard, soluble TAM receptors may have therapeutic potential in pathological conditions, such as cancer, where TAM receptor activity is upregulated. Evidence supporting endocytosis as a mechanism of TAM receptor downregulation was provided by a report which demonstrated that Gas6 stimulates interaction of Axl with the ubiquitin ligase c-Cbl and ubiquitination of Axl (138), a process that has been demonstrated with other RTKs such as the EGFR. Clearly the study of mechanisms which regulate AXL receptor function and turnover is an area that needs further investigation.

1.16. AXL and cancer

Six primary cellular functions as “Hallmarks of Cancer” which normal cells acquire during oncogenesis have been proposed by: self-sufficiency in growth signals, insensitivity to antigrowth signals, limitless replicative potential, tissue invasion and metastasis, sustained angiogenesis, and evasion of apoptosis (66). The protooncogenic TAM receptors contribute

to at least three of these six fundamental mechanisms of malignancy. The oncogenic potential of TAM receptors is related to aberrant regulation of the same signaling pathways and cellular processes in which these receptors normally play a role. To date, no activating TAM receptor mutations have been associated with development of cancer. Numerous studies have demonstrated that TAM receptors are ectopically or overexpressed in a wide array of human cancers (Table 1-2). A global survey of oncogenic phosphotyrosine signaling revealed that AXL was highly phosphorylated in both NSCLC cell lines and tumors (30).

Overexpression of AXL is associated with poor prognosis and increased invasiveness of human cancers and has been reported in lung cancer, uterine cancer, breast cancer, ovarian cancer, gastric cancer, colon cancer, prostate cancer, thyroid cancer, liver cancer, renal cell carcinoma, AML, CML, erythroid leukemia, megakaryocytic leukemia, melanoma, osteosarcoma, and glioblastoma (Table 1-3) (114). Elevated Axl expression correlated with adherence, motility, and invasiveness of osteosarcoma cell lines selected for their high metastatic ability in an *in vivo* model of lung metastasis (139). Axl expression also correlated with invasiveness of lung cancer cell lines *in vitro* (140).

Recent studies report that increased expression of AXL may play a role in resistance to imatinib in gastrointestinal stromal tumors that express cKit (141) and in resistance to chemotherapy in AML (142) as well as in lung (143) and ovarian (144) cancers.

1.17. Potential AXL-targeted therapeutic applications

Axl RTK is expressed in lung adenocarcinoma cell lines, and the level of Axl expression correlates with the invasive ability of these cell lines in vitro. Ectopic overexpression of Axl in adenocarcinoma cell lines leads to increased formation of filopodia, migration, and drug resistance. Conversely, shRNA knockdown of Axl protein levels results in decreased migration (143)Stable shRNA knockdown of Axl significantly reduced tumor growth in a xenograft model of breast carcinoma (145). In the same study, inhibition of Axl with small interfering RNA in human umbilical vein endothelial cells (HUVECs) blocked endothelial tube formation in vitro suggesting that inhibition of Axl may restrict mechanisms of angiogenesis required for breast cancer tumor cell growth.

Additional mechanisms of TAM receptor inhibition could include soluble receptors that soak up available ligand or direct binding to the receptor by monoclonal antibodies. The latter might block activation, desensitize, or downregulate the surface receptor, or call in an immune response. MP470 is a potential Axl inhibitor but also blocks other tyrosine kinases within the same concentration range (141). Sensitivity of Mer and Tyro-3 to MP470 has not been tested. Thus, it is not clear how selectively this molecule inhibits Axl. Nevertheless, MP470 reduces the metabolic activity of an Axl-expressing, drug-resistant, gastrointestinal stromal tumor (GIST) cell line, suggesting that this novel drug may provide new treatment strategies for drug-resistant cancers. More recently the AXL small molecular inhibitors, XL880 (146) and R428 (147), and monoclonal antibody (113) against AXL have been demonstrated to have antitumor effects on AXL expressing cancer cells (Table 1-3) . In

addition, these studies further validate Axl as a therapeutic target for treatment of cancer and provide promising evidence for future selective small molecule inhibitors of TAM receptors.

Table 1-3. Axl as a Therapeutic Target

Inhibitor	Outcome
Axl-DN construct	Reduced glioblastoma growth and invasiveness <i>in vitro</i> and <i>in vivo</i> ; Increased overall survival after orthotopic implantation of glioblastoma cells containing Axl-DN
shRNA Axl construct	Decreased growth of breast carcinoma tumors in an ectopic xenograft model
Axl small molecule inhibitor (MP470)	May inhibit <i>in vitro</i> Axl kinase activity with limited selectivity; cytotoxic to gastrointestinal stromal tumor cells <i>in vitro</i>
Axl small molecule inhibitor (XL880)	Restore lapatinib sensitivity in lapatinib-resistant breast cancer cells with AXL overexpression
Axl small molecule inhibitor (R428)	Blocks tumor spread and prolongs survival in models of metastatic breast cancer. Synergizes with cisplatin to enhance suppression of liver micrometastasis.
AXL mAb	Attenuate NSCLC xenograft growth by downregulation of AXL expression, reducing tumor cell proliferation and inducing apoptosis.

CHAPTER 2

DUSP6 is an ETS1-regulated negative feedback mediator of oncogenic ERK signaling in lung cancer cells

Abstract

MAPK pathway signaling plays an important role in the majority of NSCLCs. In a prior microarray analysis of EGFR inhibition in NSCLC cell lines, we noted that several DUSPs were among the most highly and immediately regulated genes. DUSPs act as natural terminators of MAPK signal transduction and therefore, we hypothesized a tumor suppressive role via feedback mechanisms. In the current study, we focus on the assessment of DUSP6, a cytoplasmic DUSP with high specificity for ERK. We demonstrate that DUSP6 expression tracks in tandem with ERK inhibition and that regulation of DUSP6 is mediated at the promoter level by ETS1, a well-known nuclear target of activated ERK. Small interfering RNA knockdown in DUSP6-high H441 lung cancer cells significantly increased ERK activation and cellular proliferation, whereas plasmid-driven overexpression in DUSP6-low H1975 lung cancer cells significantly reduced ERK activation and cellular proliferation and promoted apoptosis. Also, DUSP6 overexpression synergized with EGFR inhibitor treatment in EGFR-mutant HCC827 cells. Our results indicate that DUSP6 expression is regulated by ERK signaling and that DUSP6 exerts antitumor effects via negative feedback regulation,

pointing to an important feedback loop in NSCLC. Further studies assessing the tumour suppressive role of DUSP6 and strategies aimed at modulation of its activity are warranted.

Introduction

Lung cancer, in particular NSCLC remains the leading cause of cancer deaths in both men and women in the USA (1). Despite recent progress in the diagnosis and treatment of NSCLC, survival remains poor (148). Improved outcomes are expected from better understanding of the molecular mechanisms underlying tumorigenesis. The ERK pathway plays an important role in oncogenesis and its overactivation is present in the majority of NSCLC, particularly those with EGFR and K-RAS mutations (101). EGFR belongs to the HER (or ErbB) family of growth factor receptor tyrosine kinases. Upon ligand binding, these receptors homodimerize or heterodimerize, resulting in autophosphorylation, activation and subsequent activation of intracellular signaling cascades, most notably the RAS-RAF-MEK-ERK pathway. Small-molecule EGFR TKIs, such as gefitinib and erlotinib, have shown benefit in patients with advanced NSCLC (57, 149). The majority of patients with EGFR TKI-responsive tumors carry activating mutations of EGFR, such as L858R or exon 19 deletions (150-152). Depending on the population studied, EGFR mutations occur on average in 10–20% of patients and identify a specific subset of patients highly dependent on oncogenic EGFR signaling (76). K-RAS mutations, which appear to be mutually exclusive of EGFR mutations, occur in ~20 to 30% of adenocarcinomas and their oncogenic potential is principally mediated via overactivation of ERK (10). Therefore, ERK signaling appears important or critical in at least 30–50% of NSCLC. However, little is known regarding regulation of ERK signaling. ERK1/2 is activated by dual threonine and tyrosine phosphorylation of a TEY motif by the MAPKs, mitogen-activated protein kinase kinase 1 (MEK1) and mitogen-activated protein kinase kinase 2 (MEK2). Inactivation of ERK1/2 is achieved by dephosphorylation of this TEY motif by distinct members of the DUSP family,

including both cytoplasmic (DUSP6, 7 and 9) and nuclear DUSPs (DUSP5) (153). The specific feedback regulatory mechanisms of ERK signaling in lung cancer cells have not been defined. Defects of feedback regulation are posited to contribute to oncogenesis, and an understanding of these mechanisms could provide novel strategies for biomarker and treatment development.

Clinical experience has shown that the majority of patients who initially respond to EGFR TKI treatment eventually develop resistance, most commonly via secondary mutations in EGFR such as T790M (56, 86). Irreversible EGFR inhibitors, such as CL-387,785 or HKI-272 can overcome the resistance conferred by this secondary mutation (78, 91, 154). H1975, an NSCLC cell line harboring the EGFR-T790M mutation, is highly resistant to gefitinib/erlotinib but sensitive to CL-387,785. Using microarray transcriptional profiling of H1975 cells exposed to CL-387,785 or gefitinib, we identified candidate downstream effectors of oncogenic EGFR signaling, specifically demonstrating that the transcription of several DUSPs is highly suppressed at 6 h by CL-387,785 but not by gefitinib (98). There are ~65 genes encoding a heterogeneous group of phosphatases broadly described as DUSPs (155). The structure of DUSP proteins confers activity for both phosphoserine/threonine and phosphotyrosine residues. DUSPs are characterized by a common structure, comprising a C-terminal catalytic domain and an N-terminal non-catalytic domain. These enzymes are defined by the active-site signature motif HCX5R, in which the cysteine residue functions as a nucleophile essential to catalysis. A subgroup of DUSPs, mitogen-activated protein kinase-specific phosphatases (MKPs) display distinct patterns of induction, subcellular localization and specificity for individual MAPKs and constitute a response network of phosphatases which attenuate MAPK-dependent signaling (153).

DUSP6 (previously called MKP-3) is a prototypical member of a subfamily of cytoplasmic MKPs, which includes DUSP7 and DUSP9 as well. These enzymes all display a high degree of substrate selectivity for ERK1/2 (156). DUSP6 has been shown to act as a central feedback regulator attenuating ERK levels in developmental programs (157, 158). The cytoplasmic localization of DUSP6 is mediated by a chromosome region maintenance-1-dependent nuclear export pathway. DUSP6 appears to play a role in determining the subcellular localization of ERK by serving as a bona fide cytoplasmic anchor for ERK, thereby mediating a spatio-temporal mechanism of ERK signaling regulation. Cytoplasmic retention of ERK requires both a functional kinase interaction motif and nuclear export site. DUSP6 null mice demonstrate enhanced ERK1/2 phosphorylation leading to increased myocyte proliferation and cardiac hypercellularity (159). A recent *in vivo* study identified DUSP6 as a negative feedback regulator of fibroblast growth factor-stimulated ERK signaling during murine development (158). Several *in vitro* studies have demonstrated that DUSP6 acts as a negative regulator of fibroblast growth factor receptor signaling and endothelial cell platelet-derived growth factor receptor signaling via termination of ERK activation (160, 161). The DUSP6 gene is localized to 12q21–q22, a chromosomal region showing frequent loss of heterozygosity in pancreatic cancer (162). Immunohistochemical staining demonstrated reduced DUSP6 expression in about half of all invasive pancreatic carcinomas, whereas expression was preserved in precursor lesions suggesting that loss of DUSP6 plays a role in tumor progression (163, 164). Similarly, loss of DUSP6 expression mediated by oxidative stress-mediated degradation was also noted in ovarian cancer and correlated with high ERK1/2 activity (165). The functional and clinical significance of DUSP6-mediated regulation of ERK signaling in lung cancer has not been carefully

investigated. In the current study, we examine effects on DUSP6 expression by EGFR/ERK inhibition and study its negative feedback regulation of ERK activation in NSCLC cell lines.

Materials and Methods

Cell lines. The following NSCLC cell lines were obtained from American Type Tissue Collection (Manassas, VA): HCC827, PC9, H1975, A549, H441, H358, Calu-3, H1838, H1650, H125, H1703, H23, H2228, Calu-1, Calu-6, SW900, SK-LU-1, H1993, H1734, H520, SK-MES-1, H157, H460 and H3255. Normal human airway epithelial cell line NuLi-1 cells were provided as a gift from Dr Jeffrey Kern and cultured in F-12/Dulbecco's modified Eagle's medium (1:1 ratio) media with 10% fetal bovine serum (FBS). Lung cancer cells were grown in RPMI 1640 supplemented with 10% FBS and 1x Antibiotic/Antimycotic (Invitrogen, Carlsbad, CA) and were in the logarithmic growth phase at initiation of all experiments. EGFR inhibitor erlotinib was obtained from Selleck Chemicals (Houston, TX); irreversible EGFR inhibitor CL-387,785 and MEK1/2 inhibitor U0126 were purchased from Calbiochem (San Diego, CA). Drugs were dissolved in dimethyl sulfoxide (DMSO) at 10 mM and stored at -20°C. The final DMSO concentration in all experiments was <0.5% in medium.

Immunoblotting. Cells were serum-starved overnight and whole cell lysates were analyzed by western blotting as described previously (14). Antibodies to DUSP6, ETS1, ETS2 and hemagglutinin (HA) tag were purchased from Santa Cruz Biotechnology (Santa Cruz, CA). Antibodies against phosphor-EGFR at different tyrosine sites, total-EGFR, phosphorylated-ERK1/2, total-ERK1/2, poly ADP ribose polymerase (PARP) and Glyceraldehyde-3-phosphate dehydrogenase (GAPDH) were purchased from Cell Signaling Technology (Boston, MA).

Immunohistochemistry. Formalin-fixed primary lung tumor tissue sections were deparaffinized and rehydrated and incubated with 0.6% hydrogen peroxide in methanol,

followed by staining using the R.T.U Vectastain Universal Quick Kit (Vector Laboratories, Burlingame, CA). Antigen retrieval treatment with sodium citrate (10 mM, pH 6.0) was used for the detection of DUSP6, whereas a specific retrieving reagent (Dako, target retrieval solution, pH 9.0) was used for the detection of P-ERK1/2. Rabbit polyclonal antibody specific against DUSP6 (Santa Cruz Biotechnology) was used at a dilution of 1:100 (optimal dilution determined in serial dilution studies) and a rabbit antibody against P-ERK1/2 was used (Cell Signaling Technology) at a dilution of 1:1000 for overnight incubation at 4°C followed by hematoxylin nuclear counterstaining. The intensity of the staining of DUSP6/P-ERK was scored by a pulmonary pathologist (A.C.B.) as 0/1 (non-detectable/weak) versus 2 (strong staining).

Quantitative reverse transcription–polymerase chain reaction assay. Total RNA was collected from cultured cells using PureLink Micro-to-Midi Total RNA Purification kit (Invitrogen). Complementary DNA was synthesized and reverse transcription–polymerase chain reaction (PCR) was performed as described previously (166). The primers used for DUSP6 quantitative reverse transcription–PCR were sense 5'-GAGTCTGACCTTGACCGAGACCCAA-3' and antisense 5'-TTCCTCCAACACGTCCAAGTTGGTGGAGTC-3'.

Plasmid constructs and cellular transfection. Original vector containing the complementary DNA sequence of human DUSP6 was purchased from OPEN Biosystems (Huntsville, AL) and modified with an HA-tag at the C-terminus by overlapping PCR to distinguish plasmid derived from native protein. An enzyme-dead DUSP6 expression construct was generated via 293 Cysteine to Glycine (C293G) point mutation (167, 168) using the QuikChange Site-Directed Mutagenesis XL II kit (Stratagene, La Jolla, CA). The

accuracy of all constructs was confirmed by direct DNA sequencing. The C293G mutation was constructed using the following oligonucleotides: sense 5'-TGGTGTCTTGGTACATGGCTTGGCTGGCATTAGCC-3' and antisense 5'-GGCTAATGCCAGCCAAGCCATGTACCAAGACACCA-3'. Both variants were subcloned into the pcDNA3.1 backbone vector. COS7 cells were transiently transfected with one of three expression vectors as follows: wild-type DUSP6 (pcDNA3.1-DUSP6), enzyme-dead DUSP6 (pcDNA3.1-DUSP6-CG) with C293G mutation or empty pcDNA3.1 vector (pcDNA3.1-EV), using Fugene 6 according to the manufacturer's protocol (Roche, Indianapolis, IN). Whole cell lysates for immunoblotting were collected at indicated time points after transfection to confirm appropriate plasmid DUSP6 expression. H1975 and HCC827 cells were transfected by identical means. Stably transfected subclones were selected with G418 at a concentration of 500 µg/ml starting 48 h posttransfection.

MTS cell growth assay. H1975 stable transfectants were seeded at a density of 6000 cells per well in 96-well plates in RPMI 1640 containing 10% FBS overnight and then maintained in 0.5% FBS media for 3 days. Viable cell numbers were determined using MTS assay kit according to the manufacturer's protocol (Promega, Madison, WI). Each assay consisted of five replicate wells.

BrdU and annexin/propidium iodide assays. For both assays, samples were analyzed on a fluorescence-activated cell scan cytometer EPICS XL MCL (Beckman Coulter, Miami, FL). Bromo-deoxyuridine (BrdU) cell proliferation assay was performed according to manufacturer's instructions (FITC BrdU Flow Kit, BD Pharmingen, San Diego CA). Briefly, H1975 stably transfected subclones were cultured in the 0.5% serum media for 3 days, then pulse labeled for 60 min with 10 µM BrdU, collected by trypsinization and washed with

phosphate-buffered saline, stained with fluorescent anti-BrdU antibody, counterstained with 7-amino-actinomycin D for total DNA content and analyzed by flow cytometry. Annexin/propidium iodide (PI) apoptosis assay was performed according to the manufacturer's instructions (Annexin V-FLUOS staining kit, Roche). Briefly, H1975 stably transfected subclones were cultured in 0.5% serum media for 3 days, collected by trypsinization and washed with phosphate-buffered saline, stained with annexin/PI and analyzed by flow cytometry. In synergism studies, HCC827 cells were transiently transfected with plasmid constructs 24 h prior to 48 h treatment with erlotinib, followed by annexin/PI staining as above.

Small interfering RNA knockdown. Knockdown of DUSP6 or ETS1 was performed using specific small interfering RNA (siRNA) pools targeting DUSP6 or ETS1 (SMARTpool) purchased from Dharmacon RNAi Technologies (Thermo, Rockford, IL). SiGENOME Non-targeting siRNA Pools and siGLO Lamin A/C Control siRNA served as negative and positive control, respectively. Introduction of siRNA was performed with DharmaFect1 according to the manufacturer's instructions (Thermo). Levels of DUSP6 or ETS1 knockdown at different time points were assessed by immunoblot analysis in pools of transfected cells.

Luciferase reporter assay. HCC827 cells were grown to 40–50% confluence in triplicates on six-well plates and then transfected using Fugene HD (Roche) with 50 ng of pGL4.74-Renilla luciferase and one of the following plasmids: 0.5 µg of pGL3Basic-DUSP6-Firefly luciferase construct containing 508 bp promoter sequence (−359 to −866) upstream of the DUSP6 gene start codon, generously provided by Dr Stephen M.Keyse, Ninewells Hospital and Medical School, Dundee, UK (160), or 0.5 µg of pGL3Basic empty vector. After 24 h of

transfection, cells were treated with 1 µM erlotinib or DMSO as a vehicle control for 6 h. Cell extracts were prepared and luciferase assays were run as described previously (166).

Chromatin immunoprecipitation assay. HCC827 cells were starved with serum-free media overnight, then treated with 1 µM erlotinib or 0.01% DMSO control for 6 h, followed by chromatin immunoprecipitation assay according to manufacturer's instructions (Upstate Biotechnology, Lake Placid, NY). Briefly, cells were cross-linked with 1% formaldehyde, then chromatin was extracted, sonicated and immunoprecipitated with 5 µg of ETS1 or ETS2 antibody (Santa Cruz Biotechnology) at 4°C overnight with rotation. Prior to immunoprecipitation, 10% of each nuclear extract was set aside as input chromatin DNA for use in assay controls. Cross-linking of immunoprecipitated and input samples was reversed by heating at 65°C in the presence of 5 M NaCl for 4 h followed by DNA isolation using QIAquick PCR Purification Kit (QIAGEN, Valencia, CA). Immune complexes were collected by incubation with supplied protein A agarose/Salmon Sperm DNA beads for 1 h at 4°C with rotation. Binding of ETS1/2 to the DUSP6 promoter was assessed by nested PCR and with primer sets amplifying ETS1/2-binding site regions spanning -844 to -404 bp (441 bp in size) and -743 to -487 bp (257 bp in size) of the DUSP6 promoter. An unrelated anti-HA antibody and an unrelated primer pair was used to amplify the sequence downstream of the ETS-binding site, +995 to +1311 bp (317 bp) to serve as control. PCR products were analyzed using a 1% agarose gel run in 1x TAE and stained with ethidium bromide.

Electrophoretic mobility shift assay. All oligonucleotides probes were obtained from Invitrogen. 5'-Biotin-labeled and identical unlabeled oligonucleotide probes, corresponding to the ETS1/2-binding sequences in the DUSP6 promoter region, were used as follows: (sense) 5'-GGCTTATCCGGAGCGGAAATTCCCTTTC and (antisense) 5'-

GAAAGGAATTCCGCTCCGGATAAGCC. Two mutant oligonucleotide probes were generated by introduction of mutations within the 508 bp DUSP6 promoter sequence as follows (160): core ETS-binding site GGA (underlined) mutated to TGA; palindromic ETS-binding site TCC (underlined) mutated to GAA. Nuclear extracts were collected from HCC827 cells in presence of erlotinib (1 μ M) or 0.01% DMSO control for 6 h. Double-stranded DNA annealing was achieved by incubating complementary pairs of oligonucleotide probes at 95°C for 5 min followed by slow cooling to room temperature. Binding reactions were performed using Pierce LightShift Chemiluminescent EMSA Kit as described previously (166).

Statistical analysis. Fisher's exact test was used to estimate association between categorical measurements. Differences in a continuous measurement between two or more groups were examined by χ^2 test. All tests were two sided and P-value < 0.05 was considered statistically significant.

Results

DUSP6 protein expression correlates with ERK signaling activation in lung cancer cell lines and primary NSCLCs

We assayed cellular expression of DUSP6 by immunoblot using an anti-DUSP6 antibody in 24 NSCLC cell lines and a normal human airway epithelial cell line (NuLi-1), correlated to total and P-ERK expression to assess ERK-activation (Fig. 2-1a). We observed DUSP6 expression in the majority of lung cancer cell lines. Although DUSP6 levels varied widely among different cell lines, a positive association between DUSP6 expression and ERK activity was observed ($P = 0.011$) (Fig. 2-1c) . Only 15.4% (2/13) of cell lines with low P-ERK expression had high expression of DUSP6, whereas 72.7% (8/11) of cell lines with high P-ERK expression had high expression of DUSP6. Next, we performed an immunohistochemical study of DUSP6 and P-ERK expression on 48 primary, human non-small cell lung tumors. As expected, no nuclear expression of DUSP6 was detected consistent with exclusive cytoplasmic localization of this protein. Altogether, 15/48 (31%) of tumors showed strong expression of DUSP6, whereas 11/48 (23%) of the tumors demonstrated strong cytoplasmic and 19/48 (40%) strong nuclear P-ERK staining (Fig. 2-1b). Analogous to our cell line data, a statistically significant correlation was found between cytoplasmic P-ERK and DUSP6 expression ($P = 0.022$) (Fig. 2-1c), whereas a trend was also observed between DUSP6 expression and nuclear P-ERK ($P = 0.051$) (Fig. 2-1d). Most strikingly, 13/15 (87%) specimens with strong DUSP6 expression showed strong P-ERK staining in either cytoplasmic or nuclear localization as compared with only 11/34 (32%) samples with weak DUSP6 had strong cytoplasmic or nuclear P-ERK ($P < 0.001$) (Fig. 2-1e).

These results altogether show a close correlation between ERK pathway activation and DUSP6 expression in NSCLC.

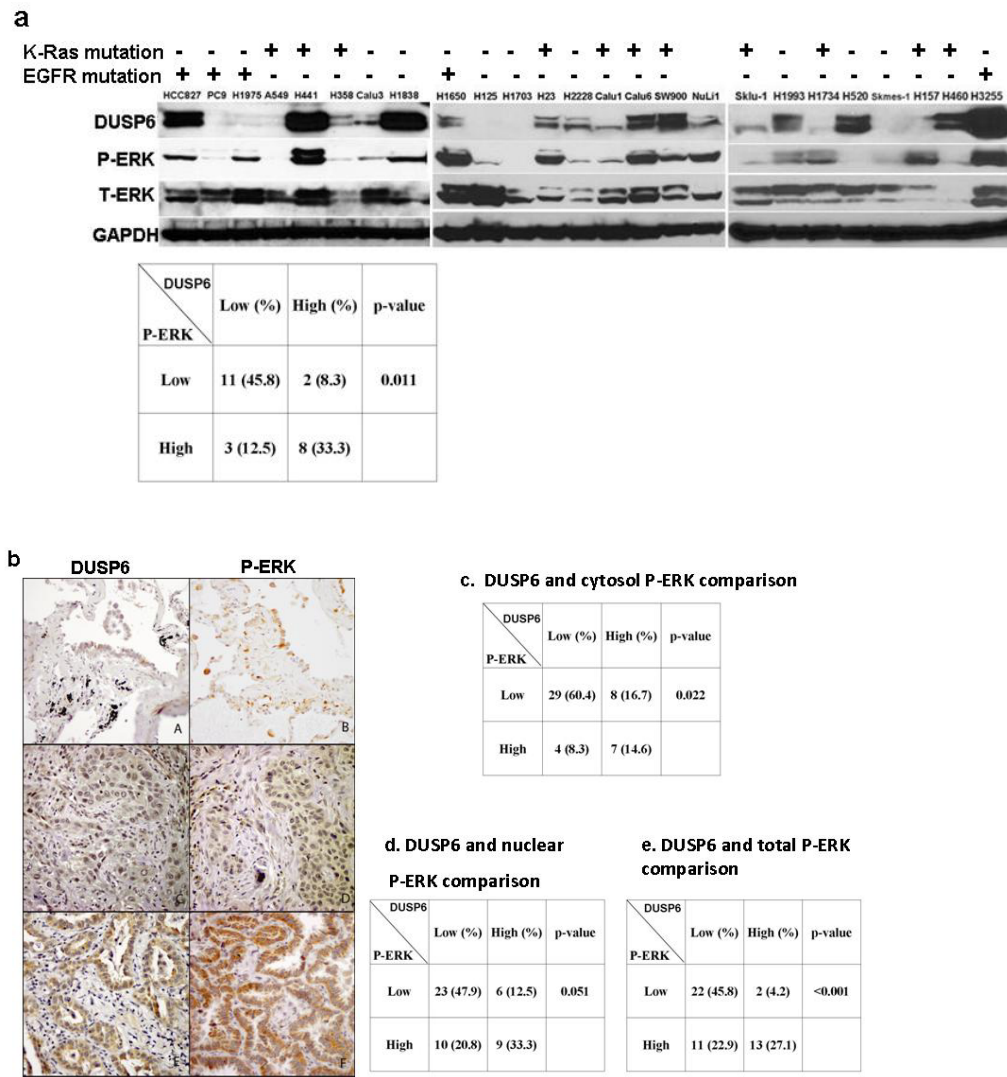
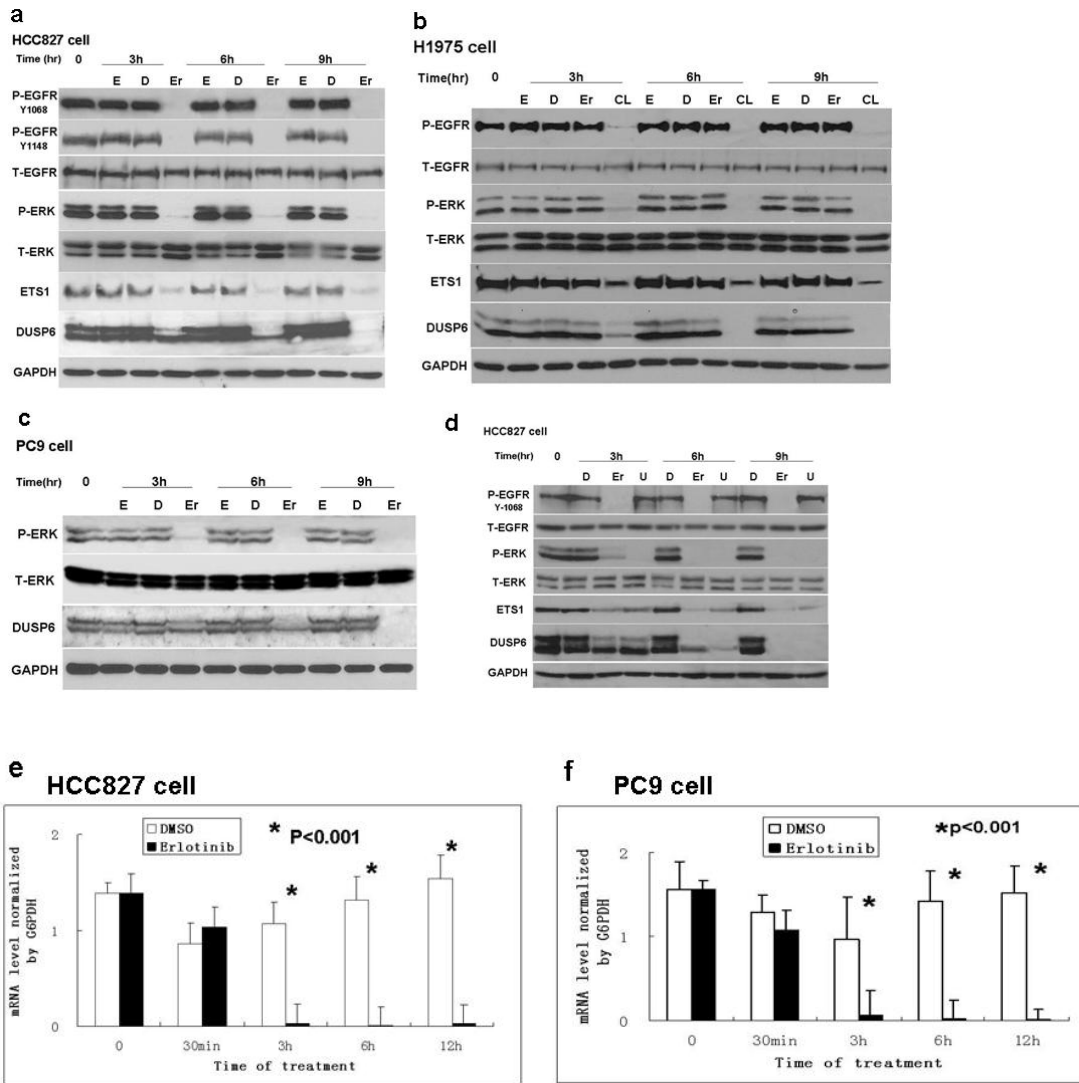


Figure 2-1. DUSP6 expression in NSCLC cell lines and primary patient samples. (a) Cells were plated and starved with serum-free media overnight, then lysed with 10% TCA lysis buffer, followed by immunoblotting for DUSP6, phosphor-ERK, total ERK, and GAPDH. Mutation status of EGFR and K-Ras was annotated for all the NSCLC cell lines. (b) Expression of DUSP6 and phospho-ERK in 48 primary NSCLC tumors. The expression of DUSP6 and P-ERK in normal lung epithelia (Panels A and B) and primary lung cancers was examined by immunohistochemistry. Cytoplasmic immunoreactivity of DUSP6 and P-ERK expression were subdivided into 2 categories: low (Panels C and D) and high (Panels E and F, A-F, DAB immunohistochemistry, original magnification $\times 100$). Fisher's Exact Test was used for the statistical analysis of the correlation between DUSP6 and P-ERK levels for both the cell lines and patient samples.

DUSP6 expression is downregulated by EGFR inhibition in EGFR-dependent NSCLC cell lines

HCC827 and PC9 are NSCLC cell lines that carry an EGFR exon 19 deletion and thereby are highly sensitive to gefitinib or erlotinib. H1975 cells harbor the T790M resistant mutation but are sensitive to the irreversible EGFR inhibitor CL-387,785. Downregulation of DUSP6 strongly correlated with effective inhibition of EGFR as well as ERK activation demonstrated by diminished P-EGFR and P-ERK expression in EGFR-dependent cell lines HCC827 (Fig. 2-2a), H1975 (Fig. 2-2b), and PC9 (Fig. 2-2c). Of note is that the anti-DUSP6 antibody detects two distinct protein bands corresponding in size to translation products initiating at the first ATG and the second ATG (Met14) as previously reported (169). Our studies reveal that the larger of these two proteins is more rapidly suppressed by TKI treatment; the mechanism is currently unclear. Quantitative reverse transcription-PCR demonstrated downregulation of DUSP6 transcription following erlotinib treatment in both HCC827 (Fig. 2-2e left) and PC9 cells (Fig. 2-2e right), in line with our prior transcriptional profiling findings in CL-387,785 treated H1975 cells (170). DUSP6 downregulation was also observed upon treatment of HCC827 cells with the MEK1/2 inhibitor U0126 accompanied by effective inhibition of P-ERK but no changes in EGFR activation status suggesting that the regulation of DUSP6 expression occurs downstream of EGFR (Fig. 2-2d).



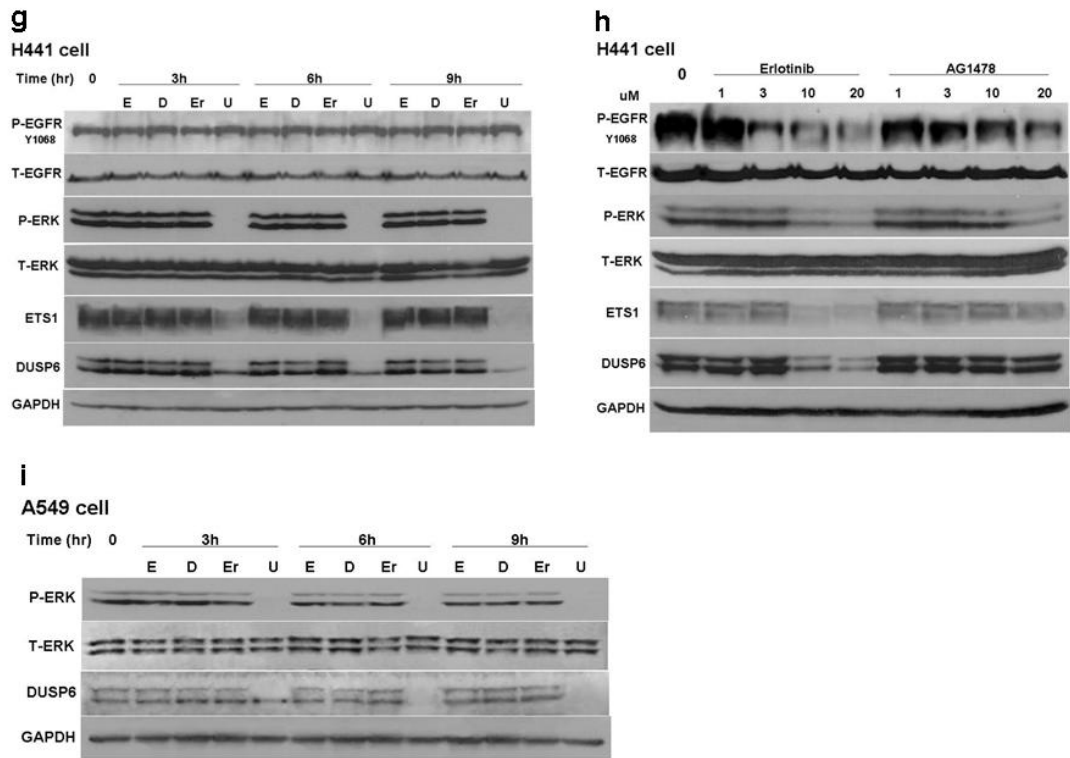


Figure 2-2. DUSP6 is regulated by EGFR/ERK inhibition in NSCLC cell lines. Protein expression levels were assayed by immunoblot for phosphor-EGFR at indicated tyrosine sites, total-EGFR, phosphor-ERK, total-ERK, ETS1, DUSP6 and GAPDH demonstrating suppression of DUSP6 followed by inhibition of activated ERK (P-ERK) and ETS1 levels in the presence of appropriate drug for each of the following cell lines: HCC827 cells treated with erlotinib(a) or U0126 (a MEK1/2 inhibitor)(d) , H1975 cells treated with CL-387,785 (an irreversible EGFR inhibitor)(b), PC9 cells treated with erlotinib(c) and H441 cells treated with erlotinib or U0126 (g, h), and AG1478 (specific EGFR inhibitor)(h), and A549 cells with erlotinib and U0126(i). Cells were starved overnight with serum-free media, then treated with drug as indicated by the following abbreviations: (E) 100ng/ml EGF; (D) 0.01% DMSO control; (Er) 1uM erlotinib, (CL) 1uM CL-387,785, (U) 20uM U0126, or AG1478. Whole cell lysates were obtained using 10% TCA lysis buffer and immunoblotting performed at indicated time points. DUSP6 gene expression is inhibited by erlotinib using quantitative real-time PCR analysis (e, f). RNA was extracted from treated HCC827 (e) or PC9 (f) cells and relative expression level standardized against GAPDH at several time points.

DUSP6 expression is downregulated by MEK inhibition but not EGFR TKI treatment in EGFR-independent lung cancer cell lines

As demonstrated above, DUSP6 expression is strongly downregulated by EGFR TKI treatment in cell lines harboring activating EGFR mutations. Next, we assessed DUSP regulation in two TKI-resistant NSCLC cell lines with wild-type EGFR, H441 and A549. Erlotinib treatment had no effects on DUSP6 expression or ERK-activity in these cell lines, whereas the MEK1/2 inhibitor U0126 reduced both ERK activation and DUSP6 expression (Fig. 2-2g, h and i). Inhibition of DUSP6 expression paralleled ERK inactivation, either through TKI treatment in EGFR-dependent NSCLC cell lines or through MEK1/2 inhibition in EGFR-independent cell lines, indicating that DUSP6 is an immediately regulated target of ERK signaling. Epidermal growth factor treatment alone, which would drive ERK activation, did not affect DUSP6 protein expression in any of the cell lines studied (Fig. 2-2a,b,c,g and i), suggesting that DUSP6 expression in these lung cancer cell lines may already be maximally saturated at baseline.

DUSP6 expression is regulated by the ERK-responsive transcription factor, ETS1

Several *in vitro* studies have demonstrated that DUSP6 is a negative regulator of fibroblast FGFR signaling and endothelial PDGFR signaling via ERK inactivation (158, 161). In a recent study, DUSP6 expression in response to fibroblast growth factor receptor signaling in fibroblasts was shown to be mediated by ETS1/2 transcription factor binding to the DUSP6 gene promoter at a consensus binding sequence (Fig. 2-3a) within a 508 bp promoter region upstream of the DUSP6 gene start codon (-359 to -866), which is highly conserved in Xenopus, Fugu, zebrafish, mouse, rat and human (160). We hypothesized that in analogous

fashion, ERK signaling may regulate DUSP6 expression in lung cancer cells through ETS1/2 factor binding of the same promoter sequence. In order to test this hypothesis, we compared promoter activity of the DUSP6 gene in the presence or absence of the EGFR inhibitor erlotinib using EGFR-dependent HCC827 cells transfected with a luciferase reporter construct (pGL3Basic-508-Firefly) containing this highly conserved sequence. Luciferase reporter assays demonstrated significantly suppressed DUSP6 promoter activity in the presence of erlotinib, not seen in the presence of DMSO vehicle control (Fig. 23b). We then sought to confirm physical binding of ETS1/2 and the DUSP6 promoter sequence in HCC827 cells using chromatin immunoprecipitation assay. A 259 bp band was amplified from either ETS1 or ETS2 immunoprecipitant from HCC827 cells by nested PCR using primers spanning the specific ETS-binding site, indicating direct binding of ETS1/2 to the DUSP6 promoter sequence (Fig. 2-3c). Erlotinib treatment reduced binding of ETS1 but not ETS2 in these assays suggestive of the direct involvement of ETS1 in erlotinib-mediated regulation of promoter activity. In order to further demonstrate erlotinib-induced attenuation of ETS1/2 promoter binding, we performed electrophoretic mobility shift assays using a labeled double-stranded oligonucleotide probe spanning the DUSP6 promoter sequence (Fig. 2-3d). Strong detection of a specific DNA–protein complex was demonstrated in the absence of erlotinib using nuclear extracts from HCC287 cells and the biotin-labeled oligonucleotide probe, whereas diminished binding was seen in the presence of erlotinib. Oligonucleotide probes with targeted mutations led to dramatically reduced complex formation (Mutant 1 and 2), and no complex was seen in the presence of excess unlabeled probe confirming binding specificity of the assay. Antibodies targeting ETS1 and ETS2 led to disappearance of the binding complex, whereas complex formation was unimpeded in the presence of anti-Foxa2

antibody, a control transcription factor again suggestive of physical binding of ETS1/2 to the binding site oligonucleotide. Supershifts in the presence of ETS1/2 antibodies were not observable in the electrophoretic mobility shift assay, potentially due to steric interference between antibody and oligonucleotide binding preventing formation of the antibody–DNA–protein super-complex, as has been previously reported for ETS1/2 by other group (171). Western blotting studies demonstrated expression of ETS1 in HCC827 cells, whereas ETS2 expression was not detectable and ETS1 expression was also found to closely track the activation status of ERK in HCC827, H1975 and H441 cells (Fig. 2-2a,b,d,g, and h). To further corroborate that indeed ETS1 is the critical mediator of DUSP6 regulation in these cells, we pursued siRNA knockdown studies of ETS1 and indeed ETS1 knockdown is accompanied by a marked reduction in DUSP6 expression confirming DUSP6 regulation by ETS1 (Fig. 2-3e)

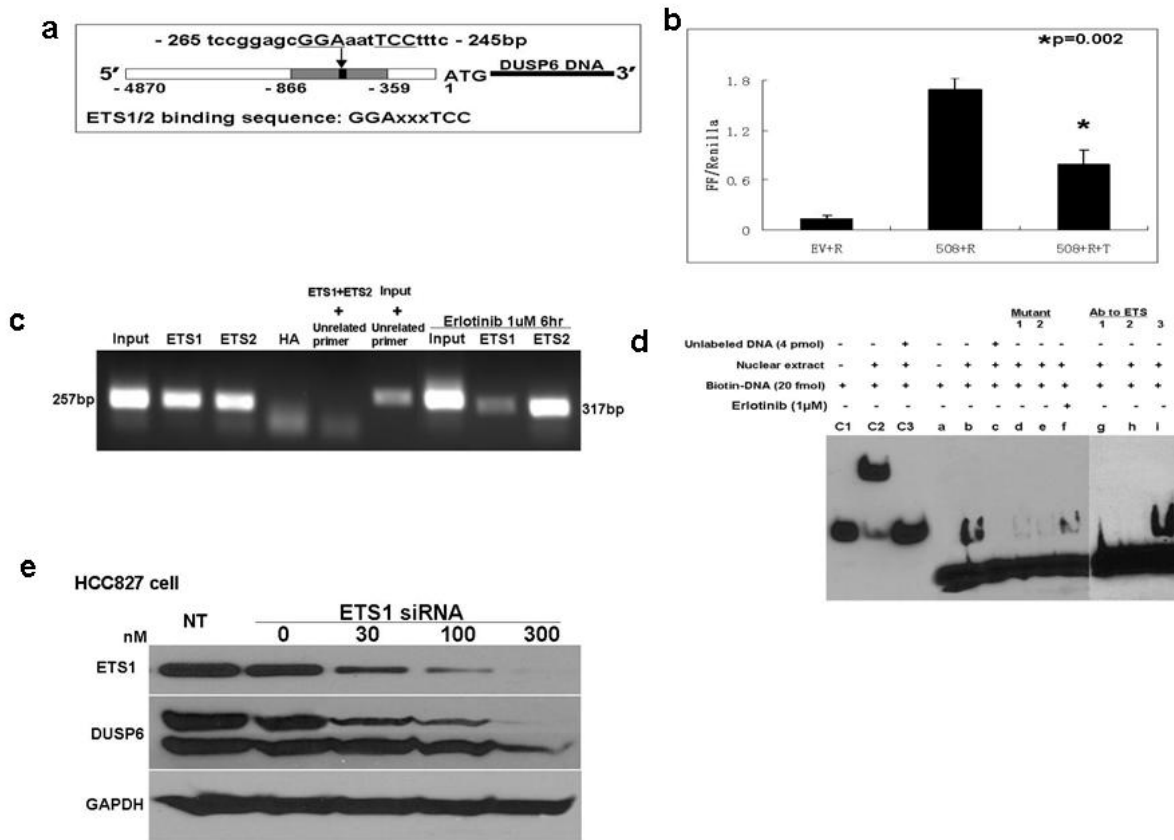


Figure 2-3. Downregulation of DUSP6 by erlotinib is mediated by the ERK-responsive ETS family transcription factor ETS1 through direct binding to the DUSP6 gene promoter. (a) A simplified structural map of the DUSP6 gene indicating the ETS1/2 binding site. (b) HCC827 cells were cotransfected with pGL4.74-renilla luciferase reporter (R) plus DUSP6 promoter-conjugated luciferase reporter, pGL3Basic-508-luciferase (508), or empty pGL3Basic reporter (EV) as a control. 24 hours following transfection, cells were treated with 1uM erlotinib or DMSO for an additional 6 hours. Dual luciferase reporter assays were conducted and Firefly luciferase was normalized to Renilla luciferase activity. (c) CHIP assay performed by nested-PCR amplified a 257 bp fragment in ETS1 or ETS2 immunoprecipitant. Anti-HA antibody was used as a negative control and pre-immunoprecipitant input as a positive control. An unrelated pair of primers amplified a 317 bp band in the positive control input, but not in the presence of ETS1 and ETS2 immunoprecipitant. (d) EMSA assay using nuclear extracts from HCC827 cells and biotin-labeled oligonucleotide probes spanning the ETS-binding site domain of the DUSP6 gene

promoter; lane b demonstrates detection of a specific DNA-protein complex in the absence of erlotinib while lane f demonstrates diminished detection of complex in the presence of erlotinib; lanes d and e show highly diminished DNA-protein complex detection when targeted mutations of the oligonucleotide probe are introduced (Mutant 1 & 2) confirming binding specificity; lane c demonstrates lack of detectable complex in the presence of competing unlabelled probe and lanes g & h demonstrate lack of detectable complex in the presence of competing antibodies targeting ETS1 and ETS2; lane i demonstrates unimpeded complex formation in the presence of anti-Foxa2 antibody, a control transcription factor; lanes c1, c2 and c3 show the EBNA control system containing (c1) biotin-labeled EBNA-binding sequence alone, or (c2) with EBNA-1 protein extract, or (c3) with protein extract as well as 200-fold excess unlabeled ENBA binding sequence. (e) Knockdown of ETS1 by siRNA inhibited DUSP6 expression in HCC827 cells in a dose-dependent manner.

DUSP6 protein localizes to the cytoplasm and functions as a negative regulator for ERK activity

DUSP activity is in part regulated by intracellular localization (172). For example, DUSP6 is primarily cytoplasmic and DUSP1 primarily nuclear, while DUSP16 shuttles between compartments (173-175). Overexpression of DUSP6 has been reported to result in aberrant accumulation within the nucleus (176). In order to assess endogenous DUSP6 localization in lung cancer cells and confirm appropriate localization of HA-tagged exogenous DUSP6, we performed immunocytochemistry by fluorescent staining using DUSP6-high HCC827, DUSP6-low H1975 cells. Anti-DUSP6 antibody was used to detect endogenous DUSP6 in naïve HCC827 cells and anti-HA antibody was used to detect exogenous DUSP6 in H1975 transfecants, demonstrating appropriate cytoplasmic localization of HA-tagged exogenous DUSP6 (Fig. 2-4a).

H1975 cells are optimal for DUSP6 functional studies in an overexpression system, given that these cells have very low baseline levels of DUSP6 protein (Fig. 2-1b), and were also used in our prior transcriptional profiling study which identified DUSP6 regulation by EGFR signaling (98). Stable pcDNA3.1-DUSP6-HA subclonal transfecants of H1975 cells with wild-type (WT), C293G-mutated enzyme-dead (CG) and empty vector pcDNA3.1 controls (EV) were generated. Appropriate plasmid expression was confirmed in transient transfection experiments of COS7 cells, which lack endogenous DUSP6 (Fig. 2-4b). To test whether HA-tagged exogenous DUSP6 preserves the functional properties expected of a dual-specificity phosphatase, we measured mitogen-stimulated ERK1/2 phosphorylation levels and observed significant reduction in P-ERK levels two hours post-EGF stimulation (Fig. 2-4c), confirming functional activity of plasmid-driven DUSP6 expression, whereas similar changes

were not observed for enzyme dead (CG) and empty vector (EV) transfectants. A recent paper also corroborates our findings by reporting analogous results by retroviral transfection of DUSP6 into immortalized normal human airway epithelial cell line NHBE-T and 3 non-small-cell lung cancer cell lines including A549, H1299, and TKB1 (177).

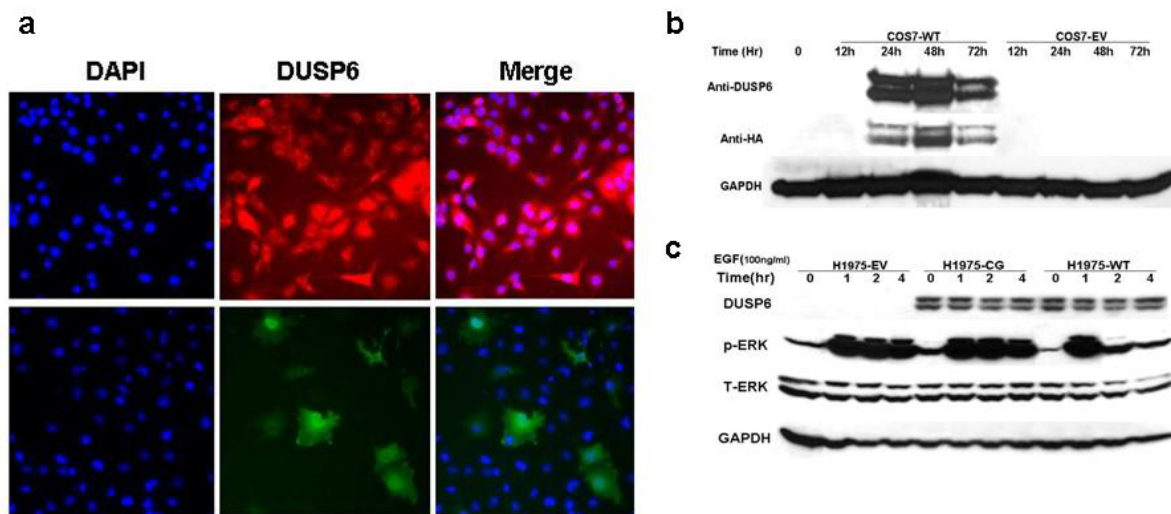


Figure 2-4. DUSP6 protein localizes to the cytoplasm and functions as a negative regulator for ERK activity. (a) DUSP6 protein is present in cytoplasm. Upper row: endogenous DUSP6 in HCC827 cells stained with fluorescent-conjugated secondary antibody after anti-DUSP6 binding, middle panel Red Alexa 560, DAPI blue nuclear stain left, merged image right. Lower row: exogenous DUSP6 in H1975 cells expressing DUSP6 stained with anti-HA antibody followed by fluorescent-conjugated secondary antibody, middle panel Green Alexa 488, DAPI left, merge right. Amplification 200 x. (b) Appropriate expression time course of the pcDNA3.1-DUSP6-HA construct was confirmed in COS7 cells by transient transfection, followed by immunoblot with anti-DUSP6 or anti-HA tag antibody, anti-GAPDH as a control. (c) Stably transfected H1975 subclones (WT) wild-type DUSP6 plasmid, (CG) enzyme-dead C293G mutant DUSP6 plasmid and (EV) empty vector pcDNA3.1 tested by immunoblot for exogenous DUSP6 (anti-HA), phosphor-ERK, total-ERK, and GAPDH control at the indicated time points following EGF stimulation.

Plasmid-driven DUSP6 overexpression decreases viability via increased apoptosis and growth arrest and synergizes with EGFR inhibitor treatment

We next examined the functional effect of overexpressed DUSP6 on cellular growth of stably transfected DUSP6-low H1975 cells. Of note is that in these studies, two independent clones of WT-DUSP6 transfectants were used and demonstrated identical findings. As determined by MTS assay under low serum culture conditions (0.5% FBS), the growth of wild-type H1975 transfectants (WT) was significantly inhibited as compared with C293G-mutated enzyme-dead (CG) and empty vector (EV) transfected cells (Fig. 2-5a). Interestingly, under higher serum culture conditions (2–10% FBS) differences in growth were not observed suggestive of less critical dependence on ERK signaling at such overstimulated conditions. In order to determine whether reduced viability was a result of decreased proliferation, increased apoptosis or a combination of both, cellular proliferation and apoptosis assays were performed under low serum conditions. We found that wild-type DUSP6 H1975 transfectants (WT) displayed a marked reduction of cells in S-phase by BrdU proliferation assay (Fig. 2-5b and table 2-1) and increased apoptosis by annexin/PI assay (Fig. 2-5c). Immunoblot studies also revealed the presence of cleaved PARP product, a marker of caspase-mediated apoptosis in wild-type transfectants (Fig. 2-5d), in marked contrast to the C293G-mutated enzyme-dead (CG) and empty vector (EV) transfected H1975 cells further confirming the induction of apoptosis by DUSP6 expression in these cells. Next, we performed synergism studies by treating stably transfected H1975 cells with CL-387,785. These studies did not demonstrate any difference in cell proliferation rates between the different clonal variants (data not shown). To rule out the possibility that this could be related to compensatory changes in other feedback mechanisms in these long-term cultured cells, we pursued

analogous studies using transient transfection of HCC827 cells with EV, CG-mutant and WT-DUSP6 plasmid constructs followed by erlotinib treatment. These studies showed marked synergism with erlotinib treatment in WT-transfected but not in EV or CG-transfected cells (Fig. 2-5e).

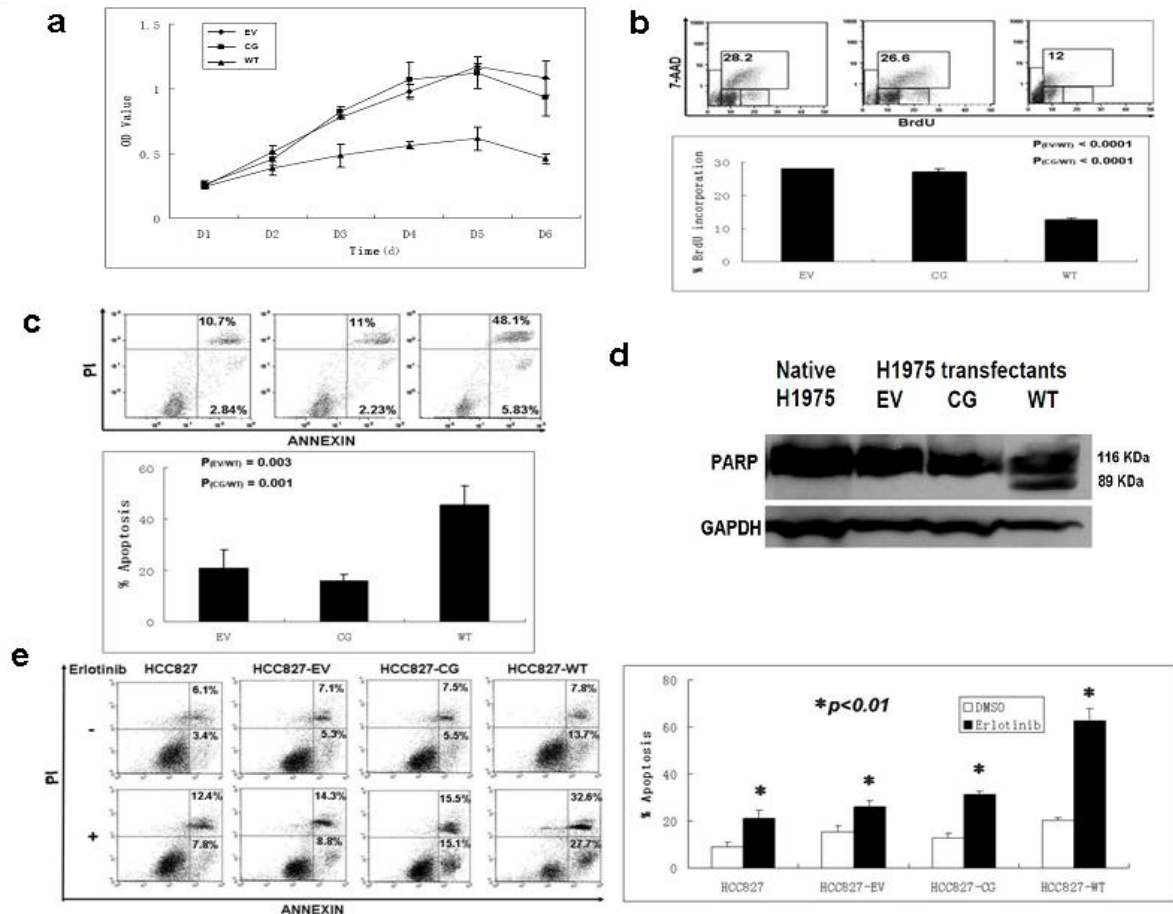


Figure 2-5. DUSP6 overexpression inhibited H1975 cell growth through a combination of increased apoptosis and decreased cell proliferation. Stably transfected H1975 subclones: (EV) empty vector pcDNA3.1; (CG) enzyme-dead C293G mut+ DUSP6; (WT) wild-type DUSP6. (a) Cellular growth curve of H1975 subclones by MTS assay. (b) BrdU assay (top): H1975 subclones were cultured in the 0.5% serum media for 3 days, and then pulse labeled for 60 min with 10uM BrdU, followed by staining with fluorescent anti-BrdU antibody and counterstaining with 7-amino-actinomycin D (7-AAD) for total DNA, then analyzed by flow cytometry; (bottom) histogram showing percentage of cells in S phases of the cell cycle by subclone. (c) Annexin/PI assay (top): H1975 subclones were grown in the 0.5% serum media for 3 days, stained with Annexin V and propidium iodide, then analyzed by flow cytometry results with percentage of cells listed for each quadrant; left lower - viable cells; right lower - early apoptosis; right upper - late apoptosis; (bottom) histogram showing percentage of cells in apoptosis by subclone. (d) PARP assay: apoptosis in wild type DUSP6

overexpressing H1975 subclone confirmed by immunoblot detection of the 89-kD PARP cleavage product. (e) Overexpression of DUSP6 synergized with erlotinib treatment to induce apoptosis in HCC827 cells by flow cytometry analysis. HCC827 cells were transiently transfected with the indicated expression plasmids as used for above H1975 cells for 48 hours before addition of 1uM erlotinib for 24 hours, followed by detection of cellular apoptosis by Annexin/PI staining by flow cytometry. Annexin/PI assay (Left): A example of the flow cytometry data. (Right) histogram showing calculated percentage of cells in apoptosis for the flow cytometry analysis.

Table 2-1. Effect of DUSP6 overexpression on H1975 cell cycle progression

	EV	DUSP6-CG	DUSP6	P value
sub-G1	15.6 ± 1.2	17.3 ± 2.4	58.5 ± 7.1	0.02
G1	49.9 ± 1.0	47.9 ± 2.0	37.4 ± 7.3	0.3
S	28.2 ± 0.1	27.1 ± 1.7	12.7 ± 1.0	<0.0001
G2/M	7.0 ± 0.4	8.1 ± 1.8	1.8 ± 1.0	0.001

EV, empty vector-transfected; DUSP6-CG, enzyme-dead DUSP6-transfected; DUSP6, wt-DUSP6 transfected cells. Mean ± Standard deviation from three independent experiments is shown; P value calculated with SPSS.

siRNA knockdown in DUSP6-high H441 cells enhances viability through prolonged ERK activation

In order to complement the overexpression experiments in cells with low expression levels of DUSP6, we pursued siRNA-mediated knockdown experiments in H441 and HCC827 cell lines. Knockdown efficiency was demonstrated by reduced DUSP6 levels in both cell lines but only H441 cells demonstrated a substantial increase in ERK activation 24 h following siRNA introduction (Fig. 2-6a and b). In H441 cells, MTS assay demonstrated increased proliferation as compared with non-targeted siRNA control, indicating that DUSP6 knockdown led to enhanced cell growth by sustained ERK activation (Fig. 2-6c and d). HCC827 cells did not demonstrate increased proliferation on MTS assay, consistent with the unchanged level of ERK activation seen on immunoblot (Fig. 2-6b). This suggests comparative variability in ERK-signaling feedback regulation in different NSCLC cell lines.

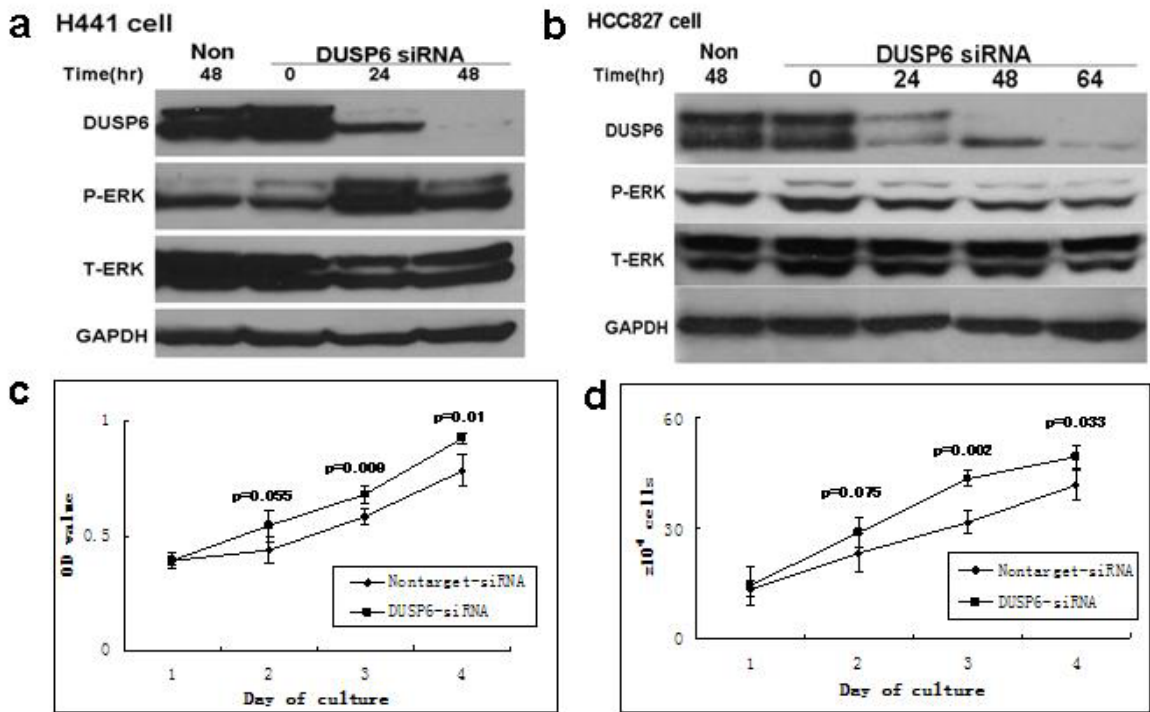


Figure 2-6. Introduction of DUSP6 siRNA reduced DUSP6 protein levels resulting in increased ERK activity and cellular proliferation. (a and b) DUSP6 siRNA was transfected into HCC827 and H441 cells; immunoblotting of cell lysates was performed at the indicated time points to assess levels of DUSP6, P-ERK, total ERK and GAPDH as control. (c) MTS assay measuring H441 cell growth at indicated time points following siRNA knockdown. (d) H441 cells were plated in 6cm-dishes at an initial concentration of 6×10^4 /mL and counted at indicated time points following introduction of DUSP6 siRNA.

Discussion

DUSP6 is a cytoplasmic DUSP with high specificity for ERK which functions as a negative feedback regulator of ERK-activation in normal developmental programs (158) and was also identified in previous studies as highly and immediately regulated by EGFR inhibitor treatment in EGFR-mutant non-small cell lung cancer cells (98). In the current study, we characterize a feedback regulation loop involving DUSP6 expression and ERK-signaling in NSCLC. First, we screened multiple NSCLC cell lines and demonstrated that DUSP6 expression tracks in tandem to ERK-activation. Next, we demonstrated that pharmacologic inhibition of ERK activity leads to dramatic downregulation of DUSP6 expression, both in an EGFR-dependent and EGFR-independent manner. We then conducted functional studies with plasmid-driven DUSP6 overexpression in stably transfected DUSP6-low lung cancer cells, demonstrating attenuation of ERK-activation which resulted in growth arrest and apoptosis as well as synergy with EGFR inhibitor treatment. Conversely, we found that siRNA knockdown in DUSP6-high lung cancer cells resulted in enhanced ERK signaling and cellular proliferation. Finally, utilizing luciferase reporter, CHIP and EMSA assays, we demonstrated that regulation of DUSP6 is mediated at the promoter level by ETS family transcription factors, well-known nuclear targets of activated-ERK, more specifically ETS1 induction through activation of the ERK pathway. Taken together, these findings indicate that DUSP6 expression is tightly regulated by ERK-signaling in NSCLC (Fig. 2-7) and exerts anti-tumor effects via negative feedback mechanisms, pointing to an important feedback loop in NSCLC, which may be prone to dysregulation in tumorigenesis.

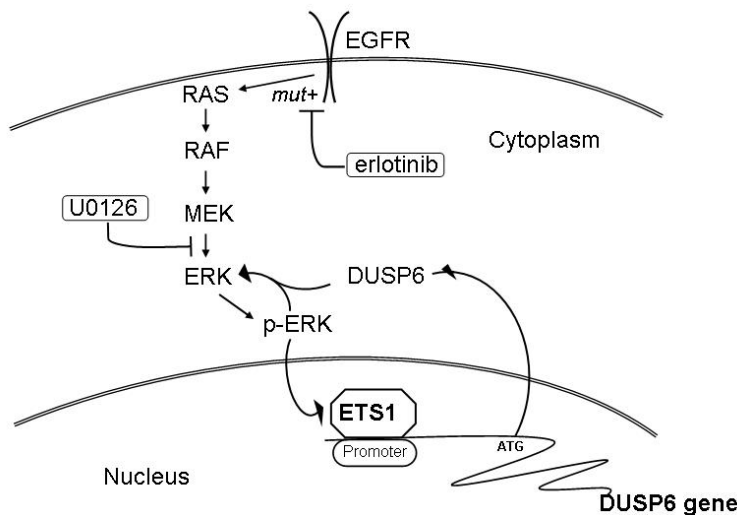


Figure 2-7. Model of MAPK pathway signal transduction in NSCLC and feedback regulation loop involving DUSP6 expression and ERK-signaling characterized in the present study. Either inhibition of EGFR in EGFR-mutated lung cancer or inhibition of ERK in lung cancer downregulates ETS1-mediated DUSP6 expression.

K-RAS mutations are common oncogenic events detectable in the majority of pancreatic cancers and 20-30% of non-small cell lung cancers. K-RAS mutation results in increased ERK-signaling output, which in turn leads to increased expression of inducible DUSPs, including DUSP6, resulting in negative feedback inhibition of ERK-signaling. Similarly, non-small cell lung cancers with constitutive activation of cell surface growth factor receptor pathways, such as EGFR or MET are also at least in part dependent on overactivation of the ERK pathway. Somatic genetic changes leading to inactivation of DUSP6 or other DUSPs and loss of negative feedback regulation of the ERK pathway could certainly represent steps in the progression of such cancers. Previous reports of DUSP6 inactivation via promoter methylation in pancreatic cancers suggest DUSP6 as a candidate tumor suppressor in that disease (178). Our cell line studies demonstrate that in many NSCLC cells, DUSP6

regulation appears intact and responsive to increased ERK-activation, arguing against DUSP6 loss as a frequent oncogenic event in NSCLC. More comprehensive studies will be needed to assess whether DUSP6 abrogation is indeed present in specific subsets of patients. The recent generation of knockout mice lacking the murine DUSP6/MKP3 gene will allow systematic evaluation of its potential role in oncogenesis, particularly for model systems of K-RAS and EGFR-driven lung cancers.

Multiple studies demonstrate that among ERK-regulated genes, DUSP6 is one of the most rapidly and significantly regulated. DUSP6 was identified as one of only three genes significantly overexpressed in myeloma cells harboring a constitutively active mutant N-RAS gene and is also overexpressed in H-RAS driven human breast epithelial cells and in human melanoma cell lines harboring potent activating mutations in B-RAF (107). Interestingly, in a study of PDGFR signaling, DUSP6 was found to be rapidly phosphorylated on Ser174 and Ser300 leading to PDGF-induced degradation while ERK-activation led to DUSP6 induction resulting in restoration of DUSP6 levels within 1-2 hours, and DUSP6 knockdown led to increased ERK-activation and mitogenic response. These results suggest that DUSP6 is an important regulator of PDGF-induced ERK phosphorylation acting in both a rapid positive feed-forward and a more delayed negative feedback loop (161). Other studies suggested that DUSP6 protein expression is also affected by post-translational regulation, principally mTOR-mediated phosphorylation of Ser159 and degradation of DUSP6 (179). Our studies as well as others point to a critical role for ETS-mediated regulation of the DUSP6 promoter in the control of DUSP6 expression (160, 180). DUSP6 was reported to be one of the most highly regulated genes in chronic myeloid leukemia cells upon imatinib treatment (181) and

similarly DUSP6 was overexpressed upon inducible expression of the EGFRvIII oncogene in glioblastoma cells (182). These data suggest that DUSP6 overexpression may be a fairly uniform phenomenon in oncogenic pathways relying on ERK-activation. A systems biological approach identified DUSP6 as a critical regulator shaping the activity of the MAPK pathway during cellular transformation by oncogenic RAS (183). DUSP6 expression was rapidly increased by inducible expression of oncogenic RAS in immortalized rat fibroblasts dampening the initial hyperactivation of ERK (184). Very interestingly, elevated DUSP6 RNA expression was reported to be a major negative predictor of survival in patients with resected non-small cell lung cancer as part of a five-gene signature model (111). The authors did not report K-RAS or EGFR-mutational data in these patients. As our data suggests, DUSP6 expression correlates with ERK-activation, and we hypothesize that tumors with DUSP6 overexpression represent a group of tumors with excessive activation of the ERK pathway explaining their poorer prognosis. This observation indeed suggests that DUSP6 expression may potentially serve as a biomarker for tumors sensitive to inhibition of the RAS-RAF-MAPK pathway.

A large number of small molecule inhibitors of the MAPK pathway are currently in development. For cancer therapy, the most relevant are inhibitors of RAF kinase and MEK1/2. Initial studies with such agents demonstrated only limited success despite the apparent importance of oncogenic ERK-signaling in cancer. The unpredictable cellular and clinical responses seen with such drugs belie a greater complexity surrounding signal regulation than previously thought. Given the critical physiological role of ERK-signaling in normal tissue maintenance and proliferation, it is not yet clear whether direct inhibition will

indeed turn out to be a successful strategy. Therefore, MAPK drug discovery will likely need to expand to include targets that are not classically druggable, though important modulators of MAPK function nonetheless. Our data suggest that modulation of DUSP-mediated feedback mechanisms in ERK-signaling may provide one such avenue for future drug development.

CHAPTER 3

Overexpression of AXL as a novel acquired resistance mechanism to erlotinib in EGFR-mutated NSCLC cells

Abstract

Activating mutations of EGFR have been characterized as important mechanisms for carcinogenesis in a subset of EGFR-dependent NSCLC. EGFR TKI, such as erlotinib and gefitinib, has dramatic clinical effects on EGFR-addicted lung cancers and are used as first-line therapy for EGFR-mutant tumors. However, eventually all tumors acquire secondary resistance to the drugs and progress. Erlotinib-resistant EGFR mutations such as EGFR T790M and MET activation have been reported in drug-resistant tumors, but the mechanism of resistance remains unclear in a significant fraction of cases. Here we report a novel molecular mechanism leading to secondary resistance to erlotinib. HCC827, an EGFR-mutant and highly erlotinib-sensitive NSCLC cell line was exposed to increasing doses of erlotinib and highly erlotinib-resistant clones were developed. In these clones no acquired alterations of EGFR or MET were found but gene expression microarray studies demonstrated in one resistant clone overexpression of AXL, a tyrosine kinase implicated in imatinib and lapatinib resistance. Further studies confirmed that co-treatment using erlotinib along with AXL knockdown or pharmacological inhibition resensitizes these resistant cells leading to cell death. Our results suggest that an oncogenic switch from EGFR-dependent to

EGFR/AXL-codependent signaling can lead to secondary EGFR-TKI resistance in NSCLC, indicating that dual blockade of EGFR and AXL may serve as a novel therapeutic strategy for the treatment of EGFR-mutant lung cancer.

Introduction

Activating mutations of EGFR have recently been identified in 10-20% of lung adenocarcinomas and their presence identifies a unique subset of cancers with exquisite sensitivity to the class of ATP-mimetic EGFR inhibitors, such as erlotinib or gefitinib. Despite dramatic initial responses, the development of acquired resistance and progression is uniform and can be associated with the acquisition of secondary mutations of EGFR, such as EGFR-T790M (185) or MET amplification (21). As a result, irreversible EGFR inhibitors and MET inhibitors are being actively investigated in this setting (79, 186). In many cases, the mechanism of acquired resistance against erlotinib/gefitinib remains ill-defined. Better understanding of resistance mechanisms will be necessary to develop strategies to overcome or prevent resistance. We developed an *in vitro* cell model system leading to the identification of AXL overexpression as one such mechanism.

Materials and Methods

Cell lines and reagents. The human lung cancer cell line HCC827 was purchased from the American Type Culture Collection. Cells were grown in RPMI 1640 supplemented with 10% FBS and 1× Antibiotic/Antimycotic (Invitrogen) and were in the logarithmic growth phase at the initiation of all experiments. Erlotinib and XL880 (GSK1363089) were purchased from Selleck Chemicals (California, USA). Drugs were dissolved in DMSO at 10 mM and stored at -20°C. The final DMSO concentration in all experiments was <0.1% in medium.

Establishment of erlotinib-resistant HCC827 subclones. HCC827 cells were exposed to increasing concentrations of erlotinib every 3 weeks from 1, 3, 5, 7, and so on until 15 µmol/L over a 5 months period. Single-cell cloning was performed by the use of cloning cylinders and two erlotinib-resistant subclones were successfully expanded with 10% fetal bovine serum culture medium containing 1 µmol/L erlotinib, named ER1 and ER2.

Ras activity measurement. Ras activity was measured by a Ras Activation ELISA Assay Kit (Upstate, Tmecula, CA). For a dose response, cells were treated with various concentrations of erlotinib for 3 hours, followed by treatment with 100ng/mL EGF for 15 minutes. For a time-course study, cells were treated with 1 µmol/L of erlotinib over varying timecourses. Samples were run in triplicates and all experiments were repeated twice.

Sequencing of AXL, EGFR, k-Ras and b-Raf. Sequencing of full length of AXL and EGFR was performed by standard methods using follow primers: AXL, 5'-

TGAAGAAAGTCCCTCGTGG-3', 5'-GATCTGTCCATCCCGAAGCC-3', 5'-
TGTCAGACGATGGGATGGGC-3', 5'-GCGTCTCCACAGGAAGCCAG-3', 5'-
TGGTAGTCAGGTACCGCGTG-3', 5'-TCCAGCTCTGACCTCGTGCAG-3', 5'-
ATATCCGGGCGTGGAGAACAGC-3', 5'-GAATCCTTAGGGTCTGGCTG-3'; EGFR,
5'-CTGCGTGAGCTTACTCGTGCCTTGG-3', 5'-AGCAGTCACTGGGGGACTTG-
3', 5'-GGTGCAGGAGAGGAGAACTGC-3', 5'-GGTTTCTGACCGGAGGTCC-3', 5'-
AGGACCAAGCAACATGGTCAG-3', 5'-TGCATCCGTAGGTGCAGTTG-3', 5'-
GATGGTGGGGGCCCTCCTCTT-3', 5'-TCCGGAACACAAAGACAATA-3', 5'-
CTTCCTCTCCGCACCCAGCAGTT-3', 5'-ATCCATCAGGGCACGGTAGAAGTT-3',
5'-AGTGCTGGATGATAGACGCAG-3', 5'-GTCAACAGCACATTGACAGC-3', 5'-
AAATTCACTGCTTGTGGCGC-3'. Sequencing of exon 2 of k-Ras and exons 11 and 15
of b-Raf was performed on isolated genomic DNA using primers and protocols previously
published (10).

Gene expression profiling. Gene expression profiling was performed using Illumina Human HT12- v3 arrays and analyzed by Illumina BeadStudio Gene Expression Module v3.2. Total RNA was extracted from serum-starved parental and ER1 and ER2 HCC827 cells, in the presence or absence of 1µM erlotinib for 12 hours using triplicate samples. Bioinformatics analysis was performed and genes were filtered to include genes with differential expression based on setting the false discovery rate (FDR) threshold at 0.05.

Quantitative real time RT-PCR. For the validation of genes identified by gene expression profiling, quantitative real-time RT-PCR was performed on RNA isolated from HCC827,

ER1, and ER2 cells. Total RNA was collected from cultured cells using PureLink Micro-to-Midi Total RNA Purification kit (Invitrogen, Carlsbad, CA, USA). cDNA was synthesized with SuperScript III reverse transcriptase with the use of oligo(dT) primers (Invitrogen) and RT-PCR was performed by using LightCycler with Syber green probes (Roche) using the following variables: denaturation at 95°C for 10 min, followed by 45 cycles of amplification (95°C 10 s, 60°C 10 s, and 72°C 15 s), and cooling to 40°C at a transition rate of 20°C/s. Levels of glyceraldehyde-3-phosphate dehydrogenase expression were used as internal reference to normalize input cDNA. Ratios of level of each gene to glyceraldehyde-3-phosphate dehydrogenase were then calculated. The primers used for qRT-PCR were: AXL, sense 5'- AGACATGCCAGTGGCATG -3' and antisense 5'- AGCGATTCCCTGCTTCAGG-3'; LUM, sense 5'- CTGGCTGATACTGGAATACCTGG-3' and antisense 5'- AGACATTCATACATACCGGTGG-3'; SLC2A3, sense 5'- TGGCTACAACACTGGGGTCATC-3' and antisense 5'- AAGAGGCCAATAACCAAGCGACC-3'; CST7, sense 5'- TTCTGCTGCCTGGTCTTGAGC-3' and antisense 5'-ACAGTCATCCAGACGCAGGTG-3'; NKD2, sense 5'- ACGCACTCCAGTGCATGTC-3' and antisense 5'- TTCACCCTCCATCCTGCAACG-3'; VGF, sense 5'- AAGTCGGGAAAGGAGTGTCC-3' and antisense 5'-TGCAGCAAATACTGGAGCAGC-3'. Primers used for EGFR and MET were as previously published (21, 78).

Western blot analysis. Cells were serum starved overnight and whole cell lysates were prepared using 10% TCA lysis buffer and clarified by centrifugation. Proteins were separated

by 10% SDS-PAGE gel and transferred onto PVDF membranes (Invitrogen) for Western blot analysis. Antibodies to AXL were purchased from Santa Cruz Biotechnology (Santa Cruz, CA). Antibodies against total ERK, phosphorylated-ERK, total MEK, phosphorylated-MEK , total AKT, phosphorylated-AKT, and GAPDH were purchased from Cell Signaling (Boston, MA). Anti-phospho-AXL antibody was purchased from R&D Systems (Minneapolis, MN). After washing and incubation with secondary antibodies, blots were developed with a chemiluminescence system (Pierce).

Fluorescence in situ hybridization (FISH). FISH was performed using standard methods on metaphase spreads prepared from cell lines. BAC clones spanning the gene AXL were obtained from a commercial source (Invitrogen). DNA was prepared from BAC clones using standard methods and labeled by nick-translation using spectrum red and spectrum green labeled tel19p used as control to enumerate chromosome numbers (Vysis, Downers Grove, IL). Hybridization signals were scored on at least 20 metaphase spreads of cell lines and 200 interphase neuclei on DAPI counterstained slides using Applied Imaging Cytovision Imaging System (Santa Clara, CA).

MTS cell growth assay. HCC827 cells were seeded at a density of 3000 cells/well in 96-well plates in RPMI 1640 containing 10% FBS overnight, then treated with respective agents for an additional 3 days. Viable cell numbers were determined using MTS assay kit according to the manufacturer's protocol (Promega, Madison, WI, USA). Each assay consisted of 3 replicate wells and was repeated at least twice. Data were expressed as the percentage survival of control calculated from the absorbance, corrected for background.

siRNA knockdown. Knockdown of AXL was performed using a specific siRNA Pool targeting AXL (SMARTpool) purchased from Dharmacon RNAi Technologies (Thermo Scientific, Rockford, IL). SiGENOME non-targeting siRNA Pools and siGLO Lamin A/C Control siRNA served as negative and positive control, respectively. Introduction of siRNA was performed with DharmaFect1 reagent over 24 hours according to the manufacturer's instructions. Levels of AXL knockdown at different time or dose points were assessed by immunoblotting.

Results

HCC827 is an EGFR-mutant (exon 19 delE746-A750) and highly erlotinib-sensitive NSCLC cell line. HCC827 cells were exposed to increasing doses of erlotinib for 5 months starting at a concentration of 1 μ mol/L and ultimately reaching a concentration of 15 μ mol/L. Two subclonal cell lines, ER1 and ER2, were established this way, both of which grow unimpeded in the presence of high-dose erlotinib (15 μ M) (Fig. 3-1A). EGFR expression was identical between parental cells and ER1 and ER2 and erlotinib treatment led to complete inhibition of p-EGFR expression in both clones at concentrations and time-course identical to parental cells (Fig. 3-1B). In contrast to parental cells, the two erlotinib-resistant cell lines demonstrated sustained activation of Ras/Mek/Erk signaling pathways (although at a lower level than without erlotinib) in the presence of erlotinib despite complete inhibition of EGFR phosphorylation both in standard signaling assays as well as Ras activation assays (Fig. 3-1B and C). Also, while treatment led to short-term inhibition of p-AKT expression, p-AKT became again detectable albeit at a lower level than in parental cells by 6 hours of treatment as opposed to parental cells where complete inhibition is sustained (Fig. 3-1B). This suggested that the molecular lesion lays downstream of EGFR and we hypothesized that it could be secondary to a kinase switch capable of sustaining sufficient activation of cell survival pathways despite complete blockade of EGFR activity. Indeed, sequencing of the entire coding sequence of EGFR demonstrated no new abnormalities.

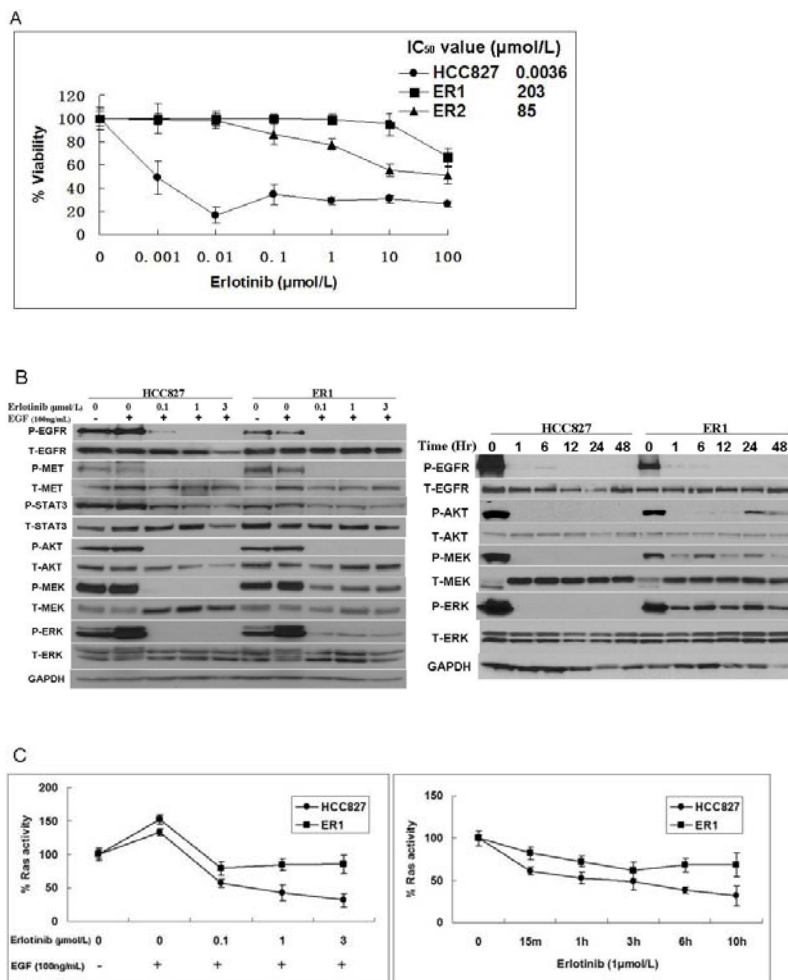


Figure 3-1. Comparison of growth and signaling of parental HCC827 and erlotinib-resistant HCC827 cells. A. Comparison of growth and IC₅₀ values to erlotinib among parental HCC827, and resistant ER1 and ER2 cells. Cells were incubated with a series of concentrations of erlotinib for 3 days and viability of cells were measured by MTS assay and IC₅₀ values were calculated. B. Comparison of signaling pathways between parental HCC827 and resistant ER1 cells. Left, Serum-starved cells were pretreated with DMSO or erlotinib for 3 hours under indicated concentrations, and then treated with 100ng/mL EGF for 15 minutes. ER1 cells were grown in the absence of erlotinib in culture for 2 weeks prior to the experiments. Right, time-course study of signaling pathways treated with 1μmol/L of erlotinib using same cells as in left. C. Ras activity is persistent in the presence of DMSO or erlotinib in ER1 cells as compared to the parental HCC827 cells. Left, erlotinib dose-response studies of Ras activity with the same conditions as in the prior signaling studies. Right, time-course study of Ras activity.

The overall level of MET expression and p-MET levels were unchanged between parental cells and ER1 and ER2 clones by immunoassays (Fig. 3-1B, left). Erlotinib treatment led to complete inhibition of p-MET expression suggestive of strong transactivation of MET by EGFR in these cells as previously seen (25, 30). Lastly, gene copy numbers of both EGFR and MET as determined by quantitative real-time PCR did not differ between parental HCC827 cells and the two clonal isolates (Data not shown).

The lack of changes in EGFR or MET suggested the presence of an alternative tyrosine kinase or other oncogenic switch rewiring the proliferative pathways in the resistant HCC827 subclones. Acquired mutations of k-ras and b-raf were ruled out by direct sequencing of exon 2 of k-ras and exons 11 and 15 of b-raf (Data not shown). In order to identify the causative lesion, we performed microarray studies in triplicate specimens of HCC827 and ER1 and ER2 cells in the presence and absence of erlotinib. Erlotinib treatment of HCC827 cells led to dramatic changes in the expression of a multitude of genes consistent with effective EGFR inhibition (170), while erlotinib treatment of ER1 and ER2 cells led to minimal detectable changes confirming functional resistance to this agent (table 3-3,4,5,6). When untreated HCC827 and ER1/ER2 cells were compared, 38 and 27 genes were upregulated and 85 and 138 genes were downregulated in the ER1 and ER2 cells respectively, with setting our threshold of detection at a p-value for FDR of <0.05 and fold-difference of 3-fold or higher (table 3-7,8,9,10). Six of the most highly upregulated genes were further confirmed using quantitative RT-PCR (Fig. 3-2A).

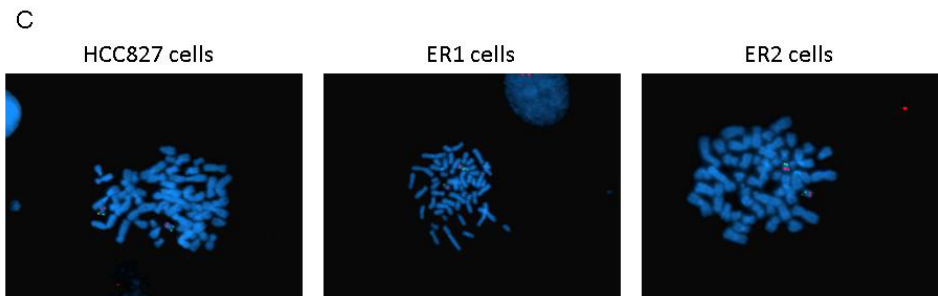
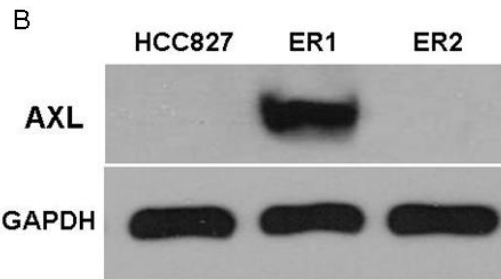
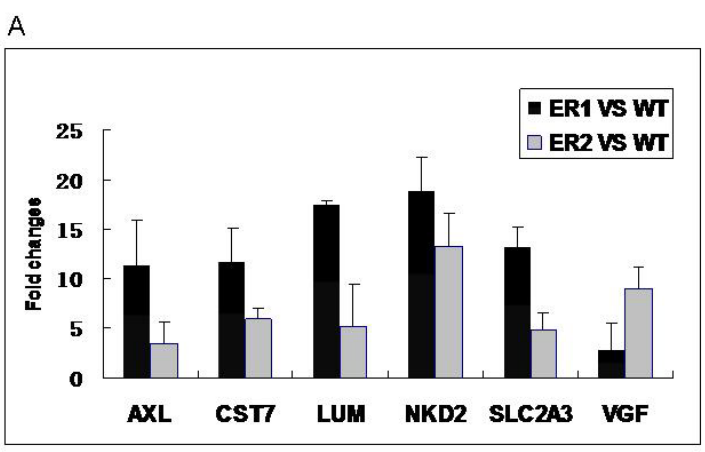


Figure 3-2. AXL is overexpressed in resistant ER1 cells. A. Quantitative real-time PCR verifies the top 6 up-regulated genes in two resistant lines compared to parental HCC827 cells. Fold increase of indicated genes in ER1 and ER2 was calculated against parental cells (results are normalized to expression of GAPDH). B. AXL protein is overexpressed in ER1 cells, but is undetectable in parental HCC827 and ER2 cells. C. FISH assay demonstrates two copies of the AXL gene (19q, red) as well as a control telomeric probe (19p, green) in parental HCC827 cells as well as ER1 and ER2 cells.

Table 3-1. Genes upregulated in HCC827 cells upon erlotinib treatment

	Gene	Fold change	t test P value	DMSO	Erlotinib		Gene	Fold change	t test P value	DMSO	Erlotinib
1	CYP1A1	13.29	0.0031	18.9	251.2	21	ID3	3.53	0.0113	148.9	525.1
2	CHIA	8.00	0.0015	30.6	244.7	22	CALCOCO1	3.45	0.0450	15.7	54.1
3	DDIT4L	6.76	0.0044	10.2	69	23	CREB3L4	3.44	0.0391	12.8	44
4	P8	6.17	0.0011	161.8	998	24	FLJ41603	3.39	0.0013	16.3	55.3
5	NUPR1	5.58	0.0007	187.7	1046.6	25	TNFSF10	3.39	0.0059	21.1	71.5
6	CAPN9	5.38	0.0036	7.9	42.5	26	BCL6	3.38	0.0032	27.8	94.1
7	MMP10	5.28	0.0051	23.3	123	27	GLT8D2	3.38	0.0055	12.9	43.6
8	PIK3IP1	4.83	0.0008	66.9	323.2	28	CHI3L2	3.37	0.0166	13.6	45.8
9	TMED6	4.54	0.0210	17.3	78.5	29	LOC730704	3.36	0.0066	15.4	51.7
10	C10orf10	4.26	0.0012	19.2	81.8	30	RNASE4	3.28	0.0059	16.2	53.1
11	PNPLA7	4.21	0.0029	30.7	129.2	31	FMO5	3.27	0.0092	45	147.3
12	C13orf15	4.20	0.0021	186.6	783.4	32	SCIN	3.23	0.0011	25.9	83.7
13	C1orf88	4.19	0.0198	6.2	26	33	RPRML	3.18	0.0024	161.8	515.1
14	YPEL3	4.06	0.0007	46.3	187.9	34	GATS	3.18	0.0016	94.2	299.4
15	BCMO1	4.05	0.0032	154.1	624	35	GFI1	3.18	0.0327	14.6	46.4
16	REEP1	4.03	0.0194	24.1	97.1	36	ANG	3.14	0.0030	30.3	95.2
17	PLA2G10	3.95	0.0014	215.5	851	37	MMP1	3.13	0.0147	17.3	54.1
18	AMHR2	3.68	0.0031	45	165.4	38	PLA2G12B	3.08	0.0005	104.9	323.1
19	SLC28A3	3.65	0.0074	16.8	61.3	39	VTCN1	3.02	0.0051	131.5	397.1
20	STOX1	3.57	0.0055	36.3	129.6						

Table 3-2. Genes downregulated in HCC827 cells upon erlotinib treatment

	Gene	Fold change	t test P value	DMSO	Erlotinib		Gene	Fold change	t test P value	DMSO	Erlotinib
1	FGFBP1	0.02	0.0009	746.5	15.9	35	SCEL	0.26	0.0017	271.5	70.8
2	FOSL1	0.09	0.0013	281.9	24.8	36	SOX9	0.26	0.0025	76.6	20
3	SPRED2	0.09	0.0074	134.9	12.4	37	NARG1	0.26	0.0006	139	36.3
4	LOC400578	0.10	0.0003	1794	172.5	38	MLF1IP	0.26	0.0497	44.8	11.7
5	CCND1	0.11	0.0038	6487	688.8	39	LOC648399	0.26	0.0126	180.9	47.5
6	SFTPA1	0.11	0.0024	92.4	9.9	40	IL8	0.27	0.0011	133.2	36
7	MGC102966	0.11	0.0002	4742	519.2	41	TIMM8A	0.27	0.0113	171.9	47.2
8	STS-1	0.12	0.0001	2013	246.1	42	CDC25A	0.27	0.0005	83.4	22.9
9	FAM46C	0.13	0.0041	152.7	19.1	43	RRM2	0.28	0.0006	255.2	70.2
10	ISG20L1	0.13	0.0019	256.3	33.6	44	CDC45L	0.28	0.0055	642.5	177.3
11	GJB2	0.15	0.0047	135.7	20.7	45	FLJ12684	0.28	0.0116	64.2	18.1
12	PTGS2	0.16	0.0003	272.6	43.1	46	ERRFI1	0.30	0.0105	3459	1024.4
13	MYB	0.17	0.0043	223.3	36.9	47	PDSS1	0.30	0.0065	212.6	63.2
14	TMEM158	0.18	0.0197	273.5	48.7	48	HSPA1B	0.30	0.0057	1774	527.7
15	SGPP2	0.18	0.0018	153.1	27.7	49	TMEM20	0.30	0.0026	67.8	20.2
16	SPRED1	0.18	0.0027	975	177.7	50	MMD	0.30	0.0181	887	264.5

17	CHAC2	0.18	0.0110	59.9	11	51	MCM6	0.30	0.0017	2465	743.8
18	MCM10	0.19	0.0129	138.7	26	52	ALDH1B1	0.31	0.0075	116.5	35.7
19	GPR116	0.19	0.0030	477.8	90	53	CCT5	0.31	0.0449	35.5	10.9
20	HSPA1A	0.20	0.0011	1190	237.7	54	FEN1	0.31	0.0045	1167	361.2
21	DUSP5	0.20	0.0150	376.4	75.4	55	PCNA	0.31	0.0009	618.4	193.3
22	LIPG	0.20	0.0038	206	41.4	56	PPRC1	0.32	0.0113	216.9	68.5
23	CTPS	0.20	0.0058	463.5	93.7	57	TP73L	0.32	0.0224	166.2	52.6
24	KCNK2	0.21	0.0203	19	4	58	BRI3BP	0.32	0.0036	116.4	37
25	ITGA2	0.22	0.0023	259.2	56.4	59	PES1	0.32	0.0480	104.9	33.5
26	PHLDA1	0.22	0.0007	809.1	176.2	60	RAD54L	0.32	0.0256	103	32.9
27	FAM43A	0.22	0.0103	133.4	29.4	61	NKD2	0.33	0.0041	167.8	54.7
28	ETV4	0.22	0.0027	59	13.1	62	ADRA1B	0.33	0.0240	82.2	26.8
29	C11orf82	0.23	0.0012	187.9	42.9	63	MAMLD1	0.33	0.0150	95.1	31.2
30	CX3CL1	0.23	0.0038	374.7	87.6	64	CD3EAP	0.33	0.0059	143.3	47.1
31	IER3	0.25	0.0016	193.3	48.3	65	C1orf135	0.33	0.0085	174.8	57.5
32	MET	0.25	0.0163	184.3	46.1	66	PAK1IP1	0.33	0.0027	311.3	103
33	FLJ14082	0.26	0.0353	53.2	13.6	67	IQCC	0.33	0.0090	42.6	14.1
34	PLAUR	0.26	0.0033	178.6	46.2	68	UTP15	0.33	0.0312	55.7	18.5

Table 3-3. Genes upregulated in ER1 cells upon erlotinib treatment

Gene	Fold change	t test P value	DMSO	Erlotinib
TCP11L2	3.219178	0.023102	14.6	47

Table 3-4. Genes downregulated in ER1 cells upon erlotinib treatment

Gene	Fold change	t test P value	DMSO	Erlotinib
FGFBP1	0.236453	0.000859	121.8	28.8

Table 3-5. Genes upregulated in ER2 cells upon erlotinib treatment

Gene	Fold change	t test P value	DMSO	Erlotinib
CYP1A1	3.455056	0.020451	17.8	61.5

Table 3-6. Genes downregulated in ER2 cells upon erlotinib treatment

Gene	Fold change	t test P value	DMSO	Erlotinib
STC1	0.168618	0.001114	85.4	14.4
EGR1	0.216925	0.003875	83.9	18.2

Table 3-7. Genes upregulated in ER1 cells compared to HCC827 cells

	Gene	Fold change	t test P value	WT	ER1		Gene	Fold change	t test P value	WT	ER1
1	SLC2A3	10.83	0.0013	61.1	661.6	20	G0S2	3.66	0.0065	63.2	231.2
2	CST7	10.00	0.0007	45.4	453.9	21	PMP2	3.59	0.0147	27.7	99.5
3	NKD2	9.15	0.0042	167.8	1535.4	22	ALDOC	3.54	0.0199	534.7	1893.8
4	AXL	8.75	0.0215	107.9	944.5	23	AFAP1L2	3.51	0.0008	99.2	348.6
5	IL23A	4.71	0.0112	15.3	72.1	24	LOC731486	3.48	0.0130	59.1	205.8
6	FAR2	4.60	0.0093	26.7	122.8	25	TUBB2B	3.45	0.0114	52.7	181.9
7	KRT86	4.43	0.0015	23.8	105.5	26	PIM1	3.45	0.0015	142.2	490.2
8	ABCB1	4.41	0.0028	29.2	128.9	27	GFI1	3.42	0.0425	14.6	50
9	MAGEB6B	4.34	0.0311	17.4	75.6	28	C20orf82	3.37	0.0038	113	380.3
10	DUSP5	4.26	0.0050	376.4	1602.8	29	FAM129A	3.31	0.0393	54.6	180.6
11	VEGFA	4.25	0.0049	40.2	170.9	30	STX1A	3.29	0.0119	56.2	184.7
12	FHL1	4.18	0.0027	26.4	110.3	31	KIAA1949	3.28	0.0040	62.8	206.2
13	PLAC8	4.08	0.0001	272.3	1110.3	32	LOC388681	3.23	0.0159	13.6	43.9
14	BCL6	3.92	0.0075	27.8	109	33	MAGEB2	3.17	0.0020	71.2	225.8
15	SLCO4A1	3.85	0.0044	118	453.9	34	C8orf46	3.17	0.0053	66.6	211
16	LOC728285	3.74	0.0040	11.9	44.5	35	C6orf65	3.15	0.0178	46.4	146.2
17	ACPL2	3.72	0.0076	27.6	102.6	36	CLIC3	3.09	0.0116	33.7	104
18	MOXD1	3.71	0.0023	39.9	148.2	37	LRRC6	3.02	0.0061	256.3	775.2
19	DDO	3.69	0.0047	8.1	29.9	38	GLIPR1	3.01	0.0041	47.5	143.2

Table 3-8. Genes downregulated in ER1 cells as compared to HCC827 cells

	Gene	Fold change	t test P value	WT	ER1		Gene	Fold change	t test P value	WT	ER1
1	PGM5	0.02	0.0006	154.4	3.5	44	PPP1R14D	0.25	0.0037	177.7	44.6
2	CD70	0.04	0.0013	362.2	13	45	LRP3	0.25	0.0161	68.7	17.5
3	GPR64	0.04	0.0026	279.5	10.5	46	LAMP3	0.26	0.0058	133.9	34.2
4	KRT4	0.06	0.0022	438.1	24.1	47	SOX21	0.26	0.0024	65.5	17.1
5	SOX2	0.06	0.0032	122.6	6.8	48	CEACAM6	0.26	0.0008	5488	1433
6	TSPAN8	0.06	0.0057	235.8	14	49	C13orf15	0.26	0.0018	186.6	49
7	ACSL1	0.08	0.0044	193.9	15.6	50	TMEM70	0.26	0.0051	221.6	58.3
8	GPR116	0.09	0.0026	477.8	44.3	51	OAS1	0.27	0.0001	392.9	106.3
9	FAM43A	0.10	0.0076	133.4	13	52	SERPINB5	0.27	0.0097	83.9	22.9
10	VTCN1	0.10	0.0117	131.5	13	53	HES6	0.28	0.0066	462.9	127.6
11	ASRGL1	0.11	0.0027	109.7	11.9	54	ACOT4	0.28	0.0196	62.3	17.2
12	TP73L	0.12	0.0142	166.2	19.2	55	FMO5	0.28	0.0227	45	12.6
13	IRX3	0.13	0.0001	648.6	86.3	56	EHF	0.28	0.0060	60.5	17.1
14	PDGFD	0.14	0.0088	81.6	11.5	57	VASH2	0.29	0.0124	63.5	18.1
15	CTDSPL	0.15	0.0036	203.4	30.3	58	PRODH	0.29	0.0084	691.6	197.8

16	ENPP4	0.15	0.0039	81.1	12.4	59	MAGEE1	0.29	0.0111	99.2	28.5
17	SOCS2	0.16	0.0013	837	131.6	60	MX2	0.29	0.0037	261.6	75.2
18	RFTN1	0.16	0.0046	646.3	102.8	61	WARS	0.29	0.0020	2048	589.3
19	MSRB3	0.16	0.0023	34.5	5.5	62	IFT57	0.29	0.0039	94.9	27.5
20	FGFBP1	0.16	0.0012	746.5	121.8	63	OAS3	0.29	0.0054	597.4	174.7
21	AMOT	0.16	0.0087	70.1	11.5	64	OSBPL5	0.29	0.0058	72.6	21.3
22	PRRX2	0.17	0.0055	132.1	22.2	65	COL4A1	0.29	0.0057	76.3	22.4
23	S100P	0.18	0.0089	170.2	30	66	BCMO1	0.29	0.0102	154.1	45.3
24	GLDC	0.19	0.0165	61.7	11.6	67	STX19	0.30	0.0082	87.4	25.8
25	SLC27A2	0.20	0.0017	173.7	34.2	68	ST8SIA4	0.30	0.0282	23.7	7
26	TGFA	0.20	0.0152	58.1	11.7	69	CTSL2	0.30	0.0084	404.1	121.4
27	SIPA1L2	0.21	0.0011	122.6	26.2	70	FAM80A	0.30	0.0070	179.8	54.1
28	DEPDC6	0.22	0.0281	28.3	6.3	71	FLJ20160	0.30	0.0113	101.8	30.7
29	RNF144B	0.22	0.0132	97.1	21.8	72	CSR2	0.30	0.0095	118.4	35.8
30	GUCY1A3	0.23	0.0014	210.9	48	73	TSPAN10	0.31	0.0242	73	22.5
31	SLC16A9	0.23	0.0020	636.4	145.1	74	STOM	0.31	0.0074	750.2	231.4
32	C11orf75	0.23	0.0102	97.5	22.7	75	EVL	0.31	0.0060	1004	311.6
33	IFI27	0.23	0.0050	12282	2886.1	76	EGR1	0.31	0.0181	304.8	94.8
34	TSPAN33	0.24	0.0037	104.7	25	77	TSHZ1	0.31	0.0043	277.5	86.6
35	MYB	0.24	0.0050	223.3	53.5	78	STAT1	0.32	0.0017	3015	951.5
36	VGLL1	0.24	0.0169	51.3	12.3	79	NOVA1	0.32	0.0230	36.9	11.8
37	LMO3	0.24	0.0028	113.3	27.2	80	PLA2G10	0.32	0.0114	215.5	69.2
38	FBLN1	0.24	0.0112	49.1	11.8	81	DOCK10	0.32	0.0037	140.7	45.3
39	OAS2	0.24	0.0016	1223	296.6	82	RGS4	0.32	0.0075	66.9	21.6
40	PTHLH	0.24	0.0027	118.7	28.8	83	YBX2	0.33	0.0056	173.7	57.2
41	OXTR	0.24	0.0039	62.6	15.3	84	LOC200810	0.33	0.0031	100.9	33.5
42	TNNC1	0.25	0.0020	126.7	31.3	85	TTC25	0.33	0.0023	93.3	31
43	C5	0.25	0.0038	124.9	31.1						

Table 3-9. Genes upregulated in ER2 cells as compared to HCC827 cells

	Gene	Fold change	t test P value	WT	ER2		Gene	Fold change	t test P value	WT	ER2
1	DDIT4L	16.08	0.0032	10.2	164	15	NOV	3.51	0.0135	10.3	36.2
2	VGF	8.88	0.0025	88	781.2	16	MT1G	3.49	0.0271	16	55.8
3	SRPX	8.44	0.0034	11.7	98.7	17	NKD2	3.47	0.0006	167.8	582.1
4	CST7	6.19	0.0014	45.4	281.2	18	PDK4	3.45	0.0245	45.9	158.4
5	LOC346887	5.40	0.0086	11.6	62.6	19	SLC2A3	3.44	0.0036	61.1	210.1
6	MAGEB6B	5.37	0.0083	17.4	93.4	20	KLF9	3.43	0.0450	27.6	94.7
7	MYOM2	5.01	0.0231	13.2	66.1	21	FHL1	3.32	0.0092	26.4	87.6
8	FAR2	5.00	0.0042	26.7	133.4	22	MAGEB2	3.21	0.0010	71.2	228.6
9	GLS	4.76	0.0006	120.5	573.6	23	LOC441054	3.19	0.0061	23.9	76.2

10	ABCB1	4.39	0.0026	29.2	128.2	24	PNCK	3.14	0.0096	11.7	36.7
11	HRASLS	4.34	0.0054	16.3	70.7	25	STC1	3.12	0.0094	27.4	85.4
12	ARMC4	4.24	0.0081	11.4	48.3	26	PFTK1	3.07	0.0076	18.7	57.4
13	GFI1	3.60	0.0179	14.6	52.5	27	CAMTA1	3.01	0.0113	10.8	32.5
14	LOC649095	3.56	0.0032	29.4	104.7						

Table 3-10. Genes downregulated in ER2 cells as compared to HCC827 cells

	Gene	Fold change	t test P value	WT	ER2		Gene	Fold change	t test P value	WT	ER2
1	GPR116	0.04	0.0021	477.8	17.9	70	SORBS2	0.24	0.0104	17.8	4.2
2	OAS1	0.04	0.0001	392.9	17.5	71	PPP1R14C	0.24	0.0076	221.8	52.5
3	PGM5	0.05	0.0006	154.4	7	72	C9orf152	0.24	0.0012	76.8	18.2
4	OAS2	0.05	0.0007	1223	63.1	73	MAPK13	0.24	0.0004	220.5	53.1
5	CD70	0.05	0.0014	362.2	19.2	74	DRAM	0.24	0.0097	376.2	90.6
6	LAMP3	0.05	0.0033	133.9	7.2	75	PRODH	0.24	0.0079	691.6	166.9
7	KRT4	0.06	0.0022	438.1	24.1	76	HERC6	0.24	0.0005	823.3	199.8
8	FGFBP1	0.06	0.0009	746.5	42.5	77	COL17A1	0.24	0.0024	121.2	29.6
9	TMEM125	0.06	0.0016	183.6	10.7	78	IFIT1	0.25	0.0033	1043	258.3
10	IFI27	0.06	0.0032	12282	751.8	79	IFIT5	0.26	0.0143	58.1	14.9
11	CEACAM6	0.07	0.0005	5488	376.7	80	LCN2	0.26	0.0117	276.1	71
12	IRX3	0.07	0.0001	648.6	47.7	81	ZNF165	0.26	0.0036	317.9	81.8
13	TMEM30B	0.08	0.0022	246.8	19.3	82	CDH1	0.26	0.0001	3079	792.9
14	MX2	0.08	0.0020	261.6	20.8	83	HEYL	0.26	0.0319	46.9	12.1
15	PLA2G10	0.08	0.0045	215.5	17.8	84	SAMD9L	0.26	0.0168	147.5	38.1
16	PROM2	0.08	0.0042	362.7	30	85	LPAR5	0.26	0.0011	134.9	35
17	MX1	0.09	0.0001	15181	1378.6	86	REC8	0.26	0.0017	98.9	25.7
18	RAB25	0.10	0.0011	135.1	13.6	87	DOCK11	0.26	0.0044	122.5	32
19	GPR110	0.11	0.0005	166.5	17.7	88	RHOD	0.26	0.0076	176.8	46.4
20	HSH2D	0.11	0.0060	161.6	17.7	89	ERP27	0.26	0.0075	519.8	136.5
21	LOC729252	0.11	0.0050	111.9	12.3	90	CDS1	0.26	0.0079	366.3	96.2
22	ASRGL1	0.11	0.0030	109.7	12.3	91	ENPP5	0.26	0.0072	47.3	12.5
23	LCP1	0.12	0.0004	2285	265.9	92	CXCL16	0.26	0.0010	470.2	124.4
24	LOC400578	0.12	0.0003	1794	218.3	93	ATP8B3	0.27	0.0051	114.5	30.8
25	FGD3	0.13	0.0033	142.6	18.5	94	LY6D	0.27	0.0092	43.8	11.8
26	GRHL2	0.14	0.0162	77.5	10.5	95	ICAM2	0.27	0.0011	140.3	38.4
27	MGC102966	0.14	0.0004	4742	642.5	96	SCEL	0.27	0.0029	271.5	74.6
28	SFTA2	0.14	0.0007	497	67.4	97	EGR1	0.28	0.0141	304.8	83.9
29	OVOL2	0.15	0.0004	298.8	45.3	98	CCL5	0.28	0.0064	268.8	74.3
30	GPR64	0.15	0.0033	279.5	43	99	MUC20	0.28	0.0080	55.6	15.5
31	MPZL2	0.15	0.0005	171.7	26.5	100	LRG1	0.28	0.0113	126.5	35.5
32	HCP5	0.16	0.0008	496	77.2	101	LOC728454	0.28	0.0131	43.6	12.3
33	GPR56	0.16	0.0007	164.6	26.5	102	GJB2	0.28	0.0081	135.7	38.4

34	ST14	0.17	0.0089	180.4	30	103	YBX2	0.28	0.0038	173.7	49.2
35	EPB41L3	0.17	0.0064	384.6	64.6	104	ERBB3	0.28	0.0096	111.5	31.7
36	MARVELD3	0.17	0.0060	58.8	10	105	SUSD2	0.29	0.0029	277.4	79.5
37	XAF1	0.17	0.0016	428.5	73.8	106	STARD10	0.29	0.0068	340.5	98.1
38	IFIH1	0.18	0.0133	304.2	53.6	107	C1orf116	0.29	0.0006	715.2	209.3
39	C13orf15	0.18	0.0023	186.6	33.7	108	SDPR	0.29	0.0018	560.5	164.1
40	EPSTI1	0.18	0.0032	2267	409.5	109	NAPSA	0.30	0.0031	1298	383.6
41	INHBB	0.18	0.0067	68.6	12.6	110	PLAC8	0.30	0.0011	272.3	81.1
42	NMNAT2	0.19	0.0112	50.1	9.3	111	PSD4	0.30	0.0317	65.1	19.4
43	ANXA8	0.19	0.0004	65.8	12.4	112	NFIA	0.30	0.0154	80.2	23.9
44	C9orf61	0.19	0.0317	64.9	12.4	113	ACSL1	0.30	0.0063	193.9	57.8
45	SCNN1A	0.19	0.0027	2141	410.7	114	SAMD9	0.30	0.0031	768.9	230.6
46	LMO3	0.20	0.0036	113.3	22.4	115	FRAS1	0.30	0.0117	39.1	11.8
47	TGFA	0.20	0.0151	58.1	11.5	116	CLDN7	0.30	0.0017	1127	340.2
48	ACOT11	0.20	0.0042	68.2	13.5	117	ZNF114	0.30	0.0244	43.6	13.2
49	STX19	0.20	0.0062	87.4	17.4	118	PRIC285	0.30	0.0032	1477	449.3
50	PTHLH	0.20	0.0017	118.7	23.7	119	TACSTD1	0.30	0.0117	2154	655.8
51	RAB17	0.21	0.0002	299.7	62	120	SP110	0.30	0.0016	521.2	158.7
52	PRSS8	0.21	0.0143	337.9	70.5	121	TNNC1	0.31	0.0025	126.7	39
53	PRRG2	0.21	0.0078	49.7	10.4	122	SLC15A3	0.31	0.0345	51.2	15.8
54	KIAA1324	0.21	0.0070	61.1	13	123	SLC27A2	0.31	0.0027	173.7	53.7
55	MEGF9	0.21	0.0196	32.6	7	124	CEACAM1	0.31	0.0004	236.4	73.6
56	LRRC6	0.22	0.0035	256.3	55.4	125	IRF6	0.31	0.0263	27.3	8.5
57	IRF9	0.22	0.0023	1903	413.4	126	GBP1	0.31	0.0151	192.2	60
58	TRIM2	0.22	0.0117	505.3	110	127	LOC648399	0.31	0.0139	180.9	56.7
59	INADL	0.22	0.0338	20.2	4.4	128	SC5DL	0.31	0.0079	981.2	308.7
60	PLSCR1	0.22	0.0029	528.3	116.9	129	WARS	0.31	0.0018	2048	644.6
61	C2orf15	0.22	0.0018	84.7	19	130	CORO1A	0.32	0.0343	38.6	12.3
62	SOX21	0.23	0.0034	65.5	14.9	131	FOXC1	0.32	0.0034	657.7	210
63	RALGPS1	0.23	0.0008	108.1	24.9	132	SLC16A9	0.32	0.0027	636.4	204.4
64	IFI44L	0.23	0.0065	3452	797	133	OSBPL5	0.32	0.0030	72.6	23.5
65	CGN	0.23	0.0004	828.7	191.5	134	IFITM1	0.32	0.0024	1990	646.3
66	MAP3K8	0.23	0.0082	56.2	13	135	SLC2A12	0.32	0.0164	51.7	16.8
67	IFI6	0.23	0.0014	4340	1011.2	136	S100A4	0.33	0.0028	258.9	84.9
68	IRF7	0.23	0.0022	420	98.4	137	FAM43A	0.33	0.0116	133.4	44
69	STAT1	0.24	0.0013	3015	711.1	138	SPDEF	0.33	0.0262	36.4	12.1

Then, we decided to focus on AXL which was overexpressed about 11-fold based on our Q-RT-PCR results in ER1 since AXL is a tyrosine kinase receptor with an emerging role in drug resistance (141, 146). Western blotting studies confirmed marked overexpression of AXL in ER1 as compared to no detectable expression in parental HCC827 and ER2 cells (Fig. 3-2B). AXL FISH studies did not show amplification of AXL in ER1 cells (Fig. 3-2C) and sequencing of the cDNA of AXL demonstrated wild-type sequences. siRNA-mediated AXL knockdown led to no significant growth reduction of parental cells in the absence of erlotinib while AXL knockdown concurrent with erlotinib treatment led to significant resensitization of ER1 cells (Fig. 3-3), although not to the level of parental cells, likely related to residual AXL activity. Signaling studies confirmed inhibition of both p-AKT and p-ERK by AXL knockdown in the ER1 cells in the presence of erlotinib.

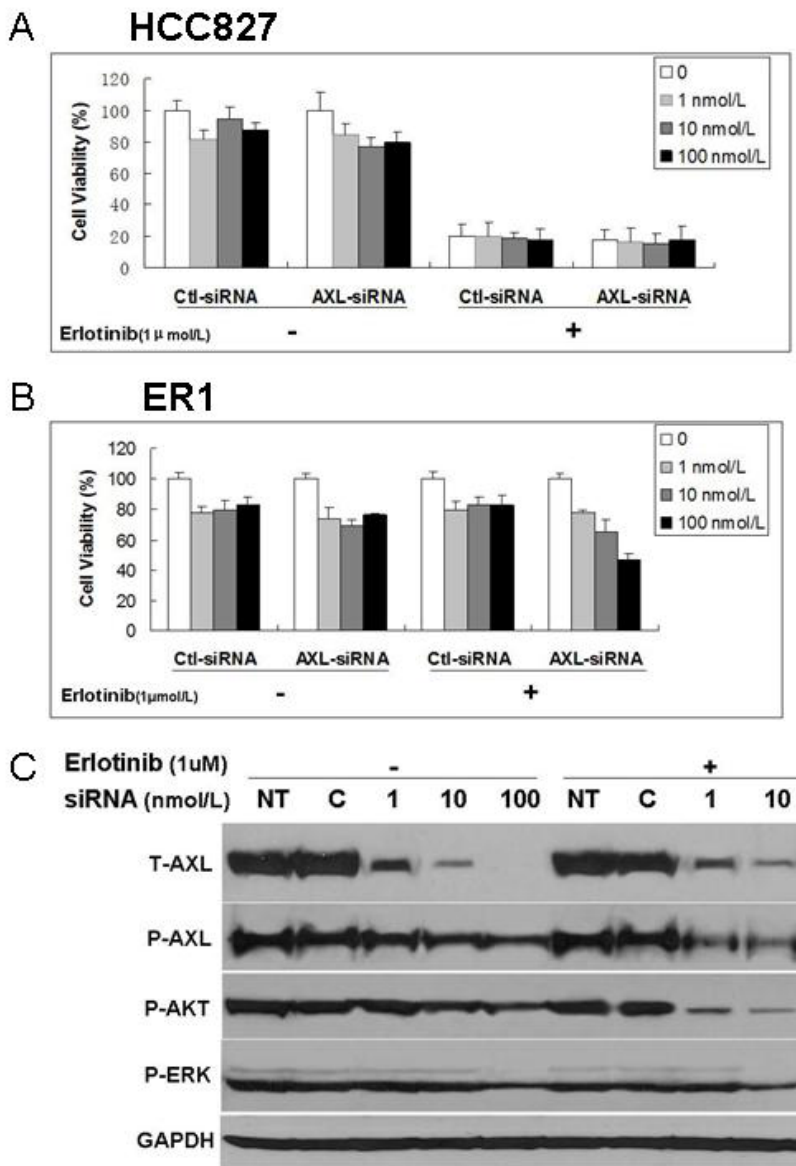


Figure 3-3. SiRNA-mediated AXL knockdown restores erlotinib sensitivity in ER1 cells leading to cell death and is accompanied by inhibition of AKT and ERK activity. A series of concentrations of AXL-targeted siRNA (1, 10, 100 nmol/mL) were transfected into HCC827 (A) and ER1 (B) cells for 72 hours, and MTS assay was performed to measure cell growth under treatment with or without 1 μmol/L of erlotinib, non-targeted siRNA served as control siRNA. C, 1, 10, or 100 nmol/mL of AXL-siRNA were transfected into ER1 cells and immunoblotting of cell lysates was performed after 48 hours of transfection to assess levels of total AXL, P-AKT, P-ERK, and GAPDH as loading control. NT, nontreated; C, non-targeted siRNA at 100 nmol/mL.

We further corroborated these findings by treating parental and ER1 cells with XL880, a multikinase inhibitor that inhibits AXL in addition to MET and VEGFR (146, 187). Similar to siRNA knockdown, XL880 alone did not induce growth inhibition in either parental or ER1 cells, while in ER1 cells co-treatment with erlotinib and XL880 significantly resensitized the cells to erlotinib inhibition with significant growth arrest seen at an XL880 concentration of 1 μ M. XL880 treatment did lead to concentration-dependent inhibition of p-AXL, p-AKT and p-ERK as expected. These results not only show restoration of erlotinib sensitivity by XL880 but also strongly suggest that this is via AXL inhibition since XL880 treatment alone did not lead to growth inhibition in parental cells at all.

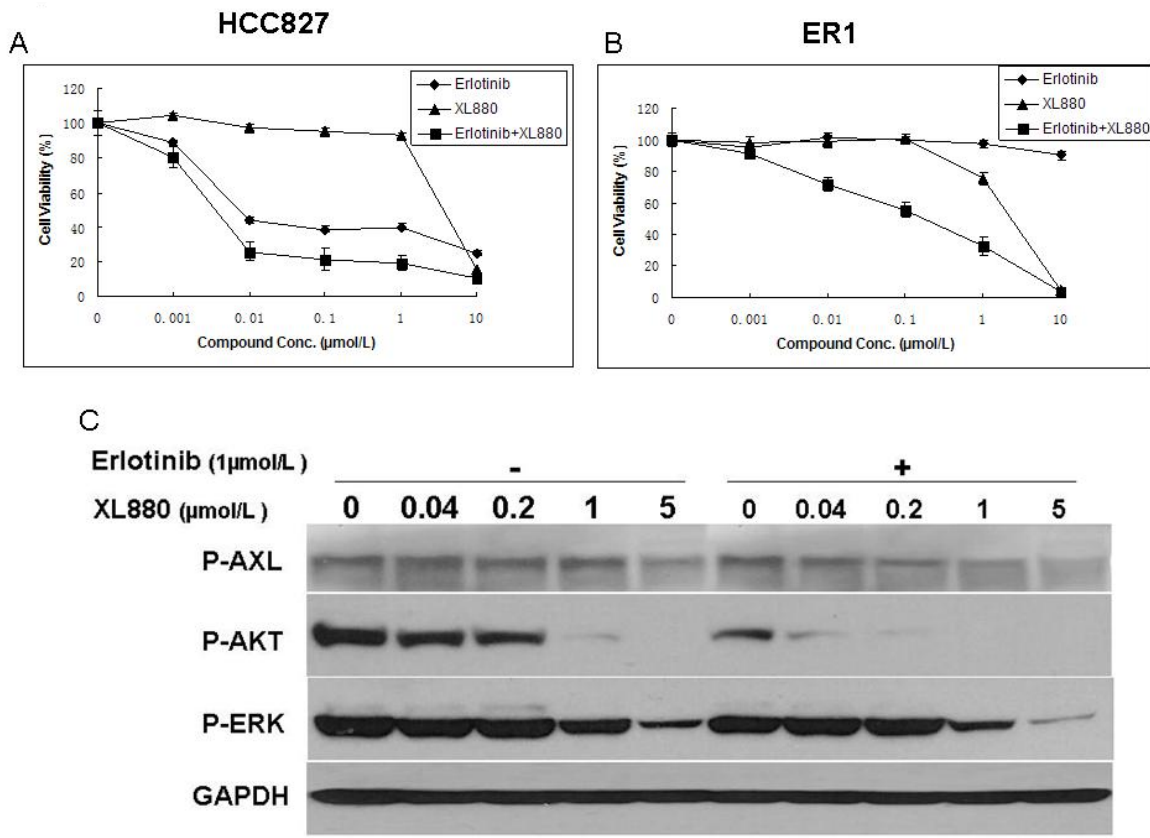


Figure 3-4. Inhibition of AXL by XL880 restores erlotinib sensitivity in ER1 cells. A. HCC827 (A) or ER1 (B) cells were treated with a series of concentrations of XL880, 1 $\mu\text{mol/L}$ erlotinib, or combination of both drugs (with fixed 1 μm of erlotinib) for 72 hours and percent cell viability was measured and calculated with MTS assay. C. Western blotting studies demonstrate that XL880 treatment leads to inhibition of p-AXL, p-AKT and p-ERK. GAPDH was used as control. ER1 cells were serum-starved overnight, followed by treatment of drugs as indicated for 3 hours before collecting of whole cell lysis.

Discussion

In summary, our results suggest that AXL overexpression is a novel mechanism of acquired resistance to EGFR TKI therapy in NSCLC. AXL is a member of the TAM (Tyro-Axl-Mer) receptor tyrosine kinases that share the vitamin K-dependent ligand Gas6 (growth arrest specific 6) (114). It consists of an extracellular region composed of two immunoglobulin-like and two fibronectin type III domains, a transmembrane alpha-helical domain and a C-terminal tyrosine kinase domain with structural similarities to the MET kinase (117). AXL activation either through ligand-dependent or independent mechanisms such as transactivation via IL-15R or HER2 is linked to several signal transduction pathways, including AKT, MAP kinases, NF-kappaB, STAT and others with the PI3kinase/AKT pathway thought to be most important for the functional effects mediated by AXL activation. AXL is expressed in many embryonic tissues and is involved in mesenchymal and neural development. In adult tissues its expression is largely restricted to smooth muscle cells. AXL was originally identified as a transforming gene from a patient with chronic myelogenous leukemia (126). Since then it has been reported to be involved in various high-grade cancers and its expression correlates with poor prognosis (113, 145). AXL is an EMT-induced effector essential for invasiveness and metastasis and it serves as a common downstream effector of the EMT program induced by Twist, Zeb2 and Snail family transcription factors (147, 188-190). This receptor can induce cell aggregation through homophilic binding. AXL is also required for xenograft growth of breast carcinoma and glioma cells and AXL knockdown reduces the growth of lung and breast cancer xenograft tumors (114). Inhibition of AXL expression attenuates breast cancer cell migration and inhibits metastasis to the lung in an orthotopic model (145). In addition to its tumorigenic and invasive properties, AXL

also plays a role in endothelial cell function and AXL knockdown in endothelial cells impairs tube formation (113). Clearly, the multiple roles AXL plays in tumorigenesis make it an attractive target for cancer therapy and recently both monoclonal antibodies as well as small molecule tyrosine kinase inhibitors blocking AXL functions have been developed (113, 146).

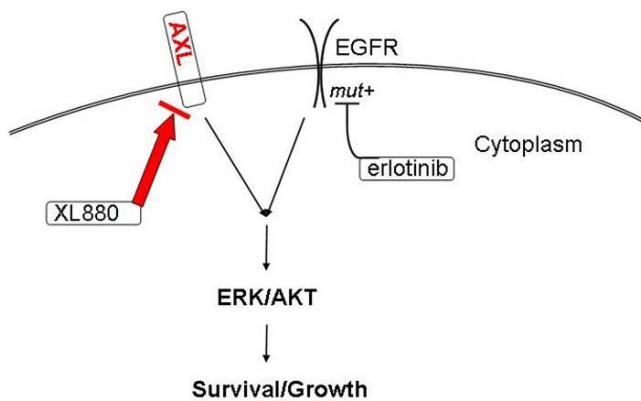


Figure 3-5. Model of oncogenic RTK switch of EGFR-TKI resistance in lung cancer with AXL overexpression. Oncogenic switch from EGFR-dependent to EGFR/AXL-codependent signaling lead to activation of ERK and AKT, resulting in secondary EGFR-TKI resistance in NSCLC. Inhibiting both EGFR and AXL is necessary to reduce the downstream ERK and AKT signaling and cell growth.

Our results suggest that an oncogenic switch from EGFR-dependent to EGFR/AXL-codependent signaling can lead to secondary EGFR-TKI resistance in NSCLC, indicating that dual blockade of EGFR and AXL may serve as a novel therapeutic strategy for the treatment of EGFR-mutant lung cancer. Interestingly, Mahadevan et al previously reported the development of an imatinib-resistant GIST cell line where imatinib-resistance similarly

was mediated by AXL overexpression in a “kinase switch” phenomenon and this switch was associated with a morphological change from spindle to epithelioid (141). Similarly, Liu et al also found that in a cell line model of lapatinib-resistance AXL overexpression led to acquired resistance which could be overcome by treatment with a small molecule inhibitor of AXL (146). Their data analogously to ours showed that in these models, neither lapatinib nor AXL inhibition alone leads to growth inhibition and suppression of both AXL and Her2/3 phosphorylation was necessary to block the interaction of AXL with p85, leading to disruption of the PI3K/AKT pathway. The mechanism of AXL overexpression in our system is unclear and will need to be further studied. We did not find gene amplification by AXL FISH, an alternative hypothesis might be promoter hypomethylation as previously found in the above listed breast cancer model (146). Further studies will also be warranted to confirm our findings in patient specimens. In the aggregate, these data put AXL into a central position as a general mediator of resistance to kinase-targeted therapy in multiple malignancies and highlight the importance of developing AXL-targeted therapeutics that could be used in combination with other targeted therapies to prevent or overcome the development of acquired resistance, one of the most important issues currently facing the development of targeted agents.

CHAPTER 4

DISSERTATION DISCUSSION

MAPK pathway signalling plays an important role in the majority of NSCLCs, whereas DUSPs act as natural terminators of MAPK signal transduction. One of the DUSPs, DUSP6 has been identified as a key target of EGFR TKI inhibition in NSCLC with EGFR superactivity, and then thoroughly studied here. I demonstrated that DUSP6 expression is actually tightly regulated by ERK activity downstream of EGFR signalling pathway and exerts anti-cancer effects in NSCLC via a negative feedback loop involving the ETS1 transcription factor which is also a target of ERK signalling. Our data and others seem to reveal a common phenomenon that DUSP6 functions as a negative mediator targeting ERK in multiple tumor types with abnormal RAS, RAF, or EGFR activation, including lung cancer, breast cancer, glioblastoma, and melanoma. We compared DUSP6 expression and ERK activity in 24 NSCLC cell lines and 48 primary NSCLC tumors and find that DUSP expression has a positive correlation with ERK activation in 19 out of 24 NSCLC cell lines and 35 out of 48 NSCLC specimens, suggesting that DUSP6 expression may potentially serve as a biomarker for the activity of RAS, RAF, or ERK in lung cancer.

On the other hand, high level of ERK activity accompanied with low DUSP6 expression has been observed in 3/24 NSCLC cell lines and 4/48 tumor specimens (i.e. about 10% of samples). Therefore while DUSP6 might overall serve as a biomarker corresponding to the intensity of ERK/MAPK signalling (higher DUSP6 protein level indicates increased oncogenic ERK signalling) in the majority of lung cancers, it could also functionally serve as

a tumor suppressor in others through its loss analogous to its role as a candidate tumor suppressor in pancreatic cancer. We therefore hypothesize that like other typical tumor suppressors, the function of DUSP6 is lost in a subset of lung cancers, resulting in oncogenesis via loss of inhibition of oncogenic MAPK signalling by DUSP6. This hypothesis further initiates other questions by which mechanisms the loss of DUSP6 occurs, for example promoter methylation and/or loss of heterozygosity. Since DUSP6 is not the only one important negative regulators of MAPK signalling, other DUSPs may also play certain roles during the disease development. For example for DUSP7, we have detected very high level of LOH rate (60%) in total 81 lung cancer cell lines, and its role in lung cancer needs to be further investigated.

Furthermore, in our study of molecular mechanisms of EGFR TKI resistance, we discover that overexpression of AXL is a novel mechanism of erlotinib-resistance in our cell model system. Inhibition of AXL by either siRNA or small molecular inhibitor resensitizes the erlotinib-resistant cells to EGFR TKI whereas inhibition of AXL or EGFR alone does not affect cell growth. Expression of AXL protein is significantly high in only one of our two erlotinib-resistant cell lines, indicating that other resistant mechanism also exist. Inhibition of both AXL and Her2/3 phosphorylation was necessary to block the interaction of AXL with p85, leading to disruption of the PI3K/AKT pathway in a lapatinib-resistant breast cancer cell model (146), but in lung cancers we will also need to confirm the physical association of AXL and P85 of PI3K and a coimmunoprecipitation experiment is needed. AXL RTK is a member of a unique class of the RTK family, and the mechanism of its overexpression is unclear in our model cells especially since we find that the AXL gene is present as normal in two copies in the genetic level analyzed by FISH in current study excluding gene

amplification as a mechanism. The oncogenic role of AXL itself is emerging as a new antitumor target in multiple cancer types including leukemia, breast cancer and lung cancer; however its relevance in oncogenesis and better understanding of its more detailed downstream signalling pathways are still incomplete.

The list of questions raised by our findings is very extensive and I have chosen to specifically focus this discussion on 3 aspects of DUSP6- and 3 aspects of AXL-related research areas, which I find particularly intriguing and worthy of further investigation. These topics include:

- (1) Further study of DUSP6 as a biomarker for NSCLC sensitive to inhibition of RAS-RAF-ERK pathway
- (2) Identification and characterization of the tumor suppressive role of DUSP6 in a subset of non-small cell lung cancer
- (3) Investigation of the mechanisms underlying the silencing of DUSP6
- (4) Characterization of the mechanisms involved in AXL overexpression in our cell model system
- (5) Study of the clinical relevance of AXL expression and EGFR TKI sensitivity/resistance in lung cancer
- (6) Study of AXL as an oncogene in lung cancer and investigation of AXL-mediated

downstream signalling pathways

(1) DUSP6 as a biomarker for NSCLC sensitive to inhibition of RAS-RAF-ERK pathway

MAPK plays an important role in the majority of NSCLCs, particularly NSCLC with constitutive activation of cell surface growth factor receptor pathways, such as EGFR, MET or the classical oncogene, K-ras. Such tumors are at least in part dependent on overactivation of the ERK pathway. Although the status of phosphor-ERK analyzed by immunohistochemistry is a direct valuable biomarker for the MAPK signalling but phosphor-antibodies are extremely difficult to adapt to routine clinical immunohistochemical use and better markers therefore are needed. A key downstream effector of this pathway could also serve as an indirect alternative marker for ERK activation, such as DUSP6 being an important negative regulator of MAPK pathway. The demonstration of the biomarker role of DUSP6 for ERK activity will help us to learn more about novel cancer-associated gene products and the mechanism by which they contribute to tumorigenesis in lung cancer, and also could lead to the development of novel strategies for diagnosis and therapy of lung cancer by targeting DUSP6.

To test this hypothesis, we will study a total of 200 NSCLC tissue slides available through our Thoracic Oncology tumor Bank at Columbia University Medical Center, and compare DUSP6 expression, ERK activity as assessed by pERK status, mutational status of kRAS and EGFR since the primary genetic abnormality driving the ERK pathway might be of critical importance. All these specimens were obtained from patients who have undergone definitive surgery for the curative management of non-small cell lung cancer and the tissues are

available in paraffin blocks. Staining intensity of DUSP6 and p-ERK will be scored by a lung pathologist using a 4-step system (0-3) and transform it into low or high (Chapter 2, fig.2-1b) based on expression as compared to that of bronchial cells available as internal controls in most specimens (Table 4-1). The correlation between DUSP6 and p-ERK will be tested by two-tailed Spearman analysis by SPSS software.

Table 4-1. Four-tier scoring system for IHC

0	Undetectable
1	Detectable, but weak;
2	Detectable, equal to normal bronchi staining (in most cases compared to normal bronchial staining in the same section)
3	Stronger than normal bronchi staining

(2) Characterization of DUSP6 as a candidate tumor suppressor in a subset of non-small cell lung cancers

In Chapter 2, we observed high level ERK activity accompanied with low DUSP6 expression in 3/24 NSCLC cell lines and 4/48 tumor specimens, i.e. approximately 10% of all specimens (Fig. 2-1a and b). We also demonstrate that ectopically expressed DUSP6 performs an anti-tumor role through the inhibition of cellular growth and promotion of cellular apoptosis in the in vitro H1975 cell model (Chapter 2, Fig. 2-4 and 5). To fully establish the candidate tumor suppressor role of DUSP6, we will further pursue in vivo confirmatory studies, such as ones utilizing DUSP6 gene knockout mice (these mice are viable and available) and test these mice for increased lung cancer susceptibility using the well-established NNK lung cancer carcinogenesis model to determine if the DUSP6 deficiency promotes carcinogen-induced lung cancer in the mouse.

After demonstration of DUSP6 as candidate tumor suppressor we want to characterize its correlation with lung cancer histological subtypes, such as adenocarcinoma, squamous carcinoma, and large cell lung cancer, other clinicopathological features related to patients, and molecular markers including EGFR and Kras levels and their mutation status since the essential direct target of DUSP6, ERK, is signalling downstream of these markers. Our convenience to access that Thoracic Oncology Tumor Bank will enable us to perform such studies. We also will learn more about the key downstream targets of DUSP6 signaling, besides ERK and ETS, by analyzing gene changes upon overexpressing of DSUP6 in a DUSP6-low NSCLC cell model by using gene expression profiling microarray.

(3) Explore the mechanisms involved in DUSP6 silencing

Genetically a classic tumor suppressor gene can generally be silenced by many ways, such as promoter methylation, loss of heterozygosity (LOH), mutations, or any of their combinations involved in any one or two alleles of the gene. The first hint that DUSP6 might be involved in the pathogenesis of human cancer came from evaluation of its possible role in pancreatic cancer associated with frequent allelic loss at 12q21. Although no gene mutations were detected, DUSP6 mRNA levels were significantly reduced in a number of pancreatic cancer cell lines (191). Loss of DUSP6 expression was reported to correlate with methylation of CpG sequences in intron 1 of the DUSP6 gene in both pancreatic cell lines and in five of eight cases of pancreatic cancer indicating that hypermethylation with modification of histone deacetylation plays an important role in transcriptional suppression of DUSP6 in pancreatic cancer (178). Currently, it is not known whether in lung cancer there might be any genetic abnormalities of DUSP6. We will focus on studies to explore the status of DUSP6

gene promoter methylation and LOH in 30 lung cancer cell lines and 200 tissue samples available for us.

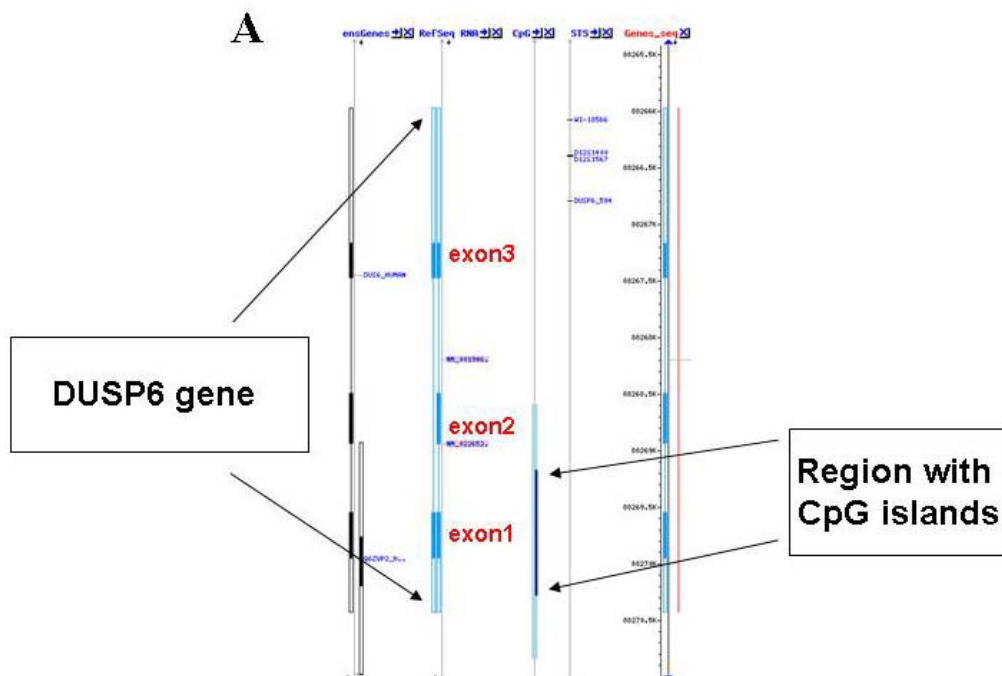
Between 60-90% of all CpG (Cytosine-phosphodiester bond-Guanine) dinucleotides are methylated in mammals whereas unmethylated CpGs are grouped in clusters called “CpG islands” that are present in the 5’ regulatory regions of many genes. In cancer, gene promoter CpG islands acquire abnormal hypermethylation, which results in heritable transcriptional silencing. DNA methylation may impact the transcription of genes by interrupting the binding of transcriptional proteins to the gene. Many tumor suppressor genes are genetically silenced by such DNA methylation mechanism. A Genebank-based search found that DUSP6 contains a cluster of CpG islands located within the promoter, exon1, and intron1 of DUSP6 gene (Fig. 4-1A). Therefore we will mainly seek to determine if methylation of this CpG island might occur in DUSP6-low NSCLC cell lines such as PC9, H1975, or A549 with very low endogenous DUSP6 expression (Fig.2-1a), then we will expand this study to further cell lines and primary specimens. 5’-Aza-2’-deoxyazacytidine (DAC) and trichostatin A (TSA), inhibitors of DNA methyltransferase (DNMT) and histone deacetylase (HDAC), will be used alone or in combination and DUSP6 mRNA level changes will be analyzed by quantitative RT-PCR. We expect that the DUSP6 mRNA will be upregulated in these 3 cell lines and if so, then will turn to investigate the methylation status of the DUSP6 gene promoter by bisulfite sequencing technique that applies routine sequencing methods on bisulfite-treated genomic DNA to determine methylation status at CpG dinucleotides. Isolated DNA from the samples will be treated with bisulfite and then nested PCR reactions of the appropriate promoter region encompassing the CpG island and sequencing will be carried out, as we described

previously (192), to establish if this CpG island is aberrantly methylated. We plan to use direct sequencing of subcloned promoter sequences of the gene to distinguish between methylated and unmethylated specimens. The primers used for this study encompass the fragment of the DUSP6 gene sequence containing the CpG island outlined above.

If indeed we find DUSP6 reactivation and promoter methylation in these samples, then we will pursue a larger study to examine the methylation status of DUSP6 in detail and correlate methylation with DUSP6 gene expression in an array of lung cancer cell lines and further in the collection of 200 primary tissue specimens as well. We will assess whether DUSP6 expression is associated with the degree of DNA methylation or the number of methylated sites detected in the DUSP6 gene sequence anticipating that cell lines with dense promoter methylation will have low or no DUSP6 expression. We will also attempt to establish a methylation-specific PCR protocol for rapid screening of a larger number of primary samples based on the results obtained with bisulfite sequencing which will be necessary for the appropriate design of primers for this assay. The primary lung cancer samples we will use will be the same that we will have used for the DUSP6 IHC study obtained through an IRB-approved study allowing genetic analysis of DUSP6 and we have selected only samples with negative lymph node blocks available. Normal lymph node DNA will be isolated for future analysis to serve as control. We hope to compare patterns of methylation (+/-) of each tumor's IHC score groups for DUSP6 expression, weak (0 or 1+) or strong (2 or 3+). The data obtained above will be correlated with the IHC-staining pattern of both DUSP6 and p-ERK expression. Our expectation would be to find a higher frequency of DUSP6 gene

methylation in tumors with low expression versus high expression of DUSP6 and we also anticipate finding a lower frequency of methylation in samples with high level of DUSP6.

Methylation-induced gene silencing is thought to be associated with a modified chromatin structure that is enriched in acetylated histones. To examine the histone acetylation status within the CpG island of the DUSP6 gene, we will perform chromatin immunoprecipitation using antibodies against the acetylated forms of histones H3 and H4 in a number of non-small cell lung cancer cell lines. We anticipate an enrichment of acetylated histones in cell lines with low as compared with cell lines with high expression of DUSP6. MeCP2 and MBD2 are methyl-CpG-binding proteins that suppress transcription from methylated promoters. To determine the binding status of MeCP2 and MBD2 within the DUSP6 CpG islands, we will again pursue chromatin immunoprecipitation assays and anticipate that binding will be directly correlated to the DNA methylation status of the DUSP6 gene and inversely with DUSP6 expression.



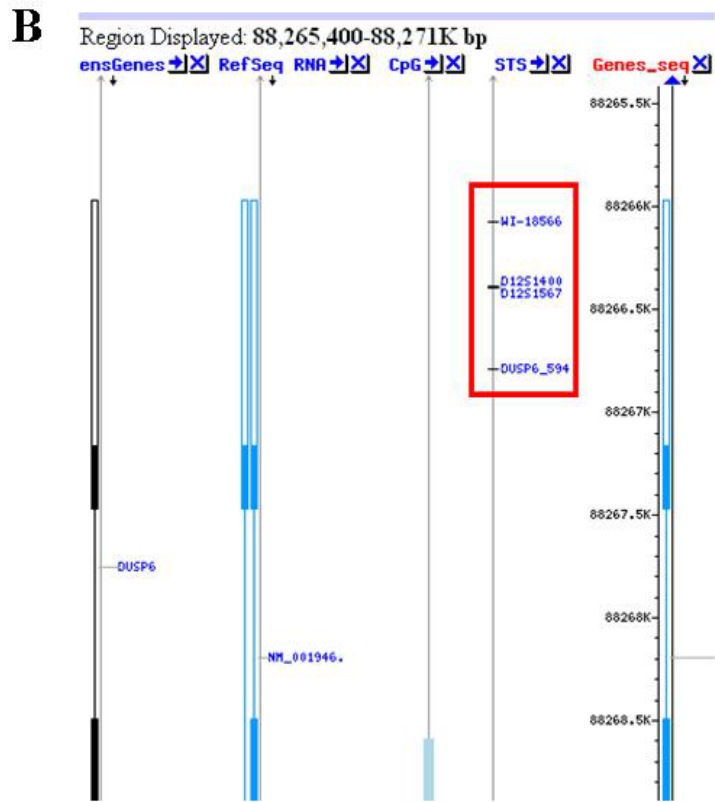


Figure 4-1. A. A cluster of CpG islands are found in the promoter region of DUSP6 gene. B. 4 Microsatellite markers for LOH analysis in DUSP6 gene are indicated as DUSP6_594, D12S1567, D12S1400, WI-18566.

Assessment of LOH of the DUSP6 gene locus in NSCLC will also be performed at the same time. LOH in a cell represents the loss of one normal allele of a gene, typically leading to the loss of the gene expression. LOH commonly occurs in cancer, where it usually indicates the presence of a functional tumor suppressor gene in the lost region. The other allele of the tumor suppressor might be affected by mutation (e.g. p53) or promoter methylation (e.g. p16). LOH has contributed significantly to the identification and characterization of tumor-suppressor genes, and can be profiled in cancers by noting the presence of heterozygosity at a

genetic locus in germline DNA, and the absence of heterozygosity at the identical locus in the cancer cells. This is often done using polymorphic markers, such as microsatellite or single nucleotide polymorphism markers. We will utilize the powerful tool of polymorphic microsatellite markers to analyze LOH of DUSP6 gene. Microsatellite markers are very short and highly polymorphic dinucleotide repeats that have a variable distribution among the population. A large number of polymorphisms are currently known and can be assessed by simple PCR. By comparing allele sizes of amplified markers, one can determine the loss of one marker allele (LOH) when comparing tumor versus normal (somatic) DNA- assuming that the patient is heterozygous for the marker to be studied. Based on a Genebank search, we will select three highly polymorphic microsatellite markers: WI-18566, D12S1400, and D12S1567, which are closest to the chromosomal locus of the DUSP6 gene on 12q21 (Fig. 4-1B). As described above we have tumor and matched normal tissue available from the entire set of 200 samples used for our DUSP6 IHC analysis thereby allowing the appropriate assessment of LOH as compared to normal somatic tissue. All patients had undergone surgical resection of primary lung cancer and had tissue blocks of tumor as well as matched uninvolved lymph node available. We will isolate tumor DNA utilizing laser capture microdissection (LCM) to ensure purity of tumor tissue and gross tissue will be scraped off of microscope slides of paraffin-embedded normal lymph node specimens using standard protocols. Microsatellite marker analysis will be performed and LOH will be scored by a loss of >50% of one of the heterozygous peaks observed in tumor versus in normal samples. LOH of DUSP6 will be correlated with baseline histological features, smoking status, age, gender as well as expression level of DUSP6, p-ERK and gene methylation status of DUSP6. We will also examine the 30 available, established non-small cell lung cancer cell lines available

in our laboratory for LOH. In the lack of normal controls for these cell lines, we will determine gene copy number changes by quantitative PCR using primers specific for the DUSP6 and as control the GAPDH gene locus.

(4) Study of the mechanisms of AXL overexpression in HCC827-ER1 cells

A kinase switch from Kit-driven cell proliferation to AXL overexpression has been reported in an imatinib-resistant GIST (gastrointestinal stromal cell tumor) cell line where imatinib-resistance is mediated by AXL overexpression where the mechanism of AXL overexpression has not been reported (141). Similarly, in a lapatinib-resistant breast cancer cell model of ErbB2-positive breast cancer, AXL overexpression has been demonstrated to be the cause of acquired resistance and this study concluded that promoter hypomethylation but not gene amplification is the mechanism of overexpression of AXL in these cells (146). The mechanism of AXL overexpression in our system is unclear but will be important to understand. We did not find gene amplification by AXL FISH analysis, and expect that promoter hypomethylation might be an alternative mechanism similar to that in the breast cancer cell model (146), but will need to be further studied. Other possibilities might include altered transcriptional regulation/ derepression or reduced RNA degradation. We will first plan to compare the methylation status of the AXL promoter with bisulfite-treated genomic DNA isolated from parental HCC827 and ER1 cells. Bisulfite-treated DNA will be amplified with two sets of methylation-specific primers by PCR as previously reported (193).

A Genebank-based search found that AXL gene contains a cluster of CpG islands located within the promoter area (41724600-41724850bp of Chromosome 19), (Fig. 4-2). Therefore we will mainly seek to determine if hypomethylation of this CpG island might develop

during chronic exposure of HCC827 cells to erlotinib in ER1 cells. We will also use DAC and TSA, alone or in combination, to restore AXL mRNA level by quantitative RT-PCR in the parental HCC827 cells. We expect that AXL mRNA expression will be upregulated in HCC827 cells upon treatment with demethylating agents and if so, then will turn to investigate the methylation status of the AXL gene promoter by bisulfite sequencing technique that we will perform on DUSP6 cells above. Isolated DNA from both parental HCC827 and ER1 cells will be treated with bisulfite and then nested PCR reactions of the appropriate promoter region encompassing the CpG island and sequencing will be carried out, as we described previously (192), to establish if this CpG island is hypomethylated. We plan to use direct sequencing of subcloned promoter sequences of the gene to distinguish between methylated and unmethylated specimens. The primers used for this study will encompass the fragment of the CpG island sequence upstream of the AXL gene (Fig. 4-2).

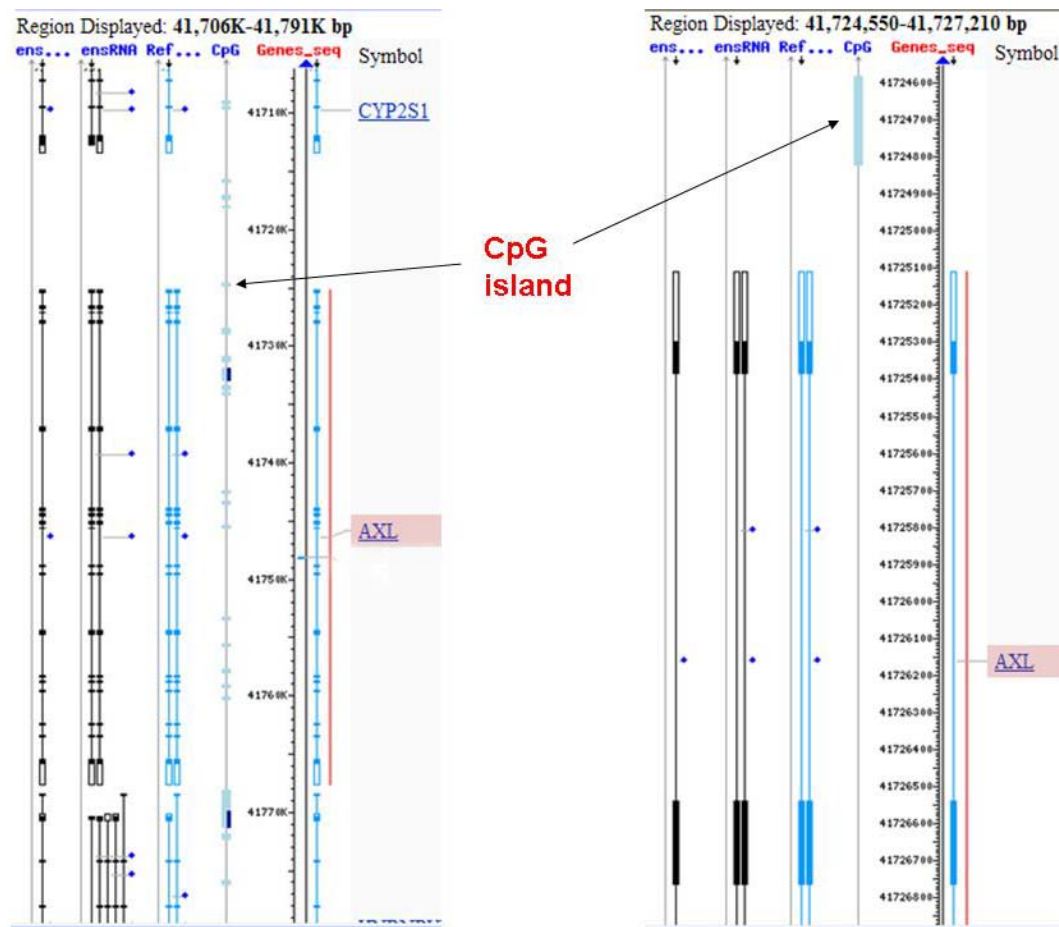


Figure 4-2. There is a CpG island within the promoter area of the AXL gene (arrow).

(5) Study of the clinical relevance of AXL expression and its implications for EGFR TKI sensitivity/resistance in lung cancer

AXL has been shown to be expressed in about 60% of NSCLC cell lines and in normal bronchial epithelial cells on both the mRNA and protein levels, but it was not seen to be expressed in cell lines of SCLC origin growing in suspension (140), suggestive of AXL expression as a histotypic biomarker for the NSCLC group of lung cancers. There is very little reported about the clinical relevance of AXL in lung cancer and much needs to be

learned, especially in light of our own findings. We will explore a significant number of NSCLC samples and assess AXL expression level by immunohistochemistry and correlate its level of expression with clinicopathological and molecular features using our Tumor Bank as described above. We will initially focus on AXL expression since no AXL gene mutation has been identified so far in any types of tumors. To our knowledge, this will be the most comprehensive study of AXL expression in lung cancer and will allow us to understand its pattern of expression by stage and histological subtype and in particular, will allow us to learn about AXL expression in relationship to key molecular alterations, such as EGFR and k-Ras mutations (Table 4-2).

Table 4-2. Correlation of AXL expression with clinicopathologic features of patients with NSCLC.

	Clinicopathologic Features	AXL Expression		
		Negative	Low	High
Gender	Male			
	Female			
Size (cm)	≤3.0			
	>3.0			
Lymph node involvement	Yes			
Type	Adenocarcinoma			
	Squamous cell carcinoma			
	Large cell lung cancer			
	Mixed type			
Staging	0			
	I			
	II			
	III			
	IV			
Prognosis	Good			
	Poor			
Response to EGFR TKI	Sensitive			
	Resistance			
EGFR level and status	High			
	Low			
	Mutation -			
	Mutation +			
k-Ras level and status	High			
	Low			
	Mutation -			
	Mutation +			

We hypothesize that a subset of lung cancers that largely depends on AXL for growth, invasion, or metastasis could be defined analogous to the concept of EGFR-addiction in lung cancer.

AXL is most closely related to the MET tyrosine kinase on the basis of the amino acid sequence of the kinase domain being more homologous with MET than other RTKs. Both AXL and MET activate common signalling molecules resulting in similar functions (116, 117). MET amplification has been well identified as an important mechanism of secondary EGFR-TKI resistance in about 20% of all EGFR-mutant lung cancers and MET mutations and overexpression have been shown to be important mechanisms of oncogenesis in both lung as well as other cancers. Similarly, we anticipate defining a certain fraction of EGFR-mutant lung cancers that overexpress AXL either at baseline or on relapse and understanding of the role of AXL will enable better therapy of tumors secondarily resistant to EGFR-TKI therapy as well.

By using an in vitro cell model system we have revealed a novel mechanism of erlotinib-resistance in EGFR-mutant NSCLCs. We will also need to confirm our findings in patient specimens by comparing AXL levels in pre- and post-EGFR-TKI treated lung tumors that have initial response but develop resistance later on. We will obtain such specimens from collaborators at Case Western Reserve University, Columbia University and Harvard Medical School. We will perform direct genomic DNA sequencing of the EGFR kinase domain, FISH analysis of gene amplification of MET and AXL (even though FISH in our HCC827-ER1 cells detected the normal number of two copies of AXL), and IHC analysis of

MET/AXL by using commercially available, optimized antibodies. We then will investigate the correlation between EGFR mutation status, MET/AXL expression level, and sensitivity/resistance of TKI on those tumor specimens. Moreover, we assume those NSCLC samples with earlier TKI-response but later TKI-resistance should contain EGFR activating mutation, and will also compare the two major EGFR mutation subtypes (exon19 deletion and L858R point mutation) and AXL expression levels. Since our HCC827 cell model carries exon19 deletion, we will need to evaluate if AXL overexpression occurs on L858R mutated tumors (Table 4-3).

Table 4-3. Study of correlaton of AXL expression with TKI resistance in NSCLC specimens

			AXL		
			Negative	Low	High
EGFR mutation	Exon19Del				
	L858R				
MET expression	FISH	-			
		+			
	IHC	-			
		+			

(6) Study of AXL as an oncogene in lung cancer and investigation of AXL-mediated downstream signalling pathways

This is the first time to define a RTK switch from EGFR-dependent to EGFR/AXL-codependent singaling that leads to secondary EGFR-TKI resistance in lung cancer. The independent oncogenic role of AXL needs to be thoroughly investigated in lung cancer tumorigenesis both in light of our findings as well as given the fact that AXL overexpression is sufficient to transform multiple cell types. Several signalling pathways such a MAPK-ERK

and PI3K-AKT have been reported to be stimulated downstream of AXL whereas more complete and detailed key effectors relying on AXL are lacking in lung cancer.

In current study we demonstrate that AXL overexpressing ER1 cells acquire erlotinib resistance. We will further verify this result by transgenecally overexpressiong AXL in the parental HCC827 cells to study if the forced expression of AXL confers resistance to erlotinib. We will clone AXL cDNA from the ER1 cells and generate an AXL expression construct with an HA as a tag and pcDNA3.1 as a backbone as we utilized for DUSP6 study (Chapter 2) (194). The cell growth inhibition and IC₅₀ analysis will be preformed by treat the AXL-expressing HCC827cells with a serious of erlotinib. The downstream signallings will also be tested meanwhile focusing on P-AXL, P-AKT, and P-ERK.

We compared AXL protein levels in 9 NSCLC cell lines by using immunoblotting (Fig. 4-3A), and found that besides our ER1 cell model, A549 is the only one with AXL expression. To test AXL oncogenic role in lung cancer, we will exogoustly overexpress AXL in cells with undetectable AXL, such as HCC827 or PC9. Expression of AXL can be established either by pcDNA3.1-driven transient, stabe expression system (Chapter 2) or by an inducible expression system generated in our lab. We will first use the inducible expression system in our comprehensive functional studies of oncogenic rolr of AXL since this retroviral inducible system has the ability to deliver all requisite transcription factors and target gene components in a single vector with a benefit of rapidness, high efficiency, more stableness, and no toxicity.

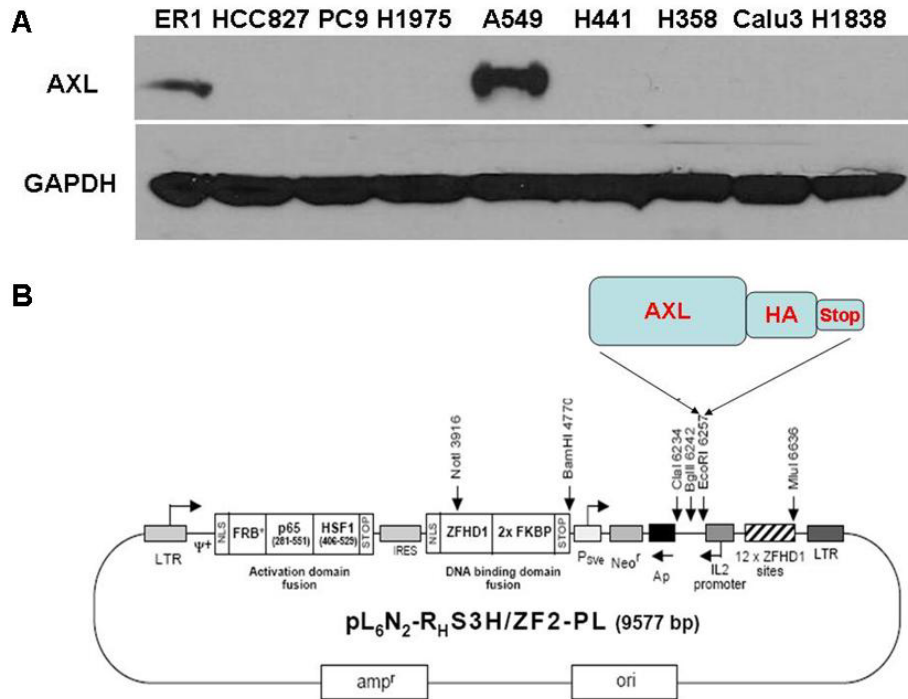


Figure 4-3. A. AXL protein expression in 9 NSCLC cell lines. ER1 and A549 cells have high AXL expression whereas AXL is undetectable in other 7 cell lines. **B. Inducible AXL expression system.** AXL-HA coding sequence was inserted into the polylinker sites (created by us) of the retroviral-based pL6N2 plasmid by standard cloning protocol.

The inducible retroviral system is generated from Argent Regulated Transcription Retrovirus Kit (ARIAD Pharmaceuticals, Inc.) that we obtained through an MTA between ARIAD and Case Western Reserve University/Columbia University. First, we introduced an additional polylinker into the vector which only contains 3 cloning sites. Two restriction enzymes (AgeI and BsiWI) were selected and introduced into the EcoRI site by standard cloning technique. These two enzyme sites will be engineered to both ends of the AXL cDNA sequence by PCR. The AXL cDNA will also be tagged with an HA-tag at the C-terminus for easier detection. In this system, activation of AXL gene expression is very tightly controlled by the induced

binding of transcription factor proteins to target genes (Fig. 4-3B). A rapamycin-based small molecule inducer (AP21967) specifically dimerizes two engineered proteins (DNA binding domain and transcriptional activation domain) to reconstitute a functional transcription factor that only targets a designed gene sequence equipped upstream of a target gene. AXL gene expression is thus activated by addition of the inducer in a dose-dependent manner. We will introduce this inducible system into HCC827 cells by transient and stable transfection. Stably transfected cells will be grown in the presence of selection medium containing G418. Clonal isolates will be obtained by limiting dilution and expanded clones will be screened for inducibility with/without AP21967 induction and immunoblotting for the presence of the HA-tag. Once the optimal experimental condition is established and inducible clones are selected, we can then perform functional assays on the stably transfected HCC827 cell model.

Functional evaluation of cell growth, proliferatin, and apoptosis will be conducted on the HCC827 cells with or without induction of AXL expression, by using the standard method as described in Chapter 2 for DUSP6 study. Three-dimensional *in vitro* colony formation assays will be performed by growing 500 cells in complete media in a liquid format and by growing 2000 cells in soft agar format for 2 weeks.

We will also pursue a transcriptional profiling study to define oncogenic targets of AXL expression by using gene expression microarray on the HCC827 cells in the absence or presence of inducer. The microarray experiments will be performed using Illumina Human HT12-v3 arrays and analysed by Illumina BeadStudio Gene Expression Module v3.2. The samples will be prepared in triplicates as we did in Chapter 3.

Interestingly we find that A549 cells contain very high level of AXL in the preliminary 9 cell lines screening, compared to all others with undetectable AXL (Fig. 4-3A). We believe this A549 cell line is an optimal model to further define the oncogenic role of AXL in lung cancer. We will conduct siRNA-mediated knockdown of AXL experiment in A549 cells to assess the functional role of AXL. Experiments of pharmacological inhibititin of AXL will also be tested using XL880 as in Chapter 3. We also will try to require more selective small molecule inhibitor of AXL kinase, like R428 from other research group (147) for our further study if possible. The functional test will include the studies of cellular growth, proliferation, apoptosis, and colony formation as above.

In addition to the functional assessments, we will investigate the downstream signalling pathways as well by focus on phosphopeptide profiling by immunoassays. Whole cell lysis will be collected from those experimental conditions above and the P-AXL, P-AKT, and P-ERK levels will be dectected by specifical antibodies.

In summary, our findings define important regulators DUSP6 and AXL related to drug sensitivity and resistance to lung cancer therapy. Our further efferts on expanding research scope on these key molecules that drive sensitivity and resistance to current targeted therapy in lung cancer will open up a new avenue of cancer research where we can identify optimal combination treatments for patients allowing to limit or potentially completely eliminate drug resistance leading to important clinical benefits for our patients given analogies of main mechanisms of sensitivity/resistance between different cancers.

BIBLIOGRAPHY

1. Jemal A, Siegel R, Ward E, Hao Y, Xu J, Thun MJ. Cancer statistics, 2009. CA Cancer J Clin 2009;59(4):225-49.
2. Hayes DN, Monti S, Parmigiani G, et al. Gene expression profiling reveals reproducible human lung adenocarcinoma subtypes in multiple independent patient cohorts. J Clin Oncol 2006;24(31):5079-90.
3. Eberhard DA, Johnson BE, Amler LC, et al. Mutations in the epidermal growth factor receptor and in KRAS are predictive and prognostic indicators in patients with non-small-cell lung cancer treated with chemotherapy alone and in combination with erlotinib. J Clin Oncol 2005;23(25):5900-9.
4. Cappuzzo F, Ligorio C, Toschi L, et al. EGFR and HER2 gene copy number and response to first-line chemotherapy in patients with advanced non-small cell lung cancer (NSCLC). J Thorac Oncol 2007;2(5):423-9.
5. Petrelli NJ, Winer EP, Brahmer J, et al. Clinical Cancer Advances 2009: major research advances in cancer treatment, prevention, and screening--a report from the American Society of Clinical Oncology. J Clin Oncol 2009;27(35):6052-69.
6. Zochbauer-Muller S GA, Minna JD. Molecular pathogenesis of lung cancer. . Annu Rev Physiol 2002;64:681-708.
7. John T, Liu G, Tsao MS. Overview of molecular testing in non-small-cell lung cancer: mutational analysis, gene copy number, protein expression and other biomarkers of EGFR for the prediction of response to tyrosine kinase inhibitors. Oncogene 2009;28 Suppl 1:S14-23.
8. Coate LE, John T, Tsao MS, Shepherd FA. Molecular predictive and prognostic markers in non-small-cell lung cancer. Lancet Oncol 2009;10(10):1001-10.
9. Sharma SV, Bell DW, Settleman J, Haber DA. Epidermal growth factor receptor mutations in lung cancer. Nat Rev Cancer 2007;7(3):169-81.
10. Pao W, Wang TY, Riely GJ, et al. KRAS mutations and primary resistance of lung adenocarcinomas to gefitinib or erlotinib. PLoS Med 2005;2(1):e17.
11. Mascaux C, Iannino N, Martin B, et al. The role of RAS oncogene in survival of patients with lung cancer: a systematic review of the literature with meta-analysis. Br J Cancer 2005;92(1):131-9.
12. Zhu CQ, da Cunha Santos G, Ding K, et al. Role of KRAS and EGFR as biomarkers of response to erlotinib in National Cancer Institute of Canada Clinical Trials Group Study BR.21. J Clin Oncol 2008;26(26):4268-75.
13. Linardou H, Dahabreh IJ, Kanaloupiti D, et al. Assessment of somatic k-RAS mutations as a mechanism associated with resistance to EGFR-targeted agents: a systematic review and meta-analysis of studies in advanced non-small-cell lung cancer and metastatic colorectal cancer. Lancet Oncol 2008;9(10):962-72.
14. Khambata-Ford S, Harbison CT, Hart LL, et al. Analysis of potential predictive markers of cetuximab benefit in BMS099, a phase III study of cetuximab and first-line taxane/carboplatin in advanced non-small-cell lung cancer. J Clin Oncol;28(6):918-27.
15. Marchetti A, Milella M, Felicioni L, et al. Clinical implications of KRAS mutations in lung cancer patients treated with tyrosine kinase inhibitors: an important role for mutations in minor clones. Neoplasia 2009;11(10):1084-92.
16. Toschi L, Janne PA. Single-agent and combination therapeutic strategies to inhibit hepatocyte growth factor/MET signaling in cancer. Clin Cancer Res 2008;14(19):5941-6.
17. Krishnaswamy S, Kanteti R, Duke-Cohan JS, et al. Ethnic differences and functional analysis of MET mutations in lung cancer. Clin Cancer Res 2009;15(18):5714-23.
18. Faoro L, Cervantes GM, El-Hashani E, Salgia R. MET receptor tyrosine kinase. J Thorac Oncol 2009;4(11 Suppl 3):S1064-5.
19. Cappuzzo F, Janne PA, Skokan M, et al. MET increased gene copy number and primary resistance to gefitinib therapy in non-small-cell lung cancer patients. Ann Oncol 2009;20(2):298-304.
20. Cappuzzo F, Marchetti A, Skokan M, et al. Increased MET gene copy number negatively affects survival of surgically resected non-small-cell lung cancer patients. J Clin Oncol 2009;27(10):1667-74.
21. Engelman JA, Zejnnullahu K, Mitsudomi T, et al. MET amplification leads to gefitinib resistance in lung cancer by activating ERBB3 signaling. Science 2007;316(5827):1039-43.

22. Bean J, Brennan C, Shih JY, et al. MET amplification occurs with or without T790M mutations in EGFR mutant lung tumors with acquired resistance to gefitinib or erlotinib. *Proc Natl Acad Sci U S A* 2007;104(52):20932-7.
23. Yano S, Wang W, Li Q, et al. Hepatocyte growth factor induces gefitinib resistance of lung adenocarcinoma with epidermal growth factor receptor-activating mutations. *Cancer Res* 2008;68(22):9479-87.
24. Turke AB, Zejnnullahu K, Wu YL, et al. Preexistence and clonal selection of MET amplification in EGFR mutant NSCLC. *Cancer Cell*;17(1):77-88.
25. Tang Z, Du R, Jiang S, et al. Dual MET-EGFR combinatorial inhibition against T790M-EGFR-mediated erlotinib-resistant lung cancer. *Br J Cancer* 2008;99(6):911-22.
26. Nguyen KS, Kobayashi S, Costa DB. Acquired resistance to epidermal growth factor receptor tyrosine kinase inhibitors in non-small-cell lung cancers dependent on the epidermal growth factor receptor pathway. *Clin Lung Cancer* 2009;10(4):281-9.
27. Soda M, Choi YL, Enomoto M, et al. Identification of the transforming EML4-ALK fusion gene in non-small-cell lung cancer. *Nature* 2007;448(7153):561-6.
28. Choi YL, Takeuchi K, Soda M, et al. Identification of novel isoforms of the EML4-ALK transforming gene in non-small cell lung cancer. *Cancer Res* 2008;68(13):4971-6.
29. Takeuchi K, Choi YL, Togashi Y, et al. KIF5B-ALK, a novel fusion oncokinase identified by an immunohistochemistry-based diagnostic system for ALK-positive lung cancer. *Clin Cancer Res* 2009;15(9):3143-9.
30. Rikova K, Guo A, Zeng Q, et al. Global survey of phosphotyrosine signaling identifies oncogenic kinases in lung cancer. *Cell* 2007;131(6):1190-203.
31. Chiarle R, Voena C, Ambrogio C, Piva R, Inghirami G. The anaplastic lymphoma kinase in the pathogenesis of cancer. *Nat Rev Cancer* 2008;8(1):11-23.
32. Soda M, Takada S, Takeuchi K, et al. A mouse model for EML4-ALK-positive lung cancer. *Proc Natl Acad Sci U S A* 2008;105(50):19893-7.
33. Horn L, Pao W. EML4-ALK: honing in on a new target in non-small-cell lung cancer. *J Clin Oncol* 2009;27(26):4232-5.
34. Inamura K, Takeuchi K, Togashi Y, et al. EML4-ALK fusion is linked to histological characteristics in a subset of lung cancers. *J Thorac Oncol* 2008;3(1):13-7.
35. Rodig SJ, Mino-Kenudson M, Dacic S, et al. Unique clinicopathologic features characterize ALK-rearranged lung adenocarcinoma in the western population. *Clin Cancer Res* 2009;15(16):5216-23.
36. Koivunen JP, Mermel C, Zejnnullahu K, et al. EML4-ALK fusion gene and efficacy of an ALK kinase inhibitor in lung cancer. *Clin Cancer Res* 2008;14(13):4275-83.
37. Shaw AT, Yeap BY, Mino-Kenudson M, et al. Clinical features and outcome of patients with non-small-cell lung cancer who harbor EML4-ALK. *J Clin Oncol* 2009;27(26):4247-53.
38. Inamura K, Takeuchi K, Togashi Y, et al. EML4-ALK lung cancers are characterized by rare other mutations, a TTF-1 cell lineage, an acinar histology, and young onset. *Mod Pathol* 2009;22(4):508-15.
39. Settleman J. Cell culture modeling of genotype-directed sensitivity to selective kinase inhibitors: targeting the anaplastic lymphoma kinase (ALK). *Semin Oncol* 2009;36(2 Suppl 1):S36-41.
40. McDermott U, Iafrate AJ, Gray NS, et al. Genomic alterations of anaplastic lymphoma kinase may sensitize tumors to anaplastic lymphoma kinase inhibitors. *Cancer Res* 2008;68(9):3389-95.
41. Takeuchi K, Choi YL, Soda M, et al. Multiplex reverse transcription-PCR screening for EML4-ALK fusion transcripts. *Clin Cancer Res* 2008;14(20):6618-24.
42. Breathnach OS FB, Conley B, Green MR, Johnson DH, Gandara DR et al. . Twenty-two years of phase III trials for patients with advanced non- small-cell lung cancer: sobering results. *J Clin Oncol* 2001;19(6):1734-42.
43. Sandler A, Gray R, Perry MC, et al. Paclitaxel-carboplatin alone or with bevacizumab for non-small-cell lung cancer. *N Engl J Med* 2006;355(24):2542-50.
44. Lee JM, Mao JT, Krysan K, Dubinett SM. Significance of cyclooxygenase-2 in prognosis, targeted therapy and chemoprevention of NSCLC. *Future Oncol* 2007;3(2):149-53.

45. Whitehead CM, Earle KA, Fetter J, et al. Exisulind-induced apoptosis in a non-small cell lung cancer orthotopic lung tumor model augments docetaxel treatment and contributes to increased survival. *Mol Cancer Ther* 2003;2(5):479-88.
46. Scagliotti G. Proteasome inhibitors in lung cancer. *Crit Rev Oncol Hematol* 2006;58(3):177-89.
47. Dragnev KH, Petty WJ, Shah SJ, et al. A proof-of-principle clinical trial of bexarotene in patients with non-small cell lung cancer. *Clin Cancer Res* 2007;13(6):1794-800.
48. Albright C, Garst J. Vaccine therapy in non-small-cell lung cancer. *Curr Oncol Rep* 2007;9(4):241-6.
49. Sun S, Schiller JH, Spinola M, Minna JD. New molecularly targeted therapies for lung cancer. *J Clin Invest* 2007;117(10):2740-50.
50. Yarden Y, Sliwkowski MX. Untangling the ErbB signalling network. *Nat Rev Mol Cell Biol* 2001;2(2):127-37.
51. Hynes NEL, H. A. . ERBB receptors and cancer:the complexity of targeted inhibitors. *Nature Rev Cancer Res* 2005;5:341-54.
52. Pao WM, V.A. Epidermal growth factor receptor mutations, small-molecule kinase inhibitors, and non-small-cell lung cancer: current knowledge and future directions. *J Clin Oncol* 2005 23(11):2556-68.
53. Hirsch FR. Epidermal growth factor receptor in non-small-cell lung carcinomas: correlation between gene copy number and protein expression and impact on prognosis. *J Clin Oncol* 2003;21:3798-807.
54. Cappuzzo F, Finocchiaro G, Metro G, et al. Clinical experience with gefitinib: an update. *Crit Rev Oncol Hematol* 2006;58(1):31-45.
55. Sequist LV, Joshi VA, Janne PA, et al. Response to treatment and survival of patients with non-small cell lung cancer undergoing somatic EGFR mutation testing. *Oncologist* 2007;12(1):90-8.
56. Kobayashi S BT, Dayaram T, Jänne PA, Kocher O, Meyerson M, Johnson BE, Eck MJ, Tenen DG, Halmos B. EGFR mutation and resistance of non-small-cell lung cancer to gefitinib. *N Engl J Med* 2005;352:786-92.
57. Shepherd FA RPJ, Ciuleanu T, Tan EH, Hirsh V, Thongprasert S, Campos D, Maoleekoonpiroj S, Smylie M, Martins R, van Kooten M, Dediu M, Findlay B, Tu D, Johnston D, Bezjak A, Clark G, Santabárbara P, Seymour L; National Cancer Institute of Canada Clinical Trials Group. Erlotinib in previously treated non-small-cell lung cancer. *N Engl J Med* 2005;353(2):123-32.
58. A. Farooq GC, S. Mujtaba, O. Plotnikova, L. Zeng, C. Dhalluin, R. Ashton, M. Zhou. Solution Structure of ERK2 Binding Domain of MAPK Phosphatase MKP-3Structural Insights into MKP-3 Activation by ERK2. . *Molecular Cell*; 7(2):387-99.
59. Harari PM. Epidermal growth factor receptor inhibition strategies in oncology. *Endocr Relat Cancer* 2004;11(4):689-708.
60. Riely GJ, Pao W, Pham D, et al. Clinical course of patients with non-small cell lung cancer and epidermal growth factor receptor exon 19 and exon 21 mutations treated with gefitinib or erlotinib. *Clin Cancer Res* 2006;12(3 Pt 1):839-44.
61. Jackman DM, Yeap BY, Sequist LV, et al. Exon 19 deletion mutations of epidermal growth factor receptor are associated with prolonged survival in non-small cell lung cancer patients treated with gefitinib or erlotinib. *Clin Cancer Res* 2006;12(13):3908-14.
62. Mok TS, Wu YL, Thongprasert S, et al. Gefitinib or carboplatin-paclitaxel in pulmonary adenocarcinoma. *N Engl J Med* 2009;361(10):947-57.
63. Riely GJ, Politi KA, Miller VA, Pao W. Update on epidermal growth factor receptor mutations in non-small cell lung cancer. *Clin Cancer Res* 2006;12(24):7232-41.
64. Hirsch FR, Witts S. Biomarkers for prediction of sensitivity to EGFR inhibitors in non-small cell lung cancer. *Curr Opin Oncol* 2005;17(2):118-22.
65. Tsao MS, Sakurada A, Cutz JC, et al. Erlotinib in lung cancer - molecular and clinical predictors of outcome. *N Engl J Med* 2005;353(2):133-44.
66. Hanahan D, Weinberg RA. The hallmarks of cancer. *Cell* 2000;100(1):57-70.
67. Gazdar AF. Personalized medicine and inhibition of EGFR signaling in lung cancer. *N Engl J Med* 2009;361(10):1018-20.

68. Shigematsu H, Gazdar AF. Somatic mutations of epidermal growth factor receptor signaling pathway in lung cancers. *Int J Cancer* 2006;118(2):257-62.
69. Greulich H, Chen TH, Feng W, et al. Oncogenic transformation by inhibitor-sensitive and -resistant EGFR mutants. *PLoS Med* 2005;2(11):e313.
70. Jiang J, Greulich H, Janne PA, Sellers WR, Meyerson M, Griffin JD. Epidermal growth factor-independent transformation of Ba/F3 cells with cancer-derived epidermal growth factor receptor mutants induces gefitinib-sensitive cell cycle progression. *Cancer Res* 2005;65(19):8968-74.
71. Thomas RK, Greulich H, Yuza Y, et al. Detection of oncogenic mutations in the EGFR gene in lung adenocarcinoma with differential sensitivity to EGFR tyrosine kinase inhibitors. *Cold Spring Harb Symp Quant Biol* 2005;70:73-81.
72. Choong NW, Dietrich S, Seiwert TY, et al. Gefitinib response of erlotinib-refractory lung cancer involving meninges--role of EGFR mutation. *Nat Clin Pract Oncol* 2006;3(1):50-7; quiz 1 p following 7.
73. Huse M, Kuriyan J. The conformational plasticity of protein kinases. *Cell* 2002;109(3):275-82.
74. Tice DA, Biscardi JS, Nickles AL, Parsons SJ. Mechanism of biological synergy between cellular Src and epidermal growth factor receptor. *Proc Natl Acad Sci U S A* 1999;96(4):1415-20.
75. Zhang X, Gureasko J, Shen K, Cole PA, Kuriyan J. An allosteric mechanism for activation of the kinase domain of epidermal growth factor receptor. *Cell* 2006;125(6):1137-49.
76. Kumar A, Petri ET, Halmos B, Boggon TJ. Structure and clinical relevance of the epidermal growth factor receptor in human cancer. *J Clin Oncol* 2008;26(10):1742-51.
77. Yun CH, Boggon TJ, Li Y, et al. Structures of lung cancer-derived EGFR mutants and inhibitor complexes: mechanism of activation and insights into differential inhibitor sensitivity. *Cancer Cell* 2007;11(3):217-27.
78. Yu Z, Boggon TJ, Kobayashi S, et al. Resistance to an irreversible epidermal growth factor receptor (EGFR) inhibitor in EGFR-mutant lung cancer reveals novel treatment strategies. *Cancer Res* 2007;67(21):10417-27.
79. Engelman JA, Janne PA. Mechanisms of acquired resistance to epidermal growth factor receptor tyrosine kinase inhibitors in non-small cell lung cancer. *Clin Cancer Res* 2008;14(10):2895-9.
80. Burris HA, 3rd. Shortcomings of current therapies for non-small-cell lung cancer: unmet medical needs. *Oncogene* 2009;28 Suppl 1:S4-13.
81. Metro G, Finocchiaro G, Cappuzzo F. Anti-cancer therapy with EGFR inhibitors: factors of prognostic and predictive significance. *Ann Oncol* 2006;17 Suppl 2:ii42-5.
82. Shih JY, Gow CH, Yang PC. EGFR mutation conferring primary resistance to gefitinib in non-small-cell lung cancer. *N Engl J Med* 2005;353(2):207-8.
83. Maheswaran S, Sequist LV, Nagrath S, et al. Detection of mutations in EGFR in circulating lung-cancer cells. *N Engl J Med* 2008;359(4):366-77.
84. Jackman DM, Yeap BY, Lindeman NI, et al. Phase II clinical trial of chemotherapy-naive patients > or = 70 years of age treated with erlotinib for advanced non-small-cell lung cancer. *J Clin Oncol* 2007;25(7):760-6.
85. van Zandwijk N, Mathy A, Boerrigter L, et al. EGFR and KRAS mutations as criteria for treatment with tyrosine kinase inhibitors: retro- and prospective observations in non-small-cell lung cancer. *Ann Oncol* 2007;18(1):99-103.
86. Pao W, Miller VA, Politi KA, et al. Acquired resistance of lung adenocarcinomas to gefitinib or erlotinib is associated with a second mutation in the EGFR kinase domain. *PLoS Med* 2005;2(3):e73.
87. Balak MN, Gong Y, Riely GJ, et al. Novel D761Y and common secondary T790M mutations in epidermal growth factor receptor-mutant lung adenocarcinomas with acquired resistance to kinase inhibitors. *Clin Cancer Res* 2006;12(21):6494-501.
88. Branford S, Rudzki Z, Walsh S, et al. High frequency of point mutations clustered within the adenosine triphosphate-binding region of BCR/ABL in patients with chronic myeloid leukemia or Ph-positive acute lymphoblastic leukemia who develop imatinib (ST1571) resistance. *Blood* 2002;99(9):3472-5.
89. Tamborini E, Bonadiman L, Greco A, et al. A new mutation in the KIT ATP pocket causes acquired resistance to imatinib in a gastrointestinal stromal tumor patient. *Gastroenterology* 2004;127(1):294-9.

90. Yun CH, Mengwasser KE, Toms AV, et al. The T790M mutation in EGFR kinase causes drug resistance by increasing the affinity for ATP. *Proc Natl Acad Sci U S A* 2008;105(6):2070-5.
91. Kwak EL, Sordella R, Bell DW, et al. Irreversible inhibitors of the EGF receptor may circumvent acquired resistance to gefitinib. *Proc Natl Acad Sci U S A* 2005;102(21):7665-70.
92. Morgillo F, Kim WY, Kim ES, Ciardiello F, Hong WK, Lee HY. Implication of the insulin-like growth factor-IR pathway in the resistance of non-small cell lung cancer cells to treatment with gefitinib. *Clin Cancer Res* 2007;13(9):2795-803.
93. Habib AA, Chun SJ, Neel BG, Vartanian T. Increased expression of epidermal growth factor receptor induces sequestration of extracellular signal-related kinases and selective attenuation of specific epidermal growth factor-mediated signal transduction pathways. *Mol Cancer Res* 2003;1(3):219-33.
94. Elkind NB, Szentpetery Z, Apati A, et al. Multidrug transporter ABCG2 prevents tumor cell death induced by the epidermal growth factor receptor inhibitor Iressa (ZD1839, Gefitinib). *Cancer Res* 2005;65(5):1770-7.
95. Wissner A, Mansour TS. The development of HKI-272 and related compounds for the treatment of cancer. *Arch Pharm (Weinheim)* 2008;341(8):465-77.
96. Gendreau SB, Ventura R, Keast P, et al. Inhibition of the T790M gatekeeper mutant of the epidermal growth factor receptor by EXEL-7647. *Clin Cancer Res* 2007;13(12):3713-23.
97. Sordella R BD, Haber DA, Settleman J. Gefitinib-sensitizing EGFR mutations in lung cancer activate anti-apoptotic pathways. *Science* 2004;305:1163-7.
98. Kobayashi S ST, Monti S, Steidl U, Hetherington CJ, Lowell AM, Golub T, Meyerson M, Tenen DG, Shapiro GI, Halmos B. Transcriptional profiling identifies cyclin D1 as a critical downstream effector of mutant epidermal growth factor receptor signaling. *Cancer Res* 2006;66(23):11389-98.
99. Wada T PJ. Mitogen-activated protein kinases in apoptosis regulation. *Oncogene* 2004;23(16):2838-49.
100. Kumar SB, J. Lee, J. C. . p38 MAP kinases: key signalling molecules as therapeutic targets for inflammatory diseases. . *Nature Rev Drug Discov* 2003; 2:717-26.
101. Dhillon AS HS, Rath O, Kolch W. MAP kinase signalling pathways in cancer. *Oncogene* 2007;26(22):3279-90.
102. Keyse SM. Dual-specificity MAP kinase phosphatases (MKPs) and cancer. *Cancer Metastasis Rev* 2008;27(2):253-61.
103. Theodosiou A AA. MAP kinase phosphatases. *Genome Biol* 2002;3(7).
104. Karlsson M MJ, Dickinson RJ, Mandl M, Keyse SM. Both nuclear-cytoplasmic shuttling of the dual specificity phosphatase MKP-3 and its ability to anchor MAP kinase in the cytoplasm are mediated by a conserved nuclear export signal. *J Biol Chem* 2004;279(40):41882-91.
105. Tárrega C RP, Cejudo-Marín R, Blanco-Aparicio C, van den Berk L, Schepens J, Hendriks W, Tabernero L, Pulido R. ERK2 shows a restrictive and locally selective mechanism of recognition by its tyrosine phosphatase inactivators not shared by its activator MEK1. *J Biol Chem* 2005;280(45):37885-94.
106. Furukawa T SM, Motoi F, Matsuno S, Horii A. Potential tumor suppressive pathway involving DUSP6/MKP-3 in pancreatic cancer. *Am J Pathol* 2003;162(6):1807-15.
107. Bloethner S, Chen, B., Hemminki, K., Muller-Berghaus, J., Ugurel, S., Schadendorf, D., et al. Effect of common BRAF and N-RAS mutations on global gene expression in melanoma cell lines. . *Carcinogenesis* 2005;26(7):1224-32.
108. Croonquist PA, Linden, M. A., Zhao, F., & Van Ness, B. G. Gene profiling of a myeloma cell line reveals similarities and unique signatures among IL-6 response, N-ras-activating mutations, and coculture with bone marrow stromal cells. *Blood* 2003;102(7):2581-92.
109. Warmka JK, Mauro, L. J., & Wattenberg, E. V. Mitogen-activated protein kinase phosphatase-3 is a tumor promoter target in initiated cells that express oncogenic Ras. *Journal of Biological Chemistry* 2004;279(32):33085-92.
110. Marchetti S GC, Roux D, Gothié E, Pouysségur J, Pagès G. Inducible expression of a MAP kinase phosphatase-3-GFP chimera specifically blunts fibroblast growth and ras-dependent tumor formation in nude mice. *J Cell Physiol* 2004 199(3):441-50.

111. Chen HY YS, Chen CH, Chang GC, Chen CY, Yuan A, Cheng CL, Wang CH, Terng HJ, Kao SF, Chan WK, Li HN, Liu CC, Singh S, Chen WJ, Chen JJ, Yang PC. A five-gene signature and clinical outcome in non-small-cell lung cancer. *N Engl J Med* 2007;356(1):11-20.
112. Perez-Soler R. Individualized therapy in non-small-cell lung cancer: future versus current clinical practice. *Oncogene* 2009;28 Suppl 1:S38-45.
113. Li Y, Ye X, Tan C, et al. Axl as a potential therapeutic target in cancer: role of Axl in tumor growth, metastasis and angiogenesis. *Oncogene* 2009;28(39):3442-55.
114. Linger RM, Keating AK, Earp HS, Graham DK. TAM receptor tyrosine kinases: biologic functions, signaling, and potential therapeutic targeting in human cancer. *Adv Cancer Res* 2008;100:35-83.
115. Yamagata M, Sanes JR, Weiner JA. Synaptic adhesion molecules. *Curr Opin Cell Biol* 2003;15(5):621-32.
116. Robinson DR, Wu YM, Lin SF. The protein tyrosine kinase family of the human genome. *Oncogene* 2000;19(49):5548-57.
117. Hafizi S, Dahlback B. Signalling and functional diversity within the Axl subfamily of receptor tyrosine kinases. *Cytokine Growth Factor Rev* 2006;17(4):295-304.
118. Crosier PS, Freeman SA, Orlic D, Bodine DM, Crosier KE. The Dtk receptor tyrosine kinase, which binds protein S, is expressed during hematopoiesis. *Exp Hematol* 1996;24(2):318-23.
119. Faust M, Ebensperger C, Schulz AS, et al. The murine ufo receptor: molecular cloning, chromosomal localization and in situ expression analysis. *Oncogene* 1992;7(7):1287-93.
120. Korshunov VA, Mohan AM, Georger MA, Berk BC. Axl, a receptor tyrosine kinase, mediates flow-induced vascular remodeling. *Circ Res* 2006;98(11):1446-52.
121. Lemke G, Lu Q. Macrophage regulation by Tyro 3 family receptors. *Curr Opin Immunol* 2003;15(1):31-6.
122. Lu Q, Lemke G. Homeostatic regulation of the immune system by receptor tyrosine kinases of the Tyro 3 family. *Science* 2001;293(5528):306-11.
123. Lu Q, Gore M, Zhang Q, et al. Tyro-3 family receptors are essential regulators of mammalian spermatogenesis. *Nature* 1999;398(6729):723-8.
124. Angelillo-Scherrer A, de Frutos P, Aparicio C, et al. Deficiency or inhibition of Gas6 causes platelet dysfunction and protects mice against thrombosis. *Nat Med* 2001;7(2):215-21.
125. Prasad D, Rothlin CV, Burrola P, et al. TAM receptor function in the retinal pigment epithelium. *Mol Cell Neurosci* 2006;33(1):96-108.
126. O'Bryan JP, Frye RA, Cogswell PC, et al. axl, a transforming gene isolated from primary human myeloid leukemia cells, encodes a novel receptor tyrosine kinase. *Mol Cell Biol* 1991;11(10):5016-31.
127. Graham DK, Bowman GW, Dawson TL, Stanford WL, Earp HS, Snodgrass HR. Cloning and developmental expression analysis of the murine c-mer tyrosine kinase. *Oncogene* 1995;10(12):2349-59.
128. Brauner J, Schleithoff L, Schulz AS, et al. Intracellular signaling of the Ufo/Axl receptor tyrosine kinase is mediated mainly by a multi-substrate docking-site. *Oncogene* 1997;14(22):2619-31.
129. Budagian V, Bulanova E, Orinska Z, et al. A promiscuous liaison between IL-15 receptor and Axl receptor tyrosine kinase in cell death control. *EMBO J* 2005;24(24):4260-70.
130. Goruppi S, Ruaro E, Varnum B, Schneider C. Gas6-mediated survival in NIH3T3 cells activates stress signalling cascade and is independent of Ras. *Oncogene* 1999;18(29):4224-36.
131. Lee WP, Wen Y, Varnum B, Hung MC. Akt is required for Axl-Gas6 signaling to protect cells from E1A-mediated apoptosis. *Oncogene* 2002;21(3):329-36.
132. Demarchi F, Verardo R, Varnum B, Brancolini C, Schneider C. Gas6 anti-apoptotic signaling requires NF-kappa B activation. *J Biol Chem* 2001;276(34):31738-44.
133. Hasanbasic I, Cuerquis J, Varnum B, Blostein MD. Intracellular signaling pathways involved in Gas6-Axl-mediated survival of endothelial cells. *Am J Physiol Heart Circ Physiol* 2004;287(3):H1207-13.
134. Hafizi S, Alindri F, Karlsson R, Dahlback B. Interaction of Axl receptor tyrosine kinase with C1-TEN, a novel C1 domain-containing protein with homology to tensin. *Biochem Biophys Res Commun* 2002;299(5):793-800.
135. Schlessinger J. Cell signaling by receptor tyrosine kinases. *Cell* 2000;103(2):211-25.
136. Hafizi S, Gustafsson A, Stenhoff J, Dahlback B. The Ran binding protein RanBPM interacts with Axl and Sky receptor tyrosine kinases. *Int J Biochem Cell Biol* 2005;37(11):2344-56.

137. Budagian V, Bulanova E, Orinska Z, et al. Soluble Axl is generated by ADAM10-dependent cleavage and associates with Gas6 in mouse serum. *Mol Cell Biol* 2005;25(21):9324-39.
138. Valverde P. Effects of Gas6 and hydrogen peroxide in Axl ubiquitination and downregulation. *Biochem Biophys Res Commun* 2005;333(1):180-5.
139. Nakano T, Tani M, Ishibashi Y, et al. Biological properties and gene expression associated with metastatic potential of human osteosarcoma. *Clin Exp Metastasis* 2003;20(7):665-74.
140. Wimmel A, Glitz D, Kraus A, Roeder J, Schuermann M. Axl receptor tyrosine kinase expression in human lung cancer cell lines correlates with cellular adhesion. *Eur J Cancer* 2001;37(17):2264-74.
141. Mahadevan D, Cooke L, Riley C, et al. A novel tyrosine kinase switch is a mechanism of imatinib resistance in gastrointestinal stromal tumors. *Oncogene* 2007;26(27):3909-19.
142. Hong CC, Lay JD, Huang JS, et al. Receptor tyrosine kinase AXL is induced by chemotherapy drugs and overexpression of AXL confers drug resistance in acute myeloid leukemia. *Cancer Lett* 2008;268(2):314-24.
143. Lay JD, Hong CC, Huang JS, et al. Sulfasalazine suppresses drug resistance and invasiveness of lung adenocarcinoma cells expressing AXL. *Cancer Res* 2007;67(8):3878-87.
144. Macleod K, Mullen P, Sewell J, et al. Altered ErbB receptor signaling and gene expression in cisplatin-resistant ovarian cancer. *Cancer Res* 2005;65(15):6789-800.
145. Holland SJ, Powell MJ, Franci C, et al. Multiple roles for the receptor tyrosine kinase axl in tumor formation. *Cancer Res* 2005;65(20):9294-303.
146. Liu L, Greger J, Shi H, et al. Novel mechanism of lapatinib resistance in HER2-positive breast tumor cells: activation of AXL. *Cancer Res* 2009;69(17):6871-8.
147. Holland SJ, Pan A, Franci C, et al. R428, a selective small molecule inhibitor of Axl kinase, blocks tumor spread and prolongs survival in models of metastatic breast cancer. *Cancer Res*;70(4):1544-54.
148. Jemal A, Thun MJ, Ries LA, et al. Annual report to the nation on the status of cancer, 1975-2005, featuring trends in lung cancer, tobacco use, and tobacco control. *J Natl Cancer Inst* 2008;100(23):1672-94.
149. Ciardiello F, Tortora G. EGFR antagonists in cancer treatment. *N Engl J Med* 2008;358(11):1160-74.
150. Lynch TJ, Bell, D. W., Sordella, R., Gurubhagavatula, S., Okimoto, R. A., Brannigan, B. W., Harris, P. L., Haserlat, S. M., Supko, J. G., Haluska, F. G., Louis, D. N., Christiani, D. C., Settleman, J., and Haber, D. A. Activating mutations in the epidermal growth factor receptor underlying responsiveness of non-small-cell lung cancer to gefitinib. *N Engl J Med* 2004;350:2129-39.
151. Paez JG, Janne, P. A., Lee, J. C., Tracy, S., Greulich, H., Gabriel, S., Herman, P., Kaye, F. J., Lindeman, N., Boggon, T. J., Naoki, K., Sasaki, H., Fujii, Y., Eck, M. J., Sellers, W. R., Johnson, B. E., and Meyerson, M. EGFR mutations in lung cancer: correlation with clinical response to gefitinib therapy. *Science* 2004.;304:1497-500.
152. Pao W, Miller, V., Zakowski, M., Doherty, J., Politi, K., Sarkaria, I., Singh, B., Heelan, R., Rusch, V., Fulton, L., Mardis, E., Kupfer, D., Wilson, R., Kris, M., and Varmus, H. EGF receptor gene mutations are common in lung cancers from "never smokers" and are associated with sensitivity of tumors to gefitinib and erlotinib. *Proc Natl Acad Sci U S A*, 2004;101:13306-11.
153. Jeffrey KL CM, Rommel C, Mackay CR. Targeting dual-specificity phosphatases: manipulating MAP kinase signalling and immune responses. *Nat Rev Drug Discov* 2007;6(5):391-403.
154. Kobayashi S JH, Yuza Y, Meyerson M, Wong KK, Tenen DG, Halmos B. An alternative inhibitor overcomes resistance caused by a mutation of the epidermal growth factor receptor. *Cancer Res* 2005;65(16):7096-101.
155. Patterson KI, Brummer T, O'Brien PM, Daly RJ. Dual-specificity phosphatases: critical regulators with diverse cellular targets. *Biochem J* 2009;418(3):475-89.
156. Keyse SM. Dual-specificity MAP kinase phosphatases (MKPs) and cancer. *Cancer Metastasis Rev* 2008;27(2):253-61.
157. Echevarria D, Martinez S, Marques S, Lucas-Teixeira V, Belo JA. Mkp3 is a negative feedback modulator of Fgf8 signaling in the mammalian isthmic organizer. *Dev Biol* 2005;277(1):114-28.
158. Li C, Scott DA, Hatch E, Tian X, Mansour SL. Dusp6 (Mkp3) is a negative feedback regulator of FGF-stimulated ERK signaling during mouse development. *Development* 2007;134(1):167-76.

159. Maillet M, Purcell NH, Sargent MA, York AJ, Bueno OF, Molkentin JD. DUSP6 (MKP3) null mice show enhanced ERK1/2 phosphorylation at baseline and increased myocyte proliferation in the heart affecting disease susceptibility. *J Biol Chem* 2008;283(45):31246-55.
160. Ekerot M, Stavridis MP, Delavaine L, et al. Negative-feedback regulation of FGF signalling by DUSP6/MKP-3 is driven by ERK1/2 and mediated by Ets factor binding to a conserved site within the DUSP6/MKP-3 gene promoter. *Biochem J* 2008;412(2):287-98.
161. Jurek A, Amagasaki K, Gembarska A, Heldin CH, Lennartsson J. Negative and positive regulation of MAP kinase phosphatase 3 controls PDGF-induced Erk activation. *J Biol Chem* 2008.
162. Furukawa T YT, Youssef EM, Abe T, Yokoyama T, Fukushima S, Soeda E, Hoshi M, Hayashi Y, Sunamura M, Kobari M, Horii A. Genomic analysis of DUSP6, a dual specificity MAP kinase phosphatase, in pancreatic cancer. *Cytogenet Cell Genet* 1998;82(3-4):156-9.
163. Muda M, Theodosiou A, Rodrigues N, et al. The dual specificity phosphatases M3/6 and MKP-3 are highly selective for inactivation of distinct mitogen-activated protein kinases. *J Biol Chem* 1996;271(44):27205-8.
164. Muda M TA, Gillieron C, Smith A, Chabert C, Camps M, Boschert U, Rodrigues N, Davies K, Ashworth A, Arkinstall S. The mitogen-activated protein kinase phosphatase-3 N-terminal noncatalytic region is responsible for tight substrate binding and enzymatic specificity. *J Biol Chem* 1998;273(15):9323-9.
165. Chan DW, Liu VW, Tsao GS, et al. Loss of MKP3 mediated by oxidative stress enhances tumorigenicity and chemoresistance of ovarian cancer cells. *Carcinogenesis* 2008;29(9):1742-50.
166. Huang G, Eisenberg R, Yan M, et al. 15-Hydroxyprostaglandin dehydrogenase is a target of hepatocyte nuclear factor 3beta and a tumor suppressor in lung cancer. *Cancer Res* 2008;68(13):5040-8.
167. Zhou B ZJ, Liu S, Reddy S, Wang F, Zhang ZY. Mapping ERK2-MKP3 binding interfaces by hydrogen/deuterium exchange mass spectrometry. *J Biol Chem* 2006;281(50):38834-44.
168. Wishart MJ, Denu JM, Williams JA, Dixon JE. A single mutation converts a novel phosphotyrosine binding domain into a dual-specificity phosphatase. *J Biol Chem* 1995;270(45):26782-5.
169. Dowd S, Sneddon AA, Keyse SM. Isolation of the human genes encoding the pyst1 and Pyst2 phosphatases: characterisation of Pyst2 as a cytosolic dual-specificity MAP kinase phosphatase and its catalytic activation by both MAP and SAP kinases. *J Cell Sci* 1998;111 (Pt 22):3389-99.
170. Kobayashi S, Shimamura T, Monti S, et al. Transcriptional profiling identifies cyclin D1 as a critical downstream effector of mutant epidermal growth factor receptor signaling. *Cancer Res* 2006;66(23):11389-98.
171. Myers E, Hill AD, Kelly G, et al. Associations and interactions between Ets-1 and Ets-2 and coregulatory proteins, SRC-1, AIB1, and NCoR in breast cancer. *Clin Cancer Res* 2005;11(6):2111-22.
172. Farooq A, Zhou MM. Structure and regulation of MAPK phosphatases. *Cell Signal* 2004;16(7):769-79.
173. Wu JJ ZL, Bennett AM. The noncatalytic amino terminus of mitogen-activated protein kinase phosphatase 1 directs nuclear targeting and serum response element transcriptional regulation. *Mol Cell Biol* 2005;25(11):4792-803.
174. Muda M BU, Dickinson R, Martinou JC, Martinou I, Camps M, Schlegel W, Arkinstall S. MKP-3, a novel cytosolic protein-tyrosine phosphatase that exemplifies a new class of mitogen-activated protein kinase phosphatase. *J Biol Chem* 1996;271(8):4319-26.
175. Masuda K, Shima H, Watanabe M, Kikuchi K. MKP-7, a novel mitogen-activated protein kinase phosphatase, functions as a shuttle protein. *J Biol Chem* 2001;276(42):39002-11.
176. Bettini ML KG. MAP kinase phosphatase activity sets the threshold for thymocyte positive selection. *Proc Natl Acad Sci U S A*, 2007;104(41):16257-62.
177. Okudela K, Yazawa T, Woo T, et al. Down-regulation of DUSP6 expression in lung cancer: its mechanism and potential role in carcinogenesis. *Am J Pathol* 2009;175(2):867-81.
178. Xu S, Furukawa, T., Kanai, N., Sunamura, M., & Horii, A. Abrogation of DUSP6 by hypermethylation in human pancreatic cancer. *Journal of Human Genetics* 2005; 50(4):159-67.
179. Bermudez O, Marchetti S, Pages G, Gimond C. Post-translational regulation of the ERK phosphatase DUSP6/MKP3 by the mTOR pathway. *Oncogene* 2008;27(26):3685-91.

180. Furukawa T, Tanji E, Xu S, Horii A. Feedback regulation of DUSP6 transcription responding to MAPK1 via ETS2 in human cells. *Biochem Biophys Res Commun* 2008;377(1):317-20.
181. Hakansson P, Nilsson B, Andersson A, Lassen C, Gullberg U, Fioretos T. Gene expression analysis of BCR/ABL1-dependent transcriptional response reveals enrichment for genes involved in negative feedback regulation. *Genes Chromosomes Cancer* 2008;47(4):267-75.
182. Ramnarain DB PS, Lee DY, Hatanpaa KJ, Scoggin SO, Otu H, Libermann TA, Raisanen JM, Ashfaq R, Wong ET, Wu J, Elliott R, Habib AA. Differential gene expression analysis reveals generation of an autocrine loop by a mutant epidermal growth factor receptor in glioma cells. *Cancer Res* 2006;66(2):867-74.
183. Warmka JK, Mauro LJ, Wattenberg EV. Mitogen-activated protein kinase phosphatase-3 is a tumor promoter target in initiated cells that express oncogenic Ras. *J Biol Chem* 2004;279(32):33085-92.
184. Marchetti S, Gimond C, Roux D, Gothie E, Pouyssegur J, Pages G. Inducible expression of a MAP kinase phosphatase-3-GFP chimera specifically blunts fibroblast growth and ras-dependent tumor formation in nude mice. *J Cell Physiol* 2004;199(3):441-50.
185. Kobayashi S, Boggon TJ, Dayaram T, et al. EGFR mutation and resistance of non-small-cell lung cancer to gefitinib. *N Engl J Med* 2005;352(8):786-92.
186. Kobayashi S, Ji H, Yuza Y, et al. An alternative inhibitor overcomes resistance caused by a mutation of the epidermal growth factor receptor. *Cancer Res* 2005;65(16):7096-101.
187. Qian F, Engst S, Yamaguchi K, et al. Inhibition of tumor cell growth, invasion, and metastasis by EXEL-2880 (XL880, GSK1363089), a novel inhibitor of HGF and VEGF receptor tyrosine kinases. *Cancer Res* 2009;69(20):8009-16.
188. Gjerdrum C, Tiron C, Hoiby T, et al. Axl is an essential epithelial-to-mesenchymal transition-induced regulator of breast cancer metastasis and patient survival. *Proc Natl Acad Sci U S A*;107(3):1124-9.
189. Vajkoczy P, Knyazev P, Kunkel A, et al. Dominant-negative inhibition of the Axl receptor tyrosine kinase suppresses brain tumor cell growth and invasion and prolongs survival. *Proc Natl Acad Sci U S A* 2006;103(15):5799-804.
190. Zhang YX, Knyazev PG, Cheburkin YV, et al. AXL is a potential target for therapeutic intervention in breast cancer progression. *Cancer Res* 2008;68(6):1905-15.
191. Furukawa T YT, Youssef EM, Abe T, Yokoyama T, Fukushige S, Soeda E, Hoshi M, Hayashi Y, Sunamura M, Kobari M, Horii A. Genomic analysis of DUSP6, a dual specificity MAP kinase phosphatase, in pancreatic cancer. *Cytogenet Cell Genet* 1998;82(3-4):156-9.
192. Halmos B BD, Monti S, D'Aló F, Dayaram T, Ferenczi K, Wouters BJ, Huettner CS, Golub TR, Tenen DG. A transcriptional profiling study of CCAAT/enhancer binding protein targets identifies hepatocyte nuclear factor 3 beta as a novel tumor suppressor in lung cancer. *Cancer Res* 2004;64(12):4137-47.
193. Mudduluru G, Allgayer H. The human receptor tyrosine kinase Axl gene--promoter characterization and regulation of constitutive expression by Sp1, Sp3 and CpG methylation. *Biosci Rep* 2008;28(3):161-76.
194. Zhang Z, Kobayashi S, Borczuk AC, et al. Dual specificity phosphatase 6 (DUSP6) is an ETS-regulated negative feedback mediator of oncogenic ERK signaling in lung cancer cells. *Carcinogenesis*;31(4):577-86.